The Influence of Myosin Regulatory Light Chain Phosphorylation on the Contractile Performance of Fatigued Mammalian Skeletal Muscle

William J. Gittings

A thesis submitted in partial fulfillment for the
requirements of a Master of Science Degree
in Applied Health Sciences (Kinesiology)

Supervisor: Rene Vandenboom, Ph.D.

Faculty of Applied Health Sciences
Brock University, St. Catharines, Ontario

ABSTRACT

The myosin regulatory light chain (RLC) of type II fibres is phosphorylated by Ca^{2+}-calmodulin dependent myosin light chain kinase (skMLCK) during muscular activation. The purpose of this study was to explore the effect of skMLCK gene ablation on the fatigability of mouse skeletal muscles during repetitive stimulation. The absence of myosin RLC phosphorylation in skMLCK knockout muscles attenuated contractile performance without a significant metabolic cost. Twitch force was potentiated to a greater extent in wildtype muscles until peak force had diminished to ~60% of baseline (37.2 ± 0.05% vs. 14.3 ± 0.02%). Despite no difference in peak force (P_o) and shortening velocity (V_o), rate of force development (+dP/d*t*) and shortening-induced deactivation (SID) were almost two-fold greater in WT muscles. The present results demonstrate that myosin RLC phosphorylation may improve contractile performance during fatigue; providing a contractile advantage to working muscles and protecting against progressive fatigue.

ACKNOWLEDGEMENTS

I want to thank everyone who contributed to the completion of this document. My hope is that this thesis will prove to useful in the future, both as a resource and as a meaningful memento of my last two years spent at Brock- only time will tell.

My friends and family have been especially encouraging throughout. I hope they realize that while my primary goal was to produce new knowledge in my field of study, their support and praise in response to my hard work and thoughtful research was the most rewarding experience of all.

The faculty support I received at Brock was influential in my decision to pursue research in the future. I would like to thank Rene for providing me with a great research opportunity and for the freedom to learn and work independently. Drs. Peters and Ditor were supportive and helpful as committee members. A special thank-you to Dr. Rob Grange for his time and expertise as my external examiner.

Thanks to all the other graduate students in the faculty with whom I spent a lot of time working and socializing. This experience, like all others to date, has shown that only a portion of my education actually occurs in the lab or classroom.

A final thank-you must be extended to Dr. Stull and colleagues at the University of Texas for their generous donation of resources and expertise in the form of the skMLCK knockout mice and myosin RLC phosphorylation analysis.

TABLE OF CONTENTS

LIST OF FIGURES

LIST OF TABLES

LIST OF ABBREVIATIONS

EDL = Extensor digitorum longus

WT, KO = Wildtype, Knockout

skMLCK, CaM = Myosin Light Chain Kinase, Calcium-Calmodulin

RLC, ELC = Regulatory Light Chain, Essential Light Chain

MHC = Myosin Heavy Chain

Tm, Tn = Tropomyosin, Troponin

F_{max}, P_o, P_t = Maximal Force, Peak Tetanic Force, Twitch Force

V_{max}, V_o = Maximal Shortening Velocity, Unloaded Shortening Velocity

$+dP/dt$, *SID* = Rate of Force Development, Shortening-Induced Deactivation

f_{app}, g_{app} = Forward & Reverse Rate Constants of Crossbridge Formation

PTP, PAP = Posttetanic Potentiation, Postactivation Potentiation

L_o = Optimal Length

HFF, LFF, PLFFD = High Frequency Fatigue, Low Frequency Fatigue, Prolonged Low Frequency Force Depression

Force-pCa = Force-Calcium Relationship (pCa = - log $[Ca^{2+}]$)

ECC = Excitation Contraction Coupling

SR = Sarcoplasmic Reticulum

ANOVA = Analysis of Variance

SEM = Standard Error of the Mean

n = Number of Subjects or Samples

GLOSSARY

Gene Ablation/Knockout: the sequence of nucleotides that code for the expression of proteins and enzymes can be manipulated to produce a specific experimental model. In this case, myosin light chain kinase (skMLCK) is selectively removed to effectively eliminate its expression within skeletal muscle.

Phosphorylation: Adenosine triphosphate (ATP) is hydrolyzed by skMLCK to produce one ADP and one inorganic phosphate (P_i) molecule. The inorganic phosphate is bound to a specific portion of the myosin neck domain, known as the regulatory light chain (RLC). This biochemical event changes the structure and function of the protein (myosin) that produces force in the muscle.

Muscle History Dependence: the phenomenon that prior contractile activity can alter subsequent performance.

Fatigue: the reversible declines in contractile and/or metabolic performance that arises from repeated contractile activity in skeletal muscle.

Conditioning Stimulus: a brief period of muscle activation that augments subsequent contractile activity.

Potentiation (Force): a greater contractile response following some type of conditioning stimulus. Also known as twitch force potentiation, Posttetanic Potentiation (PTP), Activity-dependent Potentiation, Postactivation Potentiation (PAP).

Force-pCa Relationship: using skinned-fibres, the force response of the contractile apparatus can be tested at various levels of activation by varying $[Ca^{2+}]$. In this relationship, force increases sigmoidally with increasing $[Ca^{2+}]$. The term pCa refers to the negative logarithm of calcium concentration ($-\log[Ca^{2+}]$).

Ca^{2+} Sensitivity: any factor which alters the contractile response to a given $[Ca^{2+}]$ is understood to alter the affinity of the contractile apparatus to muscle activation. Greater Ca^{2+} sensitivity will result in a greater contractile response to a given $[Ca^{2+}]$, or similarly, could allow the maintenance of some steady work output at a lower $[Ca^{2+}]$.

Contractile Apparatus: The myofilament array, composed of proteins (actin and myosin) that interact to produce mechanical forces and structural proteins that anchor the various components longitudinally and transversely. These structures make up the functional contractile unit of skeletal muscle, known as the sarcomere.

Contractile Performance: The force-producing response of the contractile apparatus, the direct result of actin-myosin interactions during muscle activation. This term includes force production, velocity of shortening, and rate of force development.

Physiological: the specific environmental conditions and functions that theoretically exist in the body.

Statistically Significant: a statistical probability that suggests how sure we can be that a given observation (within a sample) truly reflects the nature of the event or measurement in the population. The confidence interval (alpha <0.05) used in the current project suggests that the statistically significant conclusions herein would be recapitulated 95% of the time when re-sampled. It is a justifiable and economical way to infer a certain finding across a population by studying only a small sample.

I. INTRODUCTION

Performance of the contractile apparatus in fast-twitch (Type IIA, IIX, IIB) skeletal muscle is highly dependent on its previous activation history. Rapidly fluctuating intramuscular conditions following intense excitation can modulate the function of force-producing crossbridge interactions. These factors coalesce to attenuate maximal force production (F_{max}) and velocity of shortening (V_{max}), a phenomenon known as muscular fatigue. This effect has been attributed to both central and peripheral factors that alter the transmission and response of the molecular motor to motor unit activation. End-product inhibition and altered calcium (Ca^{2+}) handling have been established as the important mechanisms leading to altered excitation-contraction coupling (ECC) and subsequent fatigue (Allen, Lamb, & Westerblad, 2008b; Fitts, 2008).

The observation that previous contractile activity can augment the force response to low frequency stimulation (Bowditch, 1871; Brown & Tuttle, 1926; Lee, 1906) suggested that mechanisms, which combat the functional losses associated with muscular fatigue, might exist in skeletal muscle. One such mechanism is the contraction-activated process of myosin regulatory light chain (RLC) phosphorylation, which has been shown to potentiate muscle twitch force in skeletal muscle following a variety of conditioning stimuli. Myosin RLC phosphorylation occurs during muscle contraction when Ca^{2+} released from the sarcoplasmic reticulum (SR) binds to intracellular calmodulin (CaM) to activate the skeletal muscle isoform of myosin light chain kinase (skMLCK) (Manning & Stull, 1979; Manning & Stull, 1982). The outcome of this biochemical process is a structural change in the myosin molecule that renders the myofilaments more sensitive to intracellular calcium concentrations (Ritz-Gold, Cooke, Blumenthal, & Stull, 1980).

Structural change in the myosin head is best described as a bending or cocking movement; an alteration that shifts the population of myosin heads into a disordered array surrounding the thick filament. In this temporary state, each myosin head is thought to improve the opportunity for strong crossbridge interactions upon Ca^{2+} activation. Among the most important objectives in the study of myosin RLC phosphorylation is to elucidate (at the cellular level) the structural and functional response of the contractile apparatus to repeated contractions. Force potentiation has been implicated as a biochemical mechanism present in fast twitch skeletal muscle that may offer fatigue-resistant contractile benefits by inducing a leftward shift in the force-pCa curve at submaximal stimulation frequencies (Vandenboom, Grange, & Houston, 1993; Vandenboom & Houston, 1996; Zhi et al., 2005). This feature suggests an increased affinity of myosin crossbridges for binding sites on the thin filament and a relative increase in the number of strongly bound crossbridges in response to submaximal intracellular [Ca^{2+}]. Additional studies have shown that increased Ca^{2+} sensitivity by means of RLC phosphorylation can ameliorate the depression in muscle twitch force during prolonged contractile activity, suggesting that this mechanism may function independently of the source of fatigue (Vandenboom & Houston, 1996; Vandenboom et al., 1997). The proposed relationship between these concurrent muscle history dependent phenomena is that myosin RLC phosphorylation is an intrinsic, adaptive mechanism that maintains contractile function amidst progressive weakening of muscular activation and the sensitivity of the contractile apparatus to activation during fatigue. The fact that myosin RLC phosphorylation is simultaneously triggered with the same signal as muscular contraction suggests that it

plays an central role in the physiological design and function of fatigable type II fibers *in vivo*.

Recent technological advances in the manipulation of genetic sequencing and protein expression have established the novel ability to conduct robust mechanistic experiments with new insight. Zhi et al. (2005) generated skMLCK knockout mice to examine the physiological role of RLC phosphorylation in contractile performance. EDL muscles from skMLCK knockout mice exhibited no increase in RLC phosphorylation in response to repetitive electrical stimulation. Furthermore, in these muscles, twitch force was potentiated significantly less (>5% vs. ≥70%) than wild type mice in response to a conditioning stimulus (Zhi et al., 2005). These results confirm that RLC phosphorylation by Ca^{2+}/calmodulin-dependent skMLCK is the primary mechanism for twitch potentiation in fast-twitch skeletal muscle.

The concept that RLC phosphorylation functions as a mechanism that may transiently ameliorate myofibrillar fatigue has been challenged by Karatzaferi et al. (2008) who suggested that myosin RLC phosphorylation may act synergistically with intracellular conditions that approximate fatigue to inhibit shortening velocity up to ~40%. This outcome directly opposes previous findings (Persechini, Stull, & Cooke, 1985) and encourages additional exploration into the biochemical mechanism of RLC phosphorylation within the metabolic accumulation model of muscle fatigue. Examining the specific role that RLC phosphorylation plays in modulating contractile performance during repetitive high frequency stimulation that leads to fatigue is especially difficult because this type of muscle activation cannot be studied without concurrently elevating RLC phosphate content. Therefore, a new definitive role for force potentiation in fatigue

resistance may not be clear until repeated contractile activity can be induced in the absence of RLC phosphorylation.

The proposed study was designed to explore whether myosin RLC phosphorylation offers a fatigue resistant benefit to fast mouse muscles (EDL) during repetitive stimulation. Our primary intervention (skMLCK knockout) was expected to selectively eliminate myosin RLC phosphorylation and twitch force potentiation without influencing maximal force production or shortening velocity. The present results demonstrate that skMLCK gene ablation effectively removed myosin RLC phosphorylation, an intervention that attenuated contractile performance in KO muscles without a significant metabolic cost. Accordingly, muscle twitch force was protected in WT muscles to a greater extent during the initial stage of fatigue. As hypothesized, peak tetanic force (P_o) and shortening velocity (V_o) were not influenced by skMLCK knockout. However, the almost two-fold increase of +dP/dt observed in WT muscles suggests that elevated myosin RLC phosphorylation has the potential to maintain high frequency force production during brief contractions even at high frequencies. The secondary analysis of +dP/d*t* established that shortening-induced deactivation (SID) is significantly larger in the presence of myosin RLC phosphorylation. This is a novel finding because it demonstrates that myosin RLC phosphorylation may also improve the rapid detachment of force-producing crossbridges in addition to rate of force development. In conclusion, myosin RLC phosphorylation improves the rate and extent of force production, which may maintain contractile performance during progressive fatigue.

II. REVIEW OF LITERATURE

2.1.0 Background

Muscle twitch force potentiation has been implicated as a characteristic of fast twitch skeletal muscle that may offer fatigue resistant contractile benefits by inducing a leftward shift in the force-pCa curve at submaximal stimulation frequencies (Grange et al., 1995; Grange et al., 1998; Vandenboom et al., 1993; Vandenboom et al., 1995; Vandenboom & Houston, 1996; Vandenboom et al., 1997; Zhi et al., 2005). Characterization of skeletal muscle potentiation in recent decades has used a wide variety of methods. The gamut of these approaches ranges from robust cellular measurements of force and contraction kinetics to performance driven study of whole body dynamic movements. Fragmentation of potentiation research has resulted in specializations that differ meaningfully in the ability to characterize either *a)* the functional role of potentiation in human performance, or *b)* an accurate neuromechanical model of potentiation at the cellular level. Explaining the physiological relevance of skeletal muscle potentiation in human performance, however, may be difficult to elucidate until the precise cellular mechanisms are systematically determined.

The purpose of this review is to present a summary of biochemical and functional characteristics associated with skeletal muscle potentiation. In addition, it will present the most recent data describing the cellular mechanisms of fatigue and provide the rationale for continued study into the coincidence of these phenomena. Of special interest is the regulation and functional significance of an important contraction-activated process: myosin regulatory light chain (RLC) phosphorylation.

2.1.1 Muscle Mechanics: Experimental Models

Myosin RLC phosphorylation and muscle mechanics are studied using a variety of experimental models. In general, the most controllable experimental models are the most effective for mechanistic study but may lack physiological relevance to *in vivo* function. Of particular importance to the present discussion is the use of the skinned-fibre model. For these experiments, fast twitch fibres are extracted from an anesthetized animal and are carefully prepared by the chemical disruption of all structures other than the myofilaments (i.e., the contractile apparatus). Control of the physiological solution that surrounds the preparation is important as it contains important metabolic substrates and the Ca^{2+} that ultimately activates crossbridge cycling. This is the only model where intracellular [Ca^{2+}] can be varied to directly test mechanical function at different levels of activation. The force-pCa relationship refers to the force response of a skinned-fiber to a range of Ca^{2+} concentrations (see Figure 4 for schematic). It is within this model that the calcium sensitivity of the contractile apparatus can be directly assessed by various interventions; such as the chemical phosphorylation of the myosin RLC or the addition of various metabolites and modulators of contractile function.

2.2.0 Skeletal Muscle Microanatomy: The Contractile Apparatus

The function of skeletal muscle is to convert stored chemical energy into mechanical energy. All biological movements involve cyclic interactions between specialized motor proteins, resulting in the generation of muscular force. The seminal sliding filament theory represented years of careful research conducted most prominently by H.E. Huxley and colleagues (Hanson & Huxley, 1953; H. Huxley & Hanson, 1954; H. E. Huxley, 1953; H. E. Huxley, 1957). Although initially controversial and difficult to

substantiate, the basic concept of cross-striated myofilaments and the chemically driven power stroke has remained virtually unchanged for half a century. Technological advances in the ability to isolate and view tissue at the microscopic level has allowed researchers to further characterize the structural components comprising one of nature's most impressive designs.

Each individual contractile unit of a single muscle fibre (sarcomere) contains a network of thin (actin) and thick myofilaments (myosin) that are spatially oriented to maximize opportunities for direct physical interactions. Actin filaments are directly bound to the longitudinal ends (Z-line) of the sarcomere, while myosin is suspended at the midpoint (M-line) and anchored to the Z-line by the structural protein titin. When skeletal muscle is stimulated by peripheral alpha-motor neurons, every sarcomere along each fibre contracts synergistically as each myosin head 'pulls' the actin filament towards the M-line (H. E. Huxley, 1957; H. E. Huxley, 1969). This minute force-producing interaction of muscle proteins is turned into coordinated movement by the control of motor unit firing rates of antagonistic muscle groups attached to the appendicular skeleton.

The thin filament is formed by two actin monomers (~40kDa) bound in a helical configuration. Each regulatory protein complex of troponin (Tn) and tropomyosin (Tm) is longitudinally bound to seven actin molecules and is responsible for control of muscle contraction and propagation of cooperative myosin binding information (Gordon, Homsher, & Regnier, 2000). Actin subunits (TnC, TnI and TnT) function to control the position of Tm on the thin filament, regulating the availability of actin binding sites for weak or strong interactions with myosin. Calcium (Ca^{2+}) release from the sarcoplasmic

reticulum (SR) and subsequent binding to the specialized troponin subunit receptor (TnC) activates muscle contraction. As Ca^{2+} binds to TnC conformational changes are induced by weakening of the TnI-actin complex and strengthening of the Tn-TnI complex, a process that results in parallel sliding of Tm over the actin surface (Gordon, Homsher, & Regnier, 2000; Gordon, Regnier, & Homsher, 2001). Additionally, Tm facilitates communication along the thin filament to coordinate simultaneous availability of actin binding sites for myosin. More detailed characterizations of the thin filament regulatory protein complex have emerged but will not be discussed further in this review.

The largest muscle protein, myosin, consists of two heavy chains (~200kDa) and two pairs of light chains (~20kDa), referred to as the essential light chain (ELC) and the regulatory light chain (RLC). Many myosin isoforms exist across various species; however, the myosin II isoform is especially abundant in vertebrate skeletal muscle. There are two distinct structural regions of the myosin molecule, known as the head and tail. Dimerization of heavy chains forms the rod-like tail component opposite to the globular amino-terminus, which diverges into two distinct 'heads' (Rayment et al., 1993).

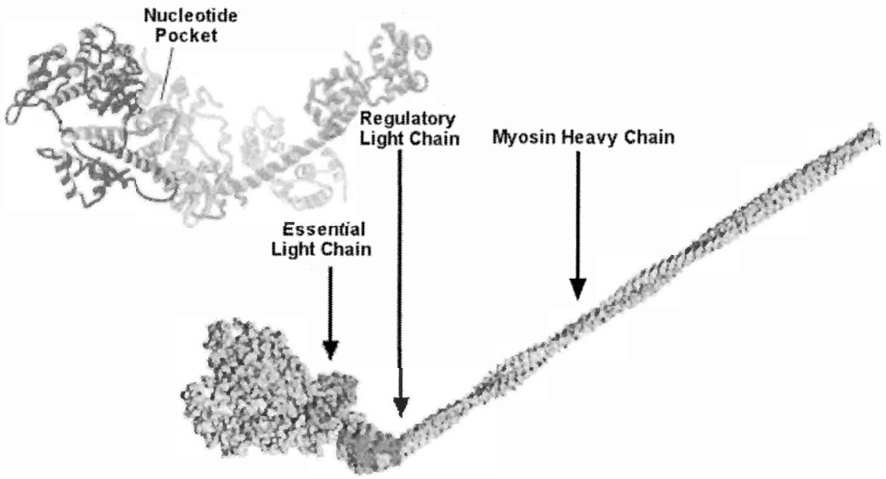

Figure 1. Myosin head microanatomy and important functional domains (Rayment et al. 1993).

The union of these distinct structural domains is an important functional location referred to as the neck and contains the essential and regulatory myosin light chains. In addition, the light chain binding domain located at the neck has been implicated as the lever arm during the power stroke of muscle contraction (Gulick & Rayment, 1997; Rayment et al., 1993). Each of the globular heads of myosin contain a nucleotide binding pocket as well as an actin binding domain which are essential to the force generating capacity of the contractile apparatus. More detailed references to the myofibrillar complex will be discussed as needed in explanation of crossbridge cycling, myosin RLC phosphorylation and mechanisms of cellular fatigue.

2.3.0 The Crossbridge Cycle & Regulation of Muscle Contraction

Cyclic conversion of chemical energy (ATP) to mechanical force (sarcomere shortening) is a dynamic process known as the crossbridge cycle. It can best be described as a series of conformational state changes in the myosin molecule and biochemical interactions between the thick and thin myofilaments (H. E. Huxley, 1969). Muscular contraction is a result of asynchronous, force-producing crossbridge interactions with the thin filament. Crossbridge cycling in this manner ensures that the number of crossbridges bound during contraction does not fall drastically due to simultaneous detachment, an event that would make coordinated movement virtually impossible. Each crossbridge independently harnesses the energy liberated from the hydrolysis of ATP to produce a conformational change known as the power stroke. Modulation of structural changes in the myosin head is controlled by the contents of the nucleotide-binding pocket (Cooke, 1997). The cycle begins with stearic ATP binding to the myosin head, which is subsequently hydrolyzed by myosin ATPase. Upon thin filament activation, the myosin

head can weakly bind to the actin filament with the ATP hydrolysis products (ADP and P_i) bound to the nucleotide-binding pocket. Release of P_i triggers a transition from weak to strong myosin binding and results in the power stroke. The power stroke is produced by a rotation of the light-chain binding domain of ~45°, displacing the thin filament longitudinally (~10nm) towards the M-line of the sarcomere (McKillop & Geeves, 1993; Rayment et al., 1993). Upon completion of the power stroke the crossbridge is in a rigor state and modulation of the actin-myosin interaction must take place before detachment can occur. ATP is rebound to the nucleotide-binding site and subsequently hydrolyzed as the myosin head detaches from the thin filament (Gordon et al., 2000).

The thin filament is regarded as the regulatory myofilament because it exists in various conformational states that alter the affinity of actin binding sites to crossbridge interactions. The three-state model described most notably by McKillop and Geeves (1993) suggests that the thin filament exists in a dynamic equilibrium between blocked, closed and open states. The thin filament regulatory complex (TnC, TnI, TnT, Tm) sterically blocks actin-binding sites during the blocked state (relaxation). Upon activation (Ca^{2+} binding to TnC), tropomyosin rolls along the surface of actin and partially exposes actin-binding sites (closed state). Crossbridges bound to the thin filament in the closed state form only weak biochemical interactions, initially. The cooperative effect of weakly bound crossbridges causes tropomyosin to roll further, fully exposing actin-binding sites (open state) for strong myosin interactions (power stroke). The thin filament will only remain in the open state in the presence of elevated myoplasmic [Ca^{2+}] and strongly bound crossbridges (Vandenboom, 2004). Regulation of crossbridge cycling and muscle contraction is modulated in the following way: *1)* movement of the thin filament

regulatory protein complex is dependent on myoplasmic [Ca^{2+}] and the relative abundance of weakly or strongly bound crossbridges, *2)* tropomyosin propagates signals of state changes (blocked-closed or closed-open) along the thin filament, *3)* a power stroke can only proceed once P_i has been released, *4)* affinity of crossbridges to actin binding sites is decreased when ATP is bound to the nucleotide pocket but increased upon hydrolysis (McKillop & Geeves, 1993; Rayment et al., 1993).

The theoretical model described above does not function optimally under all *in vivo* conditions. Dynamic physiological environments include fluctuations in calcium release, pH, temperature, muscle length, metabolic byproducts, and substrate availability that can impair ECC coupling (Allen, Lannergren, & Westerblad, 1995; Allen, Lamb, & Westerblad, 2008b; Cooke, 2007; Fitts, 2008). Of particular importance to the present review are acute causes of fatigue; impaired calcium release and accumulation of metabolic byproducts (see Appendix 4), which impair optimal contractility.

2.4.0 Muscle Memory & Contractile History

Among the most fascinating characteristics of skeletal muscle is that previous contractile activity can significantly alter subsequent performance, a phenomena often described as muscle memory. This concept was experimentally documented as early as the mid 19th century, a period of time in which novel explanations of muscle contractility were first developed by the pioneers of muscle physiology. Evidence of potentiated contractility following stimulation (Bowditch, 1871; Brown & Tuttle, 1926; Lee, 1906) suggested the existence of adaptive mechanisms that could at least temporarily improve muscle performance. This review is based on presenting a theoretical foundation for exploring skeletal muscle potentiation and how improved functional response to muscle

excitation could significantly attenuate the fatigability of fast twitch skeletal muscle. The role of myosin RLC phosphorylation in slow twitch muscle will not be discussed as the phenomenon of force potentiation does not exist in these myosin isoforms.

2.5.0 Skeletal Muscle Fatigue

Fatigue can be described as functional impairment of contractility, which is the direct result of altered muscle activation and crossbridge cycling. Prolonged muscle activation *in vivo* and through external stimulation can produce fatigue. The duty cycle (work:rest ratio) and stimulation intensity largely determine the amount of fatigue induced in skeletal muscle. Characterizing the mechanisms of fatigue during dynamic *in vivo* activity is extremely complex; therefore, this review will be limited to introducing the most important causes of fatigue and explaining how they might alter optimal contractility. The majority of applied research on fatigue has been conducted using isolated animal models, and therefore will be referred to support proposed theoretical mechanisms of fatigue.

The two types of fatigue most often cited are high frequency fatigue (HFF) and prolonged low frequency force depression (PLFFD), previously described as low frequency fatigue (LFF). Each term refers to the modality in which the fatigue-related decline in performance is measured. HFF is the impaired ability to develop maximal tension in response to high frequency muscle activation and is generally attributed to *a)* elevated extracellular [K^+], and *b)* failure at the neuromuscular junction (Allen, Lamb, & Westerblad, 2008b). This experimental model is most applicable to human tasks such as heavy lifting and maximal isometric contractions. PLFFD describes an impaired tension response to low frequency stimulation (twitch) without a concomitant impairment in high

frequency stimulation (tetanus). This phenomenon can last hours and possibly even days and is most prevalent at stimulation frequencies that correlate to low and moderate activities in humans (Rassier & Macintosh, 2000; Vandenboom & Houston, 1996).

PLFFD is most likely caused by impaired calcium release and reduced myofibrillar Ca^{2+} sensitivity, which is the result of either disrupted calcium release channels or the precipitation of calcium phosphate ($Ca_3[PO_4]_2$) in the SR (Allen, Lamb, & Westerblad, 2008a; Posterino & Dunn, 2008). In humans, PLFFD could explain the period of weakness felt after an intense bout of exercise, especially activities involving muscle stretch and resultant structural damage. Regardless of whether any functional deficits exist in producing maximal muscle tension, activities requiring low to moderate stimulation frequencies may be altered in response to PLFFD. Skeletal muscle potentiation may therefore play a significant role in improving contractile performance deficits that persist far beyond the time course required for metabolic recovery from activity (Allen, Lamb, & Westerblad, 2008b; Rassier & Macintosh, 2000).

2.6.0 Myosin Heavy Chain Phenotypes: Influence of Fibre Type

Structural and functional differences exist between different fibre types in skeletal muscle. Muscle types are classified based on the expression of different myosin heavy chain isoforms; type I, IIA, IIX and IIB. Although under considerable debate, recent evidence exists that *a)* muscle fibres can contain different myosin isoforms, and b) maximal shortening velocity between muscle cells with the same MHC expression is variable (Bottinelli, 2001; Pette & Staron, 2000). Therefore, the relationship between genetic expression of muscle protein isoforms and contractile properties is very complex. Type I fibres are far more fatigue resistance than type IIA and IIB fibres, although

oxidative capacity of type IIA fibres in rats is larger than type I fibres (Baldwin, Klinkerfuss, Terjung, Mole, & Holloszy, 1972). Type II fibres rapidly exhibit fatigue deficits in response to repeated contractions, and are commonly implicated in high intensity muscle performance due to their important role in developing maximal tension and rate of force development.

The beneficial effects of myosin RLC phosphorylation on contractile performance are present in type IIX and IIB fibres only. Twitch force potentiation and myosin RLC phosphorylation are absent in muscles with high proportions of Type IIA and I fibres, even in the presence of elevated skMLCK (Ryder et al. 2007).

2.7.0 Metabolite Accumulation & the Role of Calcium

During muscular work, flux through metabolic pathways increases in response to changing energy demands. Maintaining [ATP] is vital to provide the chemical energy to fuel crossbridge cycling, Na^+/K^+ pumps and SR Ca^{2+} reuptake. However, during high intensity activity or continuous work, fast-twitch muscle can consume ATP much faster than it can regenerate it, resulting in accumulation of metabolic byproducts (see Appendix 4). Allen et al. (2002) used the firefly luciferin/luciferase reaction to monitor intracellular ATP concentration in single mouse skeletal muscle fibres. Their results suggest that although [ATP] declines significantly during fatigue (~20-30%) it cannot be a major cause of contractile dysfunction: a conclusion that substantiates the accumulation model and the idea of end-product inhibition. At low energy demand, the creatine kinase (CK) reaction buffers ADP accumulation by regenerating ATP through the following reaction: PCr + ADP $\Leftrightarrow$ ATP + Cr. As [PCr] reaches low levels, [ATP] decreases rapidly and [ADP] accumulates in the myoplasm (Chase & Kushmerick, 1995; Cooke & Pate,

1985). During intense exercise, nucleoside diphosphate kinases can further buffer rises in [ADP] and re-synthesize ATP by facilitating reactions with other cellular high-energy phosphate donors (resulting in the accumulation of AMP, IMP). The accumulation of specific metabolic byproducts can impair actin-myosin interactions and Ca^{2+} handling (release and uptake) during muscle contraction. Appendix 4 provides a table of values that summarize the changes in metabolite concentrations that occur in skeletal muscle during fatigue. Additional factors such as muscle temperature, pH, duty cycle (work: rest ratio), and O_2 availability are dynamic during repeated contractions and interact simultaneously to impair muscle performance. The following sections will outline the functional manifestations of fatigue and refer to the putative mechanisms involved.

2.8.0 Contractile Function During Fatigue

The direct result of repeated, asynchronous crossbridge power strokes is the production of longitudinal forces, known as active muscle tension. Muscular contraction is activated by calcium released from the SR in response to nervous stimulation. In principle, altered contractile performance observed during fatigue could be caused by: *a)* reduced myoplasmic [Ca^{2+}] during contraction, *b)* reduced tension produced per crossbridge and number of crossbridges in the force-producing state, *c)* reduced sensitivity of the myofilaments to Ca^{2+}, or d) altered rate of ECC. The force-pCa curve is a graphic representation that describes how much tension a muscle fibre can produce in response to a given myoplasmic [Ca^{2+}]. Alterations in Ca^{2+} sensitivity of the myofilament shift the force-pCa curve, an effect that results in different contractile responses to a given [Ca^{2+}] signal during contraction. In fatigued skeletal muscle, this represent an alteration in EC coupling. Allen and Westerblad (1989) studied free myoplasmic [Ca^{2+}]

in isolated frog skeletal muscle fibres and concluded that [Ca^{2+}] release and reuptake are attenuated during fatigue. This resulted in a rightward shift of the force-pCa curve (decreased Ca^{2+} sensitivity), at least partially explaining the reduction in tension and slowed rate of relaxation after fatiguing tetani. The authors suggested that impaired Ca^{2+} release during fatigue might be due to alterations in calcium release channels or a reduction in SR [Ca^{2+}]. One important mechanism implicated in reduced SR [Ca^{2+}] is the precipitation of calcium phosphate in response to elevated [P_i] during fatigue (Kabbara & Allen, 1999).

Inability to develop maximal tetanic force (F_{max}) at saturating [Ca^{2+}] suggests that factors other than calcium release may cause impaired contractility at the crossbridge level. Accumulation of P_i and hydrogen ions (H^+) have been linked to altered crossbridge function during fatigue. Studies using skinned fibres have shown that F_{max} decreases exponentially with increases in [P_i], which can accumulate to 20-30mM during fatigue (Altringham & Johnston, 1985; Cooke & Pate, 1985; Debold, Dave, & Fitts, 2004). The general explanation for this effect is that accumulation of P_i may inhibit the crossbridge power stroke by inhibiting the release of P_i from the nucleotide-binding pocket, and in general causes a rightward shift in the force-pCa curve. Accumulation of P_i, however, does not significantly alter V_{max} (Cooke & Pate, 1985; Debold et al., 2004).

The effect of increased [ADP] during fatigue has been shown to increase force production by ~10% (Chase & Kushmerick, 1995; Cooke & Pate, 1985). The putative mechanism involved is that ADP accumulation may delay crossbridge detachment, resulting in longer strongly bound crossbridge associations. Despite this apparent fatigue resistant property, increased [ADP] has also been shown to significantly reduce V_{max} in

skinned muscle fibres and isolated mouse skeletal muscle (Cooke & Pate, 1985; Metzger, 1996; Westerblad, Allen, Bruton, Andrade, & Lannergren, 1998). As crossbridge detachment (ATP binding and hydrolysis) represents the rate-limiting step in the crossbridge cycle, the accumulation of [ADP] considerably attenuates ADP release- and the subsequent binding of ATP. The net effect of increased [ADP] in skeletal muscle therefore remains an impairment of contractile performance.

Historically, the effect of muscle acidosis on contractile function has been a heavily debated topic. Flux through anaerobic glycolysis in fast twitch skeletal muscle can result in up to a ten-fold increase in $[H^+]$ over resting values (Allen, 2004). Early studies showed that pH decreases during fatigue and is associated with decreases in F_{max} and V_{max}. These studies used a skinned-fibre model and confirmed that decreasing pH from ~7 to ~6 resulted in an ~ 40% decrease in V_{max} and ~50% decrease in F_{max} (Fabiato & Fabiato, 1978; Godt & Nosek, 1989). Skinned fibre models represent a highly controllable (though non-physiological) representation of muscle contraction in which the muscle membrane has been chemically dissolved- leaving only the contractile apparatus intact. Muscle contraction is therefore regulated by the addition of specific concentrations of Ca^{2+} into the muscle bath itself. It has been suggested that H^+ may compete with Ca^{2+} for binding to TnC (thus reducing thin filament activation), and additionally, that muscular acidosis may reduce the amount of energy liberated from the hydrolysis of ATP (Westerblad, Allen, & Lannergren, 2002). However, the role of reduced pH during fatigue may only be important at sub-physiological temperatures, questioning the physiological validity of past observations. Recent analysis using skinned muscle fibres have shown that at physiological temperatures fatigue may occur independent from

reductions in pH (Allen, 2004). It is increasingly apparent that Ca^{2+} signaling and sensitivity of the contractile apparatus to myoplasmic [Ca^{2+}] plays a central role in fatigue (Allen & Westerblad, 2001; Allen, Lamb, & Westerblad, 2008b; Bruton, Lannergren, & Westerblad, 1998; Westerblad & Allen, 1991). Accumulation of metabolic byproducts in the myoplasm can inhibit optimal crossbridge cycling and the sensitivity to myoplasmic [Ca^{2+}], which functionally impair muscle performance. Mechanisms that could improve or maintain contractile function in the presence of reduced myoplasmic [Ca^{2+}] and crossbridge dysfunction could therefore be highly beneficial for muscle performance. Furthermore, an increased force response to a given stimulus (Ca^{2+} sensitivity) could theoretically improve muscle economy and delay fatigue by sparing the activation component of muscle contraction (see Appendix 5 for schematic and explanation). Skeletal muscle potentiation has been implicated as such a mechanism, although an exact physiological role has remained elusive. This discussion will continue by presenting the mechanism of skeletal muscle potentiation and explain its role in modulating contractility during a variety of environmental parameters.

2.9.0 Skeletal Muscle Potentiation

The observation that previous muscle contractile activity can modulate subsequent muscular performance can be traced back to as early as the mid 19th century (Bowditch, 1871; Brown & Tuttle, 1926; Lee, 1906). This effect was termed 'treppe', which directly translated into English means staircase. Lee (1906) postulated that this phenomenon was caused by either *a)* a benefit caused by chemical substances formed during catabolism, or *b)* by the production of heat from metabolic processes. New methods of isolating skeletal muscle tissue have since developed, and rodent tissue is

used in addition to previous research using skeletal and cardiac muscle from amphibians. Close and Hoh (1968) conducted experiments on whole rat muscle (EDL) suspended in a Ringer solution, measuring posttetanic potentiation (PTP) at 35° C. Their results characterized important characteristics of skeletal muscle potentiation such as; a) the intensity (frequency & duration) of a stimulus can alter the kinetics of a muscle twitch, b) environmental factors such as temperature and pH can alter a contractile response, and c) PTP is likely related to ionic accumulation in the muscle. The study of the history dependence of skeletal muscle contractility has therefore specifically attempted to characterize the structural and functional responses of the myofilaments to repeated contractions at the cellular level. Within the study of human muscle performance, it is of special interest to establish how the act of a 'warm-up' activity or conditioning stimulus may acutely influence muscle performance during high intensity activities.

2.10.0 Myosin RLC Phosphorylation

During muscle contraction, Ca^{2+} released from the SR is an important regulator of myofilament function. In addition to activating the thin filament regulatory complex (as explained previously), myoplasmic Ca^{2+} binds to calmodulin and subsequently activates myosin light chain kinase (skMLCK). Early experiments by Manning and Stull (1979) measured myosin RLC phosphorylation in isolated EDL muscles from Sprague-Dawley rats at rest, during tetani and following relaxation. They concluded that phosphorylation of the myosin light chain was temporally correlated with a transient potentiation of posttetanic twitch force. This process is non-acutely reversed following activation by myosin light chain phosphatase, which de-phosphorylates the RLC (Morgan, Perry, & Ottaway, 1976).

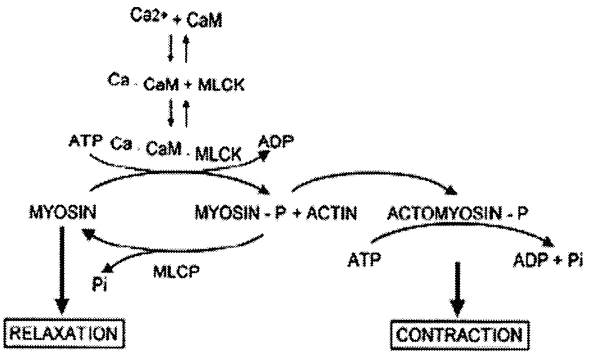

Figure 2. Myosin light chain kinase (MLCK) and myosin light chain phosphatase (MLCP) regulate the phosphate content of the regulatory light chain. MLCK is activated with muscle contraction as intracellular [Ca^{2+}] increases rapidly (Manning & Stull, 1982).

The functional alterations associated with potentiation are thought to occur during the temporal lag between muscle inactivation (declining myoplasmic [Ca^{2+}]) and the slow dephosphorylation of the RLC (Manning & Stull, 1982). It is well understood that phosphorylation of the RLC causes a conformational change in the myosin crossbridge characterized as a bending or swivel, which may be caused by an interaction between the negatively charged phosphate and the negatively charged myosin tail (Ritz-Gold et al., 1980; Yang, Stull, Levine, & Sweeney, 1998). This change is understood to disorder the distribution of myosin heads around the thick filament.

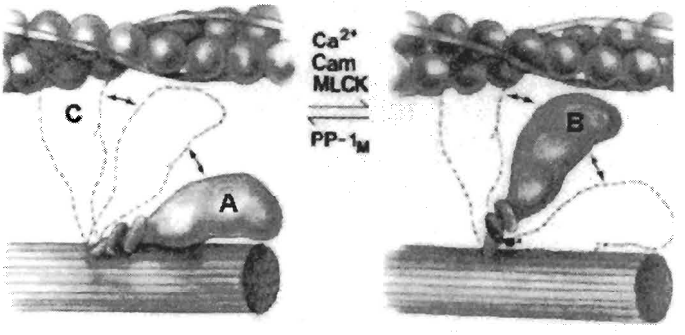

Figure 3. Myosin RLC phosphorylation causes a conformational change in the myosin head domain that improves the opportunity for strong crossbridge binding to the thin filament (Sweeney, et al., 1993).

The implicated functional benefit of this conformational change is that a decrease in the interfilament spacing can improve the capacity to form weakly bound crossbridge interactions with the thin filament. RLC phosphorylation is therefore thought to improve the Ca^{2+} sensitivity of the contractile apparatus by shifting the force-pCa curve to the left. The conformational change associated with phosphorylation is thought to induce a disordered organization of the myosin filament vs. an ordered organization during rest. Yang et al. (1998) used permeabilized rabbit psoas fibres to determine whether decreasing the lattice spacing of the thick and thin filaments could mimic the physiological effects of phosphorylation. The effect of reducing interfilament spacing using osmotic pressure (w/ Dextran) and increasing muscle length (muscle is isovolumetric) substantiated the interaction between interfilament spacing and improved Ca^{2+} sensitivity. However, RLC phosphorylation did not provide any additional contractile benefit to muscles compressed by osmotic pressure or increased length.

2.10.1 Functional Outcomes of RLC Phosphorylation

Isolated mammalian skeletal muscle models of contractility allow researchers to control environmental factors and physiological variables that may confound whole body *in vivo* studies. The most robust of these models uses skinned muscle fibres, which retain an intact myofilament lattice following chemical disruption of the plasma membrane. Persechini et al. (1985) used skinned rabbit psoas fibres to further validate the association between RLC phosphorylation and twitch potentiation. Previous studies had not measured intracellular $[Ca^{2+}]$ as a potential confounding factor causing twitch potentiation; therefore, the authors intended to measure potentiation in phosphorylated muscle with constant $[Ca^{2+}]$. Their results show that at 25°C myosin RLC

phosphorylation has little effect on twitch force at saturating free Ca^{2+} (10μM), although a large effect at 0.6 μM. Maximum shortening velocity was unaffected by RLC phosphorylation indicating cross-bridge detachment rate is also unaltered. The physiological significance of these results is that RLC phosphorylation may only alter contractile performance at free [Ca^{2+}] which are lower than those found during tetanic contractions *in vivo*.

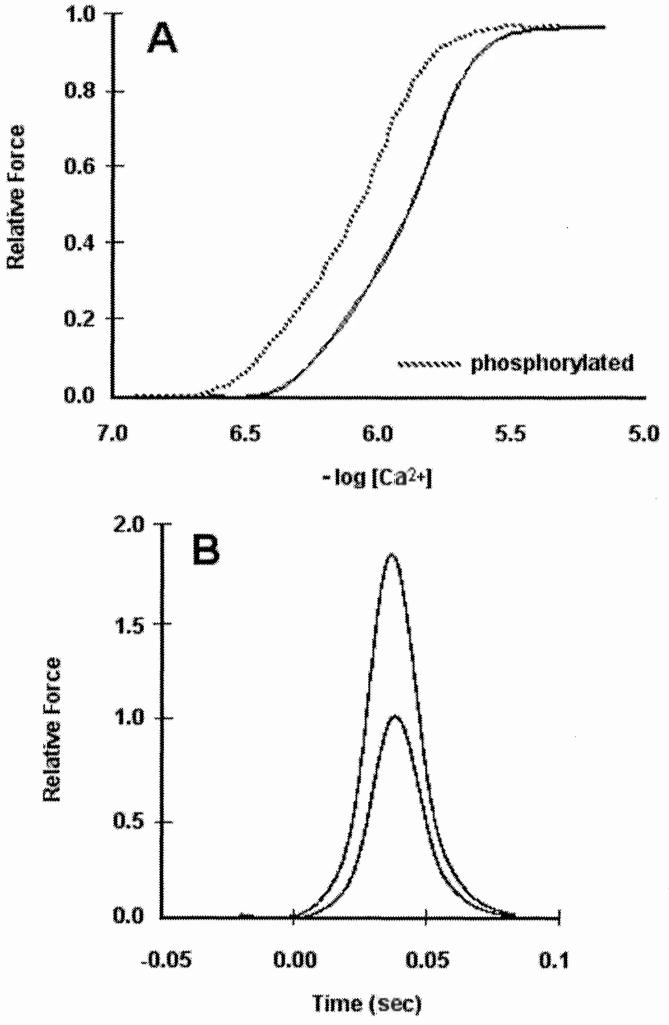

Figure 4. The functional effects of myosin RLC phosphorylation on the force-pCa curve and twitch force potentiation. A) Myosin RLC phosphorylation induces a leftward shift in the force-pCa curve; a change reflecting increased calcium sensitivity (Persechini et al., 1985). B) Posttetanic potentiation following a conditioning stimulus. Twitch force is elevated almost 2-fold due to an increase in apparent rate of crossbridge formation (Zhi et. al., 2005).

Metzger et al. (1989) subsequently designed a series of experiments to further elucidate the role of RLC phosphorylation on crossbridge interactions. Using skinned fibres from rabbit psoas and rat vastus lateralis, the authors explored the rate of force development (+dP/dt) after a step release before and after RLC phosphorylation. Their results indicate that RLC phosphorylation increases the rate of crossbridge attachment at moderate free [Ca^{2+}], an effect that would increase the rate of tension development of a twitch following conditioning activity. In 1990, Sweeney and Stull conducted experiments also using skinned rabbit psoas fibres to further characterize the actin myosin interaction in response to RLC phosphorylation. Their results were analyzed using the two-state crossbridge model first described by Brenner (1988), which classifies the transition between non-force-generating to force-generating states using the forward rate constant of crossbridge formation, $f_{app,}$ and the reverse rate constant g_{app}. The general understanding is that myosin RLC phosphorylation induces a structural modification that repositions the myosin binding domain into a more favorable position, thus facilitating more effective strong crossbridge binding. Accordingly, it is inferred that crossbridge binding can occur sooner and to a greater extent when the myosin RLC is phosphorylated; establishing that myosin RLC phosphorylation augments the rate of force development by an increase in the rate constant f_{app}. Furthermore, the observation that g_{app} is unaffected by this mechanism substantiates the previous finding that RLC phosphorylation does not modulate maximal shortening velocity (Persechini et al., 1985). In summary, the results of skinned fibre experiments provide compelling evidence for improved contractile performance mediated by RLC phosphorylation. The leftward shift of the force-pCa curve during RLC phosphorylation represents both an increased affinity

of the crossbridge to binding sites on the thin filament and a relative increase in the number of strongly bound crossbridges in response to submaximal Ca^{2+} (Persechini et al., 1985). Skinned fibre analysis, however, is not representative of *in vivo* conditions. These observations could be consistent with physiological function *in vivo* but without the experimental control of potentially confounding variables, these conclusions cannot be substantiated. However, these results do serve as a strong theoretical framework from which other models of skeletal muscle potentiation have developed.

Grange, Vandenboom and Houston (Grange et al., 1995; Grange et al., 1998) conducted studies that applied the previous data from skinned fibre experiments to whole muscle (mouse, EDL) function *in vitro* (25°C). EDL muscles phosphorylated using a 20s conditioning stimulus (5Hz) exhibited potentiation of maximal isometric twitch force (13-17%) and rate of force development (9-17%)(Grange et al., 1995). Importantly, all values correlated with a five-fold increase in RLC phosphorylation. The novel finding of potentiated displacement may also suggest a relevant correlation between RLC phosphorylation and whole body movement due to improved work and power (~22%). Studies conducted in 1998 were intended to determine the work and power response to single-twitch stimulations during sine cycles in potentiated mouse EDL. This study was intended to approximate previously documented increases in work and power under conditions that mimic *in vivo* function (i.e. locomotion), where load and velocity may vary as muscle length changes. The results indicated a potentiation of mean concentric work and power (25-50%), isometric twitch force and rate of force development (14%, 12%) with a concomitant increase in RLC phosphate content (~3.7-fold). These data clearly highlight the importance of studying force-potentiation under dynamic conditions

and further reinforce the hypothesis that RLC phosphorylation may be an important mechanism which modulates muscle performance *in vivo*.

2.10.2 Temperature & Length: Modulators of Ca^{2+} Sensitivity

Skinned fibre experiments are highly controllable and reliable however, they are limited by a lack physiological relevance due to the absence of important *in vivo* conditions. The force-pCa curve can be altered by a variety of factors, but most significantly by changes in temperature and length. It is critical, therefore, to consider these factors when describing the physiological importance of RLC phosphorylation *in vivo*. Previous studies (Close & Hoh, 1968; Krarup, 1981; Stein, Gordon, & Shriver, 1982) have highlighted the importance of temperature on muscle twitch contractility, suggesting the following: rate of force relaxation, shortening velocity and extent of tension potentiation decay proportionally with decreasing temperature, while the time course and peak tension are positively correlated to decreasing temperature.

Moore et al. (1990) reported the effects of temperature (25°, 30° and 35° C) on contractile function in mouse EDL muscles. Following a conditioning stimulus (5Hz, 20s) the extent of RLC phosphorylation and peak unpotentiated twitch tension was inversely proportional to temperature. These findings are supported by the concept that at low temperatures Ca^{2+} transients are larger and longer in duration, resulting in a larger activation of skMLCK and the thin filament. Moore et al. also observed more robust tension potentiation, increased rate of decay, and more rapid dephosphorylation as temperature increased. It is clear that the Ca^{2+}-sensitizing effect of RLC phosphorylation is more critical at higher temperatures that correspond to relatively lower [Ca^{2+}] levels. Therefore, previous skinned fibre experiments conducted at 20-25°C may have

underestimated the significance of improved Ca^{2+} sensitivity (RLC phosphorylation) that occurs at physiological temperatures where [Ca^{2+}] handling may be impaired.

To mimic the leftward shift in the force-pCa curve due to RLC phosphorylation Yang et al. (1998) increased muscle length of skinned fibres to decrease interfilament spacing. These methods successfully increased the sensitivity of the myofilament to [Ca^{2+}], but subsequent phosphorylation of the RLC had no additional effect on the force-pCa curve. Similar conclusions have been made in a variety of experiments using rat gastrocnemius *in situ* and isolated mouse EDL fibres *in vitro* (Rassier, Tubman, & MacIntosh, 1997; Rassier, Tubman, & MacIntosh, 1998; Rassier & MacIntosh, 2002). The consensus is that improved Ca^{2+} sensitivity induced by myosin RLC phosphorylation diminishes as muscle length increases due to reduced interfilament spacing. This finding that intracellular Ca^{2+} transients were not altered by length changes in mammalian single fibres (Balnave & Allen, 1996) demonstrates that the reduction in observed potentiation at long muscle lengths is likely attributed to myosin RLC phosphorylation and not some Ca^{2+} effect. An additional study conducted by Rassier and Herzog (2002) revealed the effect of pH on the length dependence of force potentiation. The results of their study indicated that as pH increased (6.6 to 7.8), the length dependence of potentiation was abolished. Therefore, a decrease in pH could attenuate Ca^{2+} sensitivity by competing for thin filament binding domains. Although not discussed by the authors this association may be significant when speculating the benefit of potentiation during fatigue at all muscle lengths, given the decline in pH during intense activity (due to accumulation of H^+ ions).

2.11.0 Coincident Potentiation & Fatigue During Repetitive Stimulation

The idea that skeletal muscle force potentiation occurs in fast twitch muscle to resist fatigue is an attractive concept, yet at present, lacks conclusive evidence. It is clear that the physiological role of RLC phosphorylation is not regulatory, but may modulate contractility enough to be considered performance enhancing. An additional challenge in characterizing this relationship is the highly complex nature of fatigue, which may arise from central nervous failure, peripheral motor unit impairment, or ECC failure in the muscle. The following discussion will attempt to explore the coincidence of potentiation and fatigue by discussing the most significant literature that has addressed this issue.

Vandenboom and Houston conducted a series of studies on fatigued mouse EDL muscle (Vandenboom & Houston, 1996; Vandenboom et al., 1997) at 25°C, to determine the effect of RLC phosphorylation-mediated increases in Ca^{2+} sensitivity on the potentiation of maximal twitch force (P_t) and rate of force development ($+dP/dt$). Initially, the authors elicited muscle fatigue using high frequency tetanic stimulation (400Hz, 150ms) for 120s (Vandenboom & Houston, 1996). After 15s of stimulation, P_t was potentiated ~18% while RLC phosphorylation was increased four-fold. Subsequent P_t measures continued to decline despite elevated RLC phosphate content, suggesting that potentiation was not strong enough to overcome the effects of HFF. During additional experiments, a LFF protocol was used to depress peak tetanic force (P_o) and twitch force (P_t) by ~ 80% and 67%, respectively. Following a conditioning stimulus, myosin RLC phosphorylation and twitch force were elevated above resting values for fatigued muscles (four-fold and 25%, respectively). These results indicated that increased Ca^{2+} sensitivity due to RLC phosphorylation abolishes the declines in twitch force during fatigue

(Vandenboom & Houston, 1996). In 1997, the same authors utilized a variety of experimental protocols to depress peak tetanic force production and stimulate RLC phosphorylation (Vandenboom et al., 1997). Stimulation of the muscles at lower frequencies (2.5-20Hz) increased RLC phosphorylation (0.23-0.82 P-skRLC/Total-skRLC), potentiated twitch force (4-28%) and rate of force development (5-28%). The novel finding from this study was that rate of force development could be augmented during fatigue and that increases were graded to contraction-induced RLC phosphate content.

The previous studies suggest a number of important concepts relating to the potential fatigue resistant properties of RLC phosphorylation and twitch potentiation, summarized below.

- Elevated RLC phosphate content following 120s of repeated tetani suggests that fatigue does not impair the underlying mechanism of twitch potentiation (RLC phosphorylation).
- The increase in P_t was similar during HFF and in non-fatigued muscle, proposing that the effects of RLC phosphorylation on twitch force development may be insensitive to myofibrillar fatigue.
- Twitch potentiation remains a transient phenomenon during the early stages of HFF, suggesting that force-diminishing processes at the myofilaments eventually overcome any benefit of RLC phosphorylation on Ca^{2+} sensitivity.

It is clear that even at the single muscle level, the interaction between fatigue and force potentiation is dynamic and transient. Criticism of these experimental models surrounds the fact that conclusions are based on the single muscle twitch, lacking physiological relevance to actual motor unit firing rates *in vivo*. The role of RLC

phosphorylation in attenuating the decline in P_o during HFF is unknown and has proven difficult to elucidate. Despite this, the exact role of twitch potentiation in fatigue resistance may not be clear until similar HFF protocols are conducted in the absence of RLC phosphorylation (see skMLCK knockout, below).

The coincidence of potentiation and fatigue has been documented by a variety of authors (Rassier & Macintosh, 2000; Rijkelijkhuizen, de Ruiter, Huijing, & de Haan, 2005) who have attempted to characterize the various roles in which RLC phosphorylation may benefit muscular performance. An important distinction between fatigue and potentiation is that each has a vastly different time-course for recovery. Potentiation is an acute phenomenon that dissipates within minutes, whereas fatigue may last for hours (PLFFD). Therefore, the relationship between potentiation and fatigue undoubtedly varies depending on the specific physiological condition of the tissue. For example; at high temperatures increased Ca^{2+} sensitivity due to RLC phosphorylation is more beneficial than at low temperature. However, fatigue may be elevated at high temperatures due to a variety of factors therefore masking this benefit. The relative importance of potentiation during fatigue may depend on the specific effects of any factor that may alter the force-pCa curve or ECC. In addition, the authors suggested it may be beneficial to study the interaction of potentiation and fatigue during incompletely fused tetanic contraction that may be representative of voluntary muscle activation (Rassier & Macintosh, 2000). The significance of this work would be exploring whether force potentiation is evident during repeated stimulation at higher frequencies (i.e., 15-60Hz), giving this effect greater physiological credence as a fatigue resistant property.

The relative importance of potentiation in human muscle performance has been addressed by a number of researchers (Baudry & Duchateau, 2007; Fowles & Green, 2003; Hodgson, Docherty, & Robbins, 2005; Sale, 2002). From a human systemic point of view, potentiation may provide a benefit in muscular performance in a few ways. First, potentiation may elevate submaximal force production so that a given force may be maintained at a lower motor unit firing rate, which may delay the onset of fatigue (see Appendix 5 for schematic). Producing a given submaximal force could potentially require less activation from the central nervous system in the phosphorylated state. This would be a functional outcome of increased Ca^{2+} sensitivity at the cellular level. Second, in the presence of PLFFD, potentiation may restore low-frequency force to near-pre fatigue levels, an effect that may attenuate prolonged ECC impairments or subjective feelings of weakness.

In summary, the integrative study of potentiation and fatigue has produced many questions that remain to be clarified. Whole body research has suggested that although potentiation may be evident during performance, the mechanisms involved are complex and dynamic. In particular, the fact that only type II fibres exhibit force potentiation limits the significance of results found in mixed human muscle studies. Great care must be taken by researchers who assess contractile performance and fatigue processes to account for the effects of potentiation in their results. The coincidence of potentiation and fatigue has clearly been established; however it is now important to further elucidate the role of myosin phosphorylation during various fatigue conditions. These could highlight important dependencies on temperature and the response to various modulators of skeletal muscle contractility (ADP, P_i, H^+, Ca^{2+}).

2.12.0 Recent Advances in the Study of Myosin RLC Phosphorylation

2.12.1 Myosin Light Chain Kinase (skMLCK) Knockout

Emerging technologies that use any type of genetic modification have become the topic of considerable ethical debate. From a scientific research standpoint, however, many of these breakthroughs provide an exceptional model for study. Among these is the concept of gene knockout, which involves the ablation of a specific gene to study a particular phenotypic characteristic associated with it. Geneticists at the Transgenic Core Facility at the University of Texas Southwestern Medical Center have recently developed independent breeds of mice that exhibit different expressions of the enzyme myosin light chain kinase. This advance permits an unprecedented ability to study potentiation in the absence or over-expression of its putative biochemical mechanism, myosin RLC phosphorylation.

Prof. James Stull and colleagues have since used these mice in two noteworthy research studies to substantiate the mechanism of potentiation. Zhi et al. (2005) used skMLCK knockout mice to examine the physiological role of RLC phosphorylation. Their results showed that in isolated EDL muscle from skMLCK knockouts, there is no significant increase in RLC phosphorylation in response to repetitive electrical stimulation. Furthermore, EDL muscles from knockout mice potentiated significantly less than wild type mice in response to a conditioning stimulus. These results confirm that RLC phosphorylation by Ca^{2+}/calmodulin-dependent skMLCK is the primary mechanism for twitch potentiation in fast-twitch skeletal muscle. This study produced two unexpected findings, however. First, knockout mice showed a small amount of RLC phosphorylation located near the serine residue phosphorylated by skMLCK. This

suggests the existence of additional kinases that are capable of phosphorylating the RLC. Alternate possibilities could be that this unknown kinase may be an adaptation to skMLCK knockout or that other isoforms of skMLCK could exist which may phosphorylate the myosin RLC.

The second finding was that knockout mice showed a potentiated force response to staircase stimulation (up to ~30%). The authors suggested that myosin RLC phosphorylation contributes greater to twitch potentiation than staircase in response to low frequency stimulation for long durations. This effect on Ca^{2+} handling may be attributed to calmodulin effects on the dihydropyridine and ryanodine receptors (Zhi et al., 2005). This concept was presented by Rassier & MacIntosh (2000), who suggested that the mechanism for enhancement for staircase and PTP during fatigue might be different. Furthermore, Rassier et al. (1999) noted that staircase might occur in the absence of RLC phosphorylation at low levels of Ca^{2+}. Subsequent research was conducted by Ryder et al. (2007) on transgenic mouse EDL with enhanced skMLCK expression (~22 fold) to determine whether skMLCK or its putative activator Ca^{2+}-calmodulin (CaM) is limiting to twitch potentiation. The transgenic mice showed greater RLC phosphorylation and force potentiation in response to conditioning stimulation than wild type mice. Interestingly, transgenic soleus fibres exhibited significant myosin RLC phosphorylation but no twitch potentiation. This study provided additional evidence that myosin RLC phosphorylation contributes to muscle force potentiation in type IIB fibres but not type IIA or I fibres. Finally, given that the transgenic mouse EDL exhibited greater twitch potentiation than wild type mice, the authors suggested that skMLCK is

limiting and essential to myosin RLC phosphorylation *in vivo* rather than Ca^{2+}-calmodulin (Ryder, Lau, Kamm, & Stull, 2007).

2.12.2 Myosin RLC Phosphorylation as a Contributor to Fatigue

The concept of force potentiation as a mechanism that may counteract myofibrillar fatigue has been questioned in a series of experiments conducted by Dr. R. Cooke and colleagues at the University of California (Franks-Skiba, Lardelli, Goh, & Cooke, 2007; Karatzaferi, Franks-Skiba, & Cooke, 2008). Karatzaferi et al (2008) imitated *in vivo* fatigue conditions by varying the myosin light chain phosphorylation (<10% to >50%); pH (7.0 to 6.2) and phosphate (5mM to 30mM) content of skinned fibre preparations using a temperature jump protocol (5 and 30° C). These authors showed that myosin light chain phosphorylation may act synergistically with increased P_i and decreased pH at 30° C to inhibit shortening velocity of fully activated muscle fibres (~40%.) It is important to note the temperature dependency of this effect, however, as experiments conducted at 10° C did not recapitulate these results. The manner in which temperature influences the intracellular environment during extreme fatigue remains unclear. There are two hypotheses that may explain the mechanism by which RLC phosphorylation may inhibit maximal shortening velocity. The first suggests that as RLC phosphorylation alters the structural configuration of the thick filament, disordered myosin heads can more easily interact weakly with the thin filament. These weak interactions may have a braking effect on the contractile apparatus during activation that may attenuate filament velocity (Karatzaferi et al., 2008). This hypothesis is speculative and furthermore does not include an explanation for its sole existence during conditions with low pH and elevated P_i concentrations. The second gives explanation for altered

kinetics of the actin-myosin interaction by lowered pH, elevated P_i and myosin light chain phosphorylation. The authors discuss an altered affinity for nucleotides may account for slower shortening velocity. Although the sites of phosphorylation and ATP binding are not directly associated with each other spatially, there is a possibility that the two sites may interact biochemically to result in altered contractile properties.

The conclusions reported above represent a novel concept questioning the physiological role of RLC phosphorylation. Is it possible that this biochemical process contributes to fatigue despite the previous body of research touting its existence as a fatigue resistant mechanism? The answer to this question remains equivocal but may partially be explained by the following ideas:

- Extrapolating the physiological relevance of skinned-fibre experiments to whole muscle or *in vivo* contractile function may be problematic. Shortening velocity was limited only under circumstances that may not be considered physiological except under extreme circumstances (6.2 pH, 30mM P_i). It is important, however, that experiments were conducted at 30° C: much closer to physiological temperature than used by other contractile models.
- Although not discussed, the data from Karatzaferi (2008) demonstrate that during all trials where P_i was elevated to 30mM, the addition of myosin phosphorylation increased the force-producing ability in skinned fibres (~4%).

2.12.3 Myosin RLC Phosphorylation & the Energy Cost of Muscular Work

The effect of posttetanic potentiation on muscular work and energy cost in skeletal muscle was studied on *in situ* rat gastrocnemius muscles by Abbate et al. (2001). The purpose of these experiments was to elucidate a clearer understanding of the ecomomy of skeletal muscle contraction in the 'potentiated' state. Contractile

performance was measured during a sequence of 10 submaximal (60Hz) concentric contractions at rest (control) or following a short conditioning stimulus (potentiated). The conditioning stimulus used in these experiments was a sustained maximal tetanic contraction for 1 second (160Hz). Their results demonstrated that total work was potentiated to a greater extent following the conditioning stimulus (vs. the control group), but the relative energy cost of contraction was significantly greater. This finding suggests that energy cost of contraction is increased relatively more than mechanical output when myosin RLC phosphorylation is elevated. It is important to note, however, that the submaximal concentric contractions used to assess contractile performance elevated the myosin RLC phosphate content to the same extent as the conditioning stimulus itself. Therefore, the control group itself was not studied in the absence of myosin RLC phosphorylation. The authors suggested that the increased number of strongly bound crossbridges available for binding in the phosphorylated state could possibly account for a higher rate of ATP turnover during repeated contractions. Furthermore, the addition of each phosphate to the myosin RLC represents an additional energy cost to muscular contraction. The experiments by Abbate et al. (2001) may not completely account for the increased energy cost associated with the 1-second conditioning stimulus, however. More important, the RLC phosphate content and total work output in the control (non-potentiated) group was steadily increasing throughout the 10 concentric contractions, suggesting that these muscles were in a transitional state. These results highlight the numerous methodological concerns and future questions associated with studying myosin RLC phosphorylation. First, the choice of conditioning stimulus utilized to 'potentiate' a muscle is critical. Sustained contractions at high frequencies elevate the myosin RLC

phosphate content to a higher extent while concurrently inducing significant fatigue. The conditioning stimulus employed will therefore only highlight a different 'window' to study the coincidence of potentiation and fatigue. Second, assessing the cost/benefit relation of myosin RLC phosphorylation during muscle work is likely dependent on contraction type and stimulation frequency. For example, is the role of myosin RLC phosphorylation in modulating contractile function more or less important during isometric and/or eccentric contractions? Additionally, is the potentiation of muscle work at 20Hz more or less energy efficient than the 60Hz contractions studied by Abbate et al. (2001)?

It seems plausible that the degree of myosin RLC phosphorylation for optimal mechanical efficiency of muscle contraction is variable and may depend on the type of muscle work being executed. Last, and most importantly, studying the net balance between contractile performance and energy cost establishes the rationale for determining whether myosin RLC phosphorylation truly exhibits fatigue resistant properties during fatigue.

2.12.4 Shortening-Induced Deactivation (SID)

Researchers have explored additional kinetic properties of skeletal muscle that modulate contractile performance. Through influential research by Edman (1975) with single skeletal muscle fibres, it was first observed that active shortening reduces a muscle fibre's ability to produce tension and that this depressant effect increased with the magnitude of shortening. These results suggested that the activation state of the thin filament (and regulatory protein complex) is affected during active shortening, leading to a transitory impairment of force-producing interactions between the thin and thick

filaments. Although the terms relaxation and deactivation may seem interchangeable, they occur in response to distinct mechanisms. Relaxation has been cited as the decline in active force production following muscle activation. It is most often quantified as rate of relaxation and is calculated by finding the ½ relaxation time of the force-time profile. This process is mitigated by the re-sequestration of Ca^{2+} into the sarcoplasmic reticulum and is rate-limited by the activity of the SERCA Ca^{2+}-ATPase pump. Shortening-induced deactivation (SID) refers to the rapid dissociation of Ca^{2+} and myosin crossbridges from the thin filament during active shortening (see below).

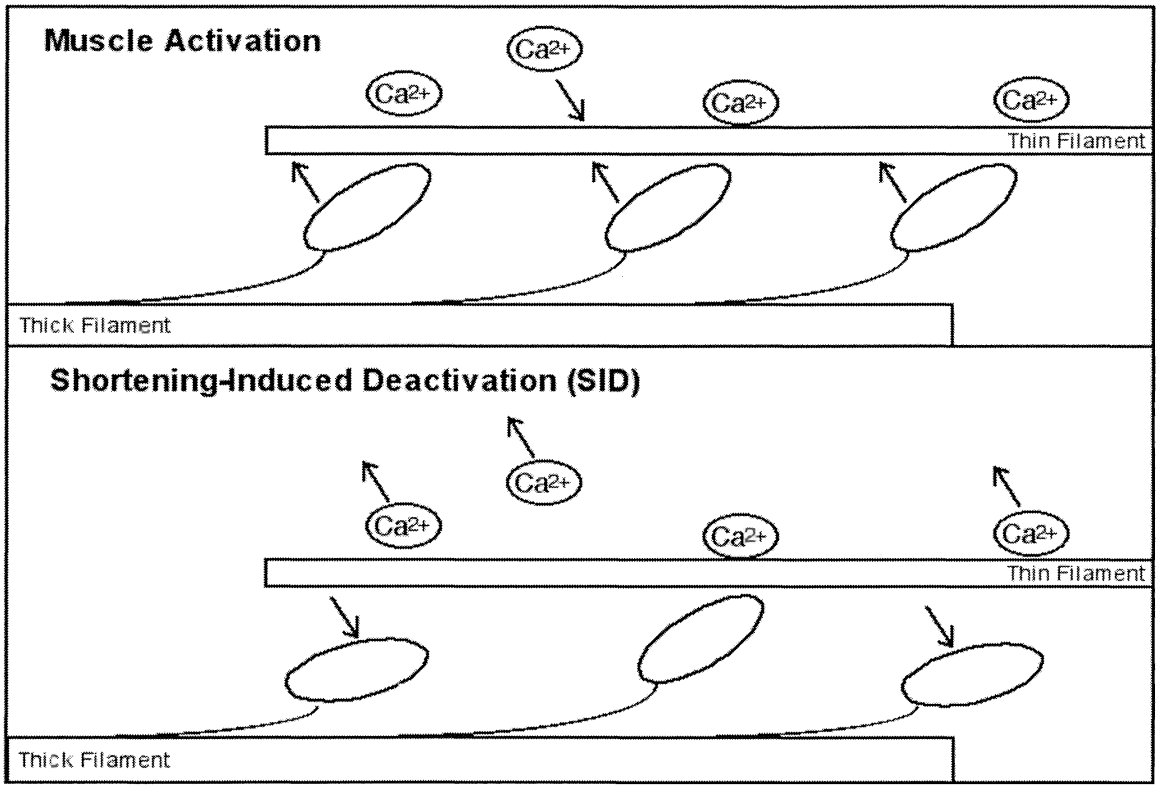

Figure 5. The mechanism of Shortening-Induced Deactivation (SID). Rapid shortening of muscle length during active crossbridge cycling induces the inactivation of the actin filament as both Ca^{2+} and force-producing crossbridges dissociate from their respective binding domains. The extent of this deactivation is observed by a reduction in the subsequent rate of force development following the length shortening, which is governed by the rate at which Ca^{2+} and force-producing crossbridges can rebind to the actin filament. Thin filament deactivation, like activation, relies on both the Ca^{2+} occupancy of the thin filament as well as the number of strongly bound crossbridges (i.e., cooperative binding model). The relative effect of each factor in causing shortening-induced deactivation is presently unknown, however.

As the relative ease to which myosin crossbridges can bind with the actin filament depends on the activation level of the thin-filament regulatory complex, the concept of SID is that the opposite process of deactivation occurs when the muscle undergoes shortening during a muscle contraction, allowing more efficient sliding of the thin filaments and possibly minimizing any negative forces exerted by a population of strongly bound crossbridges. This history-dependent mechanism in skeletal muscle was established as intracellular Ca^{2+} measurements were taken throughout a fused tetanic contraction in which various shortening protocols were induced (Vandenboom, Claflin & Julian, 1998; Jiang & Julian, 1999; Vandenboom, Hannon & Sieck, 2002). Jiang and Julian (1999) observed that intracellular [Ca^{2+}] increased during rapid shortening and this mechanism was more extreme as the speed of shortening and magnitude of shortening increase. Importantly, these experiments established that the acute consequence of SID is the attenuation of the rate of force development (+dP/d*t*) following rapid muscle shortening. SID can therefore be observed by comparing the initial rate of force development during an isometric contraction with the rate of force development following a rapid shortening of muscle length.

There are no reports at present that have specifically explored the effect of myosin RLC phosphorylation on SID. It is understood that SID represents a history-dependent mechanism that transiently decreases contractile performance (Edman, 1996). The rationale for exploring the influence of myosin RLC phosphorylation on SID is to establish whether the mechanism that potentiates rate of force development may also influence thin filament deactivation at various stages of fatigue. Given that muscle function *in vivo* is likely altered by SID during rapid cycles of activation during

concentric and eccentric work, the magnitude of deactivation and its influence on subsequent force redevelopment is of considerable importance to the current study. If total muscle work is determined by the work performed during each cycle of activation and the frequency of activation, SID may improve the ability of a muscle to rapidly deactivate at a small cost to the subsequent contraction (attenuated $+dP/dt$). The balance of these two factors may determine the effect of SID on contractile performance during fatigue.

2.13.0 Contractile Performance During Fatigue: A Brief Overview

The various factors that influence contractile function during repetitive stimulation of skeletal muscle coalesce into a complicated model of peripheral/cellular fatigue. New technologies and models of research used in carefully controlled experiments can progressively be applied to improve the understanding of this model. The following schematic describes the relevant factors that may help determine whether myosin RLC phosphorylation can truly be described as a fatigue-resistant mechanism.

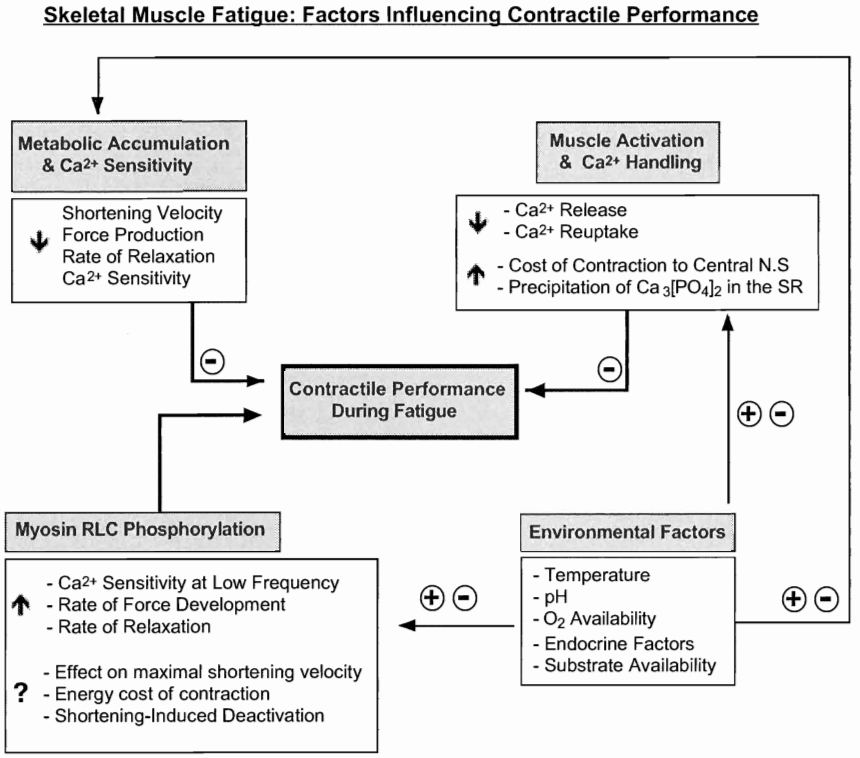

Figure 6. The coincidence of myosin RLC phosphorylation and fatigue is a complicated system of positive and negative influences that modulate contractile performance *in vivo*. Environmental factors are highly dynamic during fatigue and influence all components of the system.

III. STATEMENT OF THE PROBLEM

3.1.0 Central Research Question

Does myosin RLC phosphorylation resist fatigue by maintaining the performance response of the contractile apparatus during repeated activation?

The crucial problem is that fatigue cannot be studied in the absence of myosin RLC phosphorylation, as both occur concurrently during repeated muscle activation. Consequently, the specific physiological role of myosin RLC phosphorylation as a modulator of crossbridge function cannot be revealed until muscle performance during fatigue is studied in its absence.

The proposed study was therefore designed to test whether EDL muscles from skMLCK knockout mice exhibit more fatigue compared to wildtype EDL muscles. Biochemical analysis supplements the investigation of contractile performance by quantifying the myosin RLC phosphate content and accumulation of metabolic byproducts throughout the fatigue protocol.

3.2.0 Hypothesis

EDL muscles from skMLCK knockout mice will exhibit more fatigue in response to repetitive, high frequency stimulation. Low frequency force production will be maintained longer in wildtype muscles during the early stage of fatigue. The manifestation of fatigue in contractile function will be characterized by the analysis of force (P_o and P_t), velocity (V_o), rate of force development ($+dP/dt$), and shortening-induced deactivation (SID). The following observations are expected to result from the current experiments:

1. Myosin light chain kinase (skMLCK) gene ablation is expected to prevent phosphorylation of the myosin RLC in KO muscles in response to all type of stimulation. Predictably, myosin RLC phosphate content in wildtype EDL muscles should increase significantly in response to the repeated muscle activation.
2. WT muscles are expected to display twitch force potentiation following the standard conditioning stimulus and transiently during the early stages of fatigue. This contractile phenomenon is not anticipated in skMLCK knockout muscles, an observation which would be evident by the expected absence of elevated RLC phosphate content.
3. Repeated tetanic contractions during fatigue protocols are expected to depress both peak tetanic force (P_o) and twitch force (P_t) in both WT and KO muscles, although force potentiation is initially expected to protect twitch force degradation in WT muscles.
4. High frequency fatigue is expected to be insensitive to the extent of RLC phosphorylation, as tetanic contractions represent saturating intracellular [Ca^{2+}].
5. Maximal unloaded shortening velocity (V_o) is expected to diminish equally in both groups during fatigue, as end product inhibition and muscle activation impede maximal crossbridge cycling rate. No significant difference in V_o is anticipated between WT and KO muscles, as maximal crossbridge cycling rate should not be altered by myosin RLC phosphorylation (Persechini et al., 1985).
6. Rate of force development (+dP/d*t*) is expected to be elevated in wildtype EDL muscles, as RLC phosphorylation should increase the rate of crossbridge binding.

IV. METHODS

4.1.0 Wild-Type (WT) & skMLCK Knockout (K_o) Mice

Two independent strains of C57BL/6 Mice were acquired from the lab of Dr. James Stull at the University of Texas Southwestern Medical Center at Dallas (Contract ID #800186). The non-dominant coat color allele is spatially associated with the targeted gene for myosin light chain kinase knockout, allowing convenient manipulation of coat phenotype as a marker for each genetic strain. As such, all wild-type (WT) mice are black (homozygous for the recessive non-agouti allele) and all skMLCK knockout (KO) mice are agouti (light brown). Disregarding coat color, there were no clear differences in phenotypic expression between WT and KO animals- including body mass, total muscle length, muscle diameter, and/or absolute peak force-producing capability.

Mice were sent to the Brock University Animal Facility (Animal Care Technician: Dayle Belme) approximately 2 months after date of birth, where they were housed in small groups (1-5) and given free access to standard chow and water until required for experimental procedures. All experiments were approved by the Brock University Animal Care and Use Committee (Protocol #060102).

4.2.0 Experimental Apparatus

All contractile experiments were completed using a custom-designed apparatus capable of accurately controlling muscle length and a variety of environmental factors. The mouse extensor digitorum longus (EDL) muscle was chosen because it is comprised almost entirely of the fast myosin isoforms (63% IIB, 36% IIX, 1% I), that display twitch force potentiation and myosin RLC phosphorylation (Crow, M. T., & Kushmerick, M. J.

(1982a, 1982b). Additionally, the mouse EDL muscle is small enough to ensure that most fibres remain viable by receiving sufficient oxygen and substrates purely through diffusion (Barclay, C.J., 2005). All muscles were suspended in an oxygenated organ bath (Radnoti Glass Technology, Inc) containing a physiological salt solution maintained at constant temperature using an Isotemp 3013S circulator (Fisher Scientific). Muscle stimulation was applied using flanking platinum electrodes driven by a Model 701B biphase stimulator (Aurora Scientific, Inc.). Muscle length and diameter was monitored separately using a horizontal stereo zoom microscope (Bausch & Lomb. Contractile data were collected at 1000Hz from a 305B servomotor acquired through a 604C analog to digital interface, and controlled by a dual-mode lever system (ASI). Data acquisition and basic analysis was performed using ASI 600a software (Version 1.60) and further examined using SigmaStat.

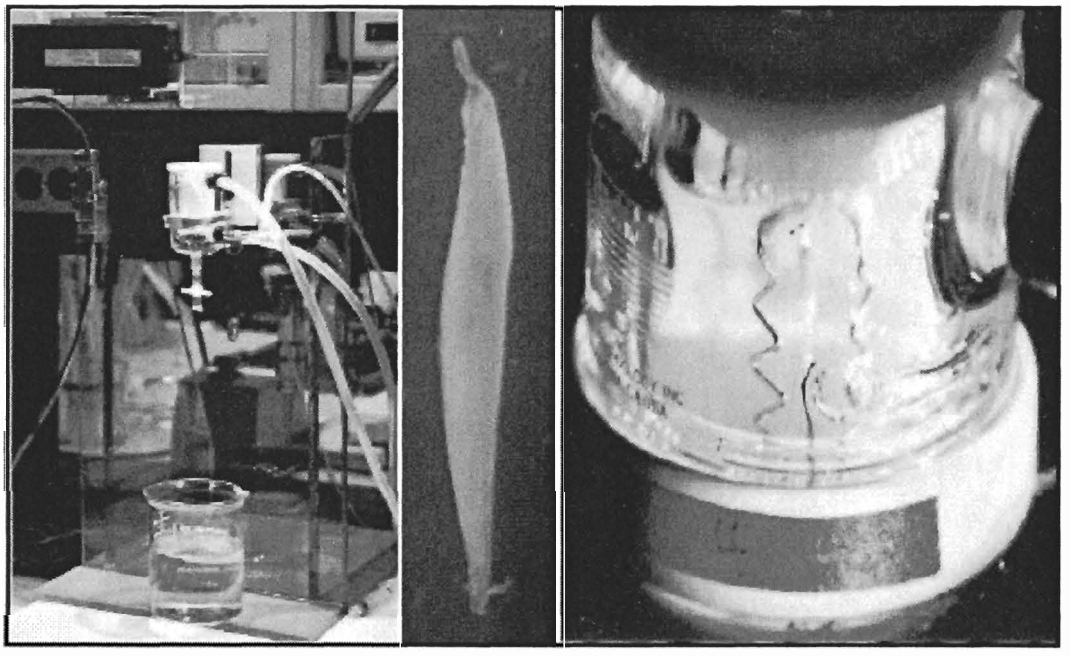

Figure 7. *In vitro* mouse EDL model at 25°C.

4.3.0 Surgical Removal of EDL & Muscle Preparation

Animals were initially sedated with a peritoneal injection of Euthanol diluted 1:10 with saline (0.025mg/g body weight). The EDL was carefully excised from each hind limb after a non-absorbable braided silk (4-0) suture was fastened to the proximal and distal tendons. One EDL was mounted into the experimental apparatus immediately while the other was maintained in an oxygenated dissecting medium on ice (see below for recipe). Following EDL removal, the animals were euthanized by lethal injection of Euthanol into the heart (0.05ml/g body weight) and disposed of according to the established Brock University Animal Facility protocol.

The physiological solution used in all experiments served as a favorable environment for muscle contraction and was intended to provide contracting muscle tissue with the essential substrates and ions present *in vivo*. Final ionic concentrations were (in mM): 121 NaCl, 5 KCl, 24 $NaHCO_3$, 0.4 NaH_2P0_4, 0.5 $MgCl_2$, 1.8 $CaCl_2$, 5.5 D-Glucose, and 0.1 EDTA. The solution was continuously gassed (95% O_2, 5% CO_2) using a scintillated glass dispersion valve (Radnoti) and maintained at 25° C (± 0.05 ° C).

4.4.0 Experimental Design

The isolated EDL *in vitro* model was used for all experiments to elucidate the role of RLC phosphorylation in modulating isometric contractile properties at rest and during fatigue. Two identical sets of experiments were conducted on EDL muscles from WT and KO mice for analysis of: 1) contractile function, and 2) biochemical quantification of muscle metabolites and myosin RLC phosphorylation.

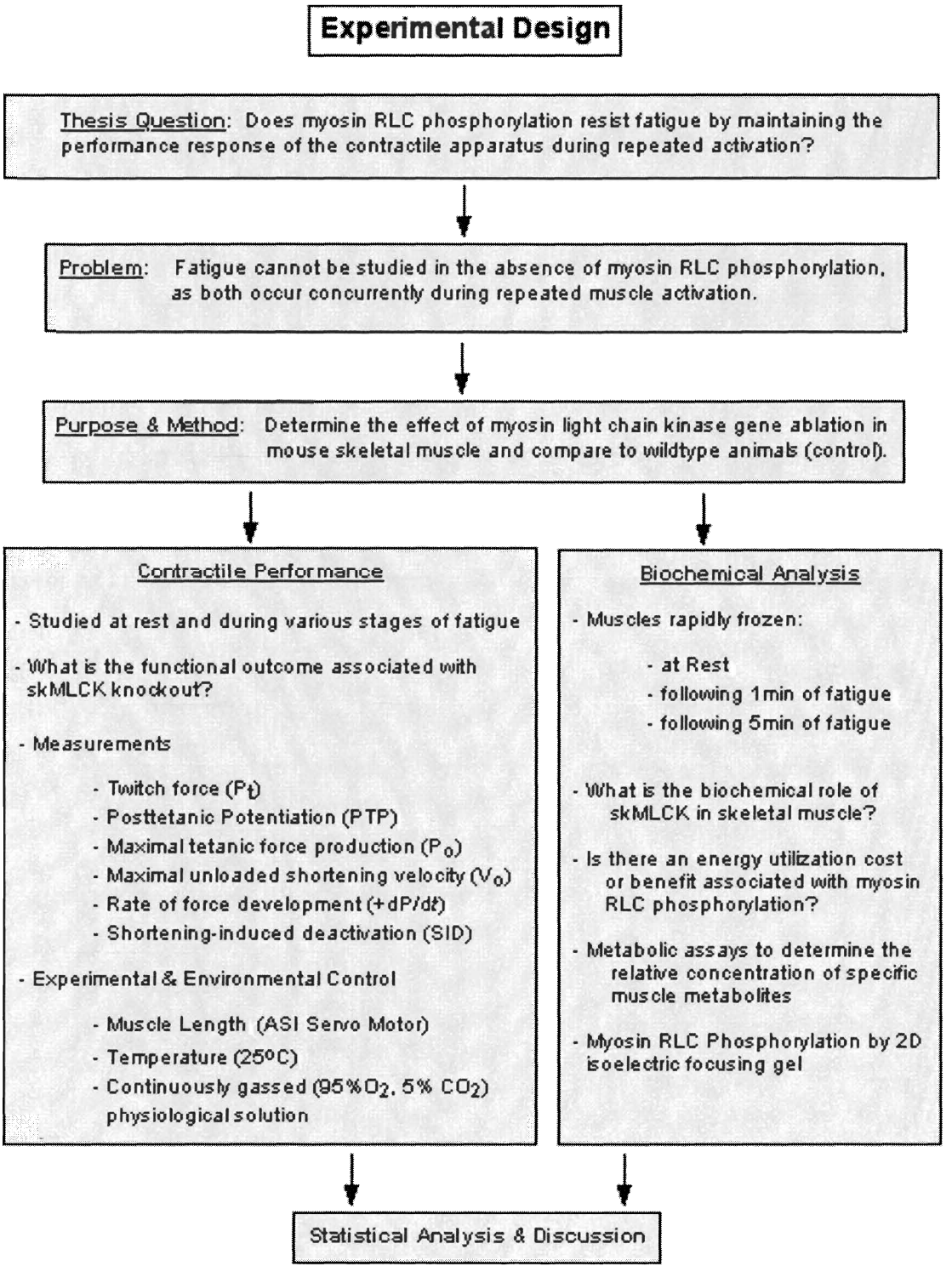

Figure 8. Experimental design flow chart.

As phosphorylation of the regulatory light chain is a contraction-activated process characterized by rapid activation and comparatively slow deactivation, great care was taken in controlling the duty cycle and rest intervals during all experiments. Each set of contractile experiments involved the quantification of posttetanic potentiation and contractile performance during various phases of high frequency fatigue. Contractile data was collected from a total of 12-15 muscles from each group (WT and KO) using identical experimental procedures.

The second set of experiments was conducted to fatigue muscles until specific reference points (Rest, 1min, 5min), when the EDL was rapidly removed from the bath (<10s) and freeze clamped for biochemical analysis. After freezing, each muscle sample was split into two equal halves to be analyzed for muscle metabolites (PCr, Cr, ATP, ADP, P_i, La^-) and myosin RLC phosphorylation. The collective data contained in this study therefore represents an analysis of twitch force modulation by posttetanic potentiation during resting conditions and a more comprehensive account of contractile function and physiological status during various stages of fatigue.

4.5.0 Force & Length Control Measures

4.5.1 Muscle Length & Optimal Length (L_o)

To normalize all force data, optimal muscle length (L_o) was measured during initial force-length measurements (see Preliminary Experimental Procedures). Optimal length (L_o) was defined as the length at which peak active twitch force (P_t) was elicited and was used as the reference length for all shortening amplitudes. Considerable attention was given to the control of muscle length, as the phenomenon of twitch force potentiation is highly length-dependent and may be mimicked on the descending limb of the force-

length curve due to decreased interfilament spacing (Yang et al., 1998). All experiments were therefore conducted at 0.9 L_o and 1.0 L_o to explore the length dependency of force potentiation in both wildtype and skMLCK KO muscles. A shorter muscle length was expected to abolish this length-dependent force potentiation and magnify the difference between wildtype and skMLCK knockout muscles.

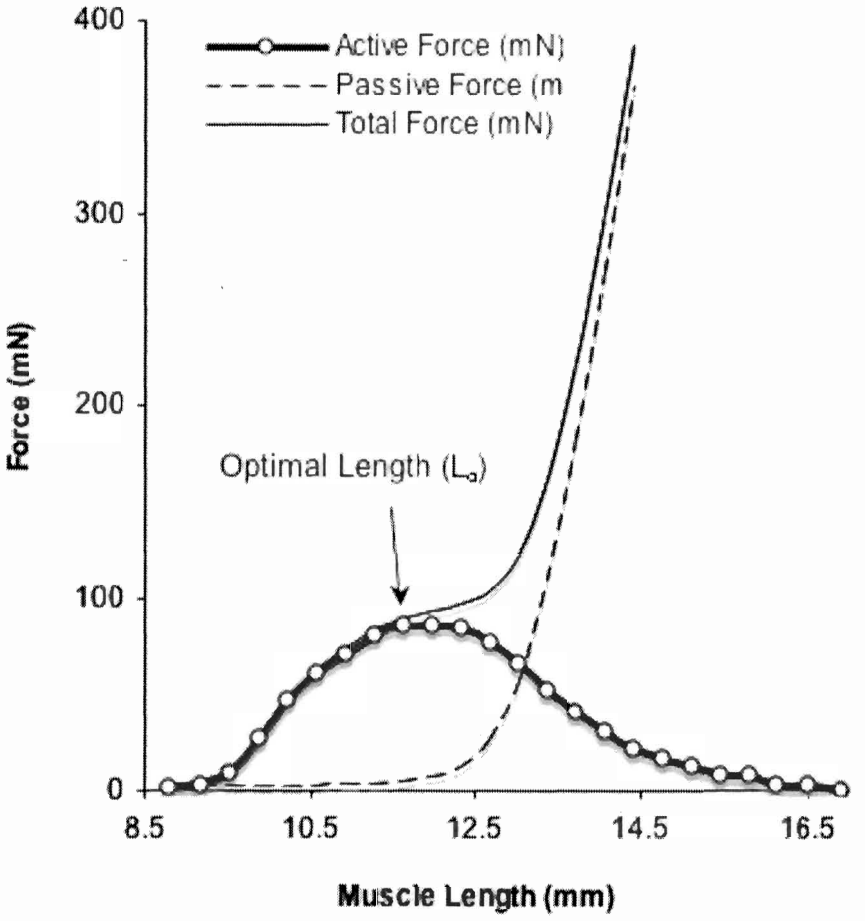

Figure 9. Example of a force-length relationship in a mouse EDL muscle. Optimal length (L_o) was determined as the length at which peak active force was reached. This data was collected from one Wildtype EDL muscle during the present study.

4.5.2 Determination of Reference Twitch (P_t) & Tetanic (P_o) Force Values

Central to the calculation of relative measures such as force potentiation and fatigue is the determination of a representative control contraction to serve as a reference. In the 60 seconds prior to each potentiation and fatigue protocol, a reference twitch value was calculated from the average active force (total tension- resting tension) of at least five reference twitches. The initial tetanic contraction of each fatigue protocol was used as the reference force (P_o) for quantification of high frequency fatigue. These reference force values were also used to compare the absolute tetanic and twitch force created in WT and KO muscles.

4.5.3 Twitch Pacing

It was necessary to continuously monitor contractile function throughout each protocol to assess tissue viability. To this end a single muscle twitch was elicited at 0.05Hz during all periods of quiescence, a method termed twitch pacing. Muscle twitches in isolation have negligible influence on RLC phosphorylation (Klug et al. 1982) and fatigue, but are included: a) to track the decay of twitch potentiation, and b) as a marker for any changes in the physiological state of the EDL preparation (i.e. hypoxia).

4.6.0 EDL Stimulation

Five pre-programmed stimuli were used to excite the EDL preparations during all contractile experiments. All were applied at supramaximal voltage to ensure that all motor units were fully activated. For tetanic contractions, 150Hz stimulation represents a supramaximal motor-unit firing rate to ensure completely fused tetani. Stimulation S2 was used for tetanic contractions during each slack test to allow an adequate force

regeneration period following rapid muscle shortening. The conditioning stimulus for the potentiation protocol was intended to maximize RLC phosphorylation while simultaneously minimizing fatigue.

4.6.1 Stimulation Profiles

- S1. Standard Tetanic Contraction → 1000ms at 150Hz
- S2. Tetanic Contraction [for Slack Test] → 1500ms at 150Hz
- S3. Single Muscle Twitch → 1Hz
- S4. Conditioning Stimulus → 150Hz, 400ms, 0.2Hz, 20s

4.7.0 Mechanical Data Collection

4.7.1 Peak Force Production

Peak force was defined as the highest or maximal tension produced in response to a given twitch (P_t) or tetanic (P_o) stimulation, measured in mN. As the shape of tetanic force production varied with changing physiological conditions of the muscle (rest vs. fatigue), this analysis did not differentiate at which point during a contraction the peak force occurred.

4.7.2 Maximal Rate of Force Development (+dP/dt)

The relative rate of force development was measured during the first contraction of each slack test (Rest, 1min, 5min), before and after a length step of 20% L_o (1.1 L_o to 0.9 L_o). The initial rise in force was used to compare the maximal rate of force development between WT and KO groups, while the rate of force development following the 20% L_o was utilized for calculation of SID. These values were determined using the ASI 600a software package, which plots a rate function of instantaneous values of +dP/d*t* following smoothing using a Savitsky-Golay Filter. Maximal +dP/d*t* was calculated as the instantaneous rate of force development at the point when tetanic force has reached

20% of maximum force. This approach was chosen as an objective method for quantifying a relative +dP/d*t* value, permitting effective comparison between muscles and to eliminate highly variable absolute values.

4.7.3 Slack Test for Maximal Unloaded Shortening Velocity (V_o)

The Slack Test (Edman, 1979) was used as an indicator of the maximally capacity to shorten the contractile apparatus during rest and fatigue conditions. Slack was briefly produced in the EDL preparation by rapidly shortening muscle length to a pre-determined position during a fused tetanic contraction. The time required for a contracting EDL to actively take up the compliance (slack) and produce measurable force was termed the slack time. It has been shown (Edman, 1979) that the size of the length step is positively correlated with slack time in a robust linear relationship (see below).

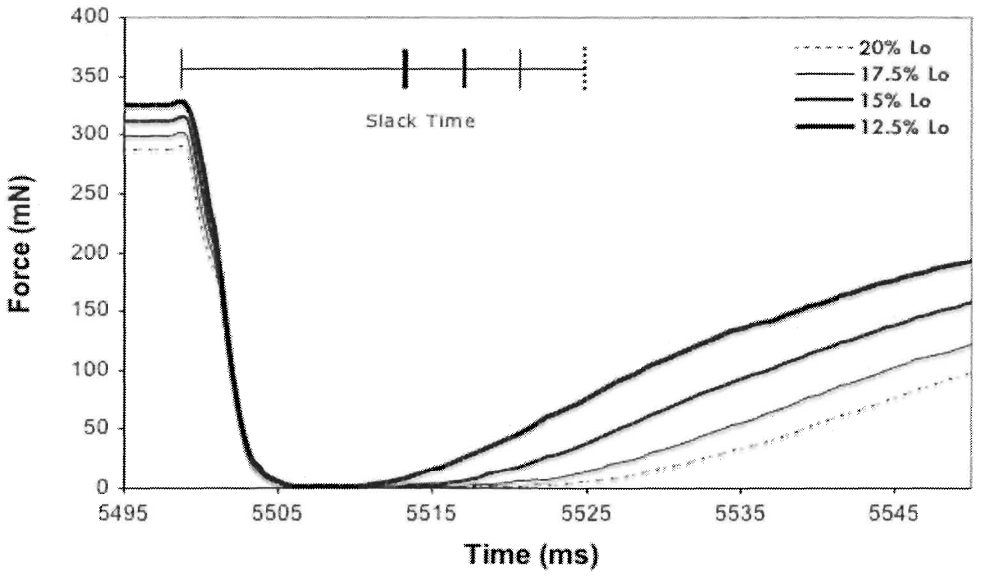

Figure 10. Force redevelopment traces of 4 tetanic contractions during the slack test to illustrate the positive correlation between step size and slack time.

Given that step size (% L_o) is a quantifiable distance (mm) and slack time (ms) is a measure of time, the slope of the linear regression represents a velocity (distance/time). Therefore at each time point, for each individual muscle, the appropriate step sizes were graphed against slack time to obtain measures of V_o and were pooled within group to create mean V_o values. Five length steps were applied during sequential tetanic contractions (10, 12.5, 15. 17.5. 20 % L_o) to create a strong linear relationship ($\geq$0.99). Slack time was determined using a calculation-based method due to the difficult nature of discerning the exact moment of force redevelopment. This calculation involved differentiation of the force-time function and subsequent quantification of 20% of the peak rate of force development (+dP/d*t*). The time that corresponded to 20% of peak +dP/d*t* was subtracted from the time at which the length step was initiated to calculate slack time (see below).

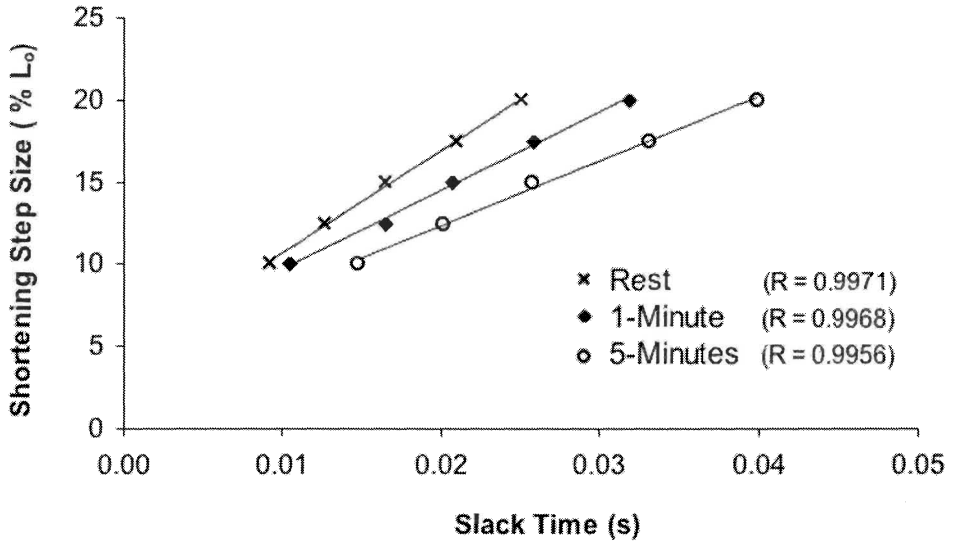

Figure 11. Example plot for quantification of maximal unloaded shortening velocity (V_o). Mean slack times from the current study (n=10) were graphed against the five shortening steps used during the slack test (10, 12.5, 15, 17.5, and 20%L_o). Throughout fatigue, muscles exhibited significantly larger slack times for a given step size, effectively decreasing the slope of the linear regression. The slope of each line was used to calculate V_o at each time point, as it represents a distance (%L_o) divided by time (s) (i.e., velocity = distance/time).

The slack test was manipulated to control for the opposing processes of fatigue and recovery, to ensure that the physiological status of the muscle remained relatively stable across each of the five sequential tetanic contractions. This was accomplished by varying the rest period between each successive contraction. This rest period was intended to stabilize the status of high frequency fatigue in the EDL (% P_o), while presenting a duty cycle that would limit the extent of force recovery between contractions. The slack test was initially applied during a quiescent period (Rest), following 60-seconds of fatiguing contractions (1min fatigue), and in the fatigued state following the full five minutes of repetitive stimulation (5min fatigue). Slack test data was collected from a total of 20 EDL muscles (10 WT, 10 KO) and provides a clear indication of whether myosin RLC phosphorylation influences how fast the actual molecular machinery (myosin crossbridge) can cycle along the thin filament against zero external load (slack).

4.7.4 Shortening-Induced Deactivation (SID)

Shortening-induced deactivation (SID) was quantified in WT and KO muscles during the first contraction of each slack test (Rest, 1min, 5min). The rapid length step (20% L_o) was applied once the muscle had reached maximal isometric force. A ratio was calculated using the rate of force development measurements taken during the initial rise in force and following the 20% L_o length step during force redevelopment.

$$[+dP/dt_{Post\text{-}length\ step}] \ / \ [+dP/dt_{Pre\text{-}length\ step}] = SID$$

The 20% L_o length step was chosen for analysis of SID for two reasons:

- The 20% L_o length step was the largest length step implemented during the slack test protocol. As SID has been shown to increase as the magnitude of shortening increases, this was assumed to magnify a potential difference between groups (should one exist).
- Comparison of +dP/d*t* before and after a length step may be problematic because myofilament overlap at the shortened length could change significantly, thus influencing the results. The 20% L_o length step was initialized at 1.1 L_o and reduced muscle length to 0.9 L_o. As both pre and post length step values are approximately equidistant from optimal length (~0.1 L_o), this length step was assumed to minimize the significance of force-length variations.

4.8.0 Contractile Experiments

4.8.1 Laboratory Procedures

Prior to a standard 20-minute equilibration period, the EDL was stimulated (150Hz, 1000ms) to produce a contraction forceful enough to remove any compliance and possible slippage of the tendon-suture unions. Subsequently, a single twitch was applied at 0.05Hz while sequentially increasing current intensity until a maximum twitch force was reached. The stimulus intensity was then increased ~25% and remained at this magnitude for the duration of each experiment to ensure maximal excitation of all motor units. Following the equilibration period, the optimal length (L_o) was determined. Initially, L_o was estimated by stretching the muscle to 10mN of passive tension; a value that generally corresponded to peak active force production in previous experiments. This initial muscle length became the temporary L_o for the optimal length protocol. From ~0.7L_o the muscle was lengthened at 0.02 L_o increments while being stimulated at each length. The muscle length at which active twitch force reached a maximum was

documented as L_o and used as the reference length for all subsequent length steps. The accuracy of all length changes and positions was corroborated manually using a stereo zoom microscope (Bausch & Lomb) to provide measurements of muscle length (mm).

Following these standard preliminary procedures, a contractile experiment was conducted. Each experiment was officially terminated when the EDL was rapidly frozen in liquid nitrogen and stored at -80° C for future biochemical analysis. Prior to the mounting of each fresh EDL muscle, the Tyrode solution was replaced with a fresh aliquot and given sufficient time to equilibrate (~15min).

4.8.2 Quantifying Posttetanic Potentiation (PTP)

The PTP protocol was designed to examine the hypothesis that only EDL muscles from WT mice would exhibit potentiated twitch force in response to a conditioning stimulus (vs. EDL muscles from skMLCK KO). Each muscle was tested for force potentiation at 2 muscle lengths (L_o and 0.9 L_o) to explore the expected length-dependency of force potentiation. After collecting a reference twitch value at each length (L_o and 0.9 L_o) and applying the standard conditioning stimulus, twitch force was measured at 9, 11, 13, 17, 19 and 21-seconds (following cessation of the conditioning stimulus). Muscle length was shortened from L_o to 0.9 L_o 15-seconds following the conditioning stimulus, ensuring that three twitches were available for analysis at each muscle length. The order of length changes within the protocol was reversed for at least five muscles per group to remove a potential order effect, where measured PTP would be insensitive to the process of lengthening and shortening. The twitches collected before and after the length change were designed to be equidistant to the 15-second time point-the instant at which pilot experiments exhibited maximal twitch potentiation.

4.8.3 High Frequency Fatigue and Unloaded Shortening Velocity

The objective of these experiments was to collect a variety of contractile data during a fatigue protocol. Slack Tests were conducted before; during, and following a 5-minute fatigue protocol to measure unloaded shortening velocity (V_o) in a variety of physiological conditions (rest, moderate fatigue, severe fatigue). Muscle length remained constant throughout the standard fatigue protocol, at 0.9 L_o. During each period of fatiguing contractions the EDL muscle received one tetanic (S1) and one twitch (S3) stimulus every 5 seconds (0.2Hz). At the conclusion of each contractile experiment, the protocol was terminated by rapidly freeze-clamping the muscle with pre-cooled pliers. Muscles samples were then stored at -80° C until biochemical analysis. Figure 12 illustrates the timeline and design of all experimental protocols.

Figure 12. Schematic of contractile experiments. Separate groups of muscles were frozen prior to (Rest), during (1Min), & following (5Min) repetitive stimulation.

4.9.0 Biochemical Analysis of Muscle Tissue

4.9.1 Quantifying Metabolic Conditions During Fatigue

The purpose of the second set of experiments was to freeze muscles at specific time points for quantification of muscle metabolites. Measurement of metabolic byproducts during fatigue was intended to establish the relative cost (or benefit) of myosin RLC phosphorylation during repetitive stimulation. The procedure of the contractile experiments was precisely replicated until premature termination by rapid freezing of the EDL (parallel incubations). Muscles were frozen prior to any fatiguing contractions (Rest), following 1min of fatigue (moderate fatigue), and following all contractile protocols.

The variability of data associated with running metabolic assays with very small muscle samples ($\leq$1mg. dry weight^{-1}) is inescapably high. It was necessary, therefore, to pool muscle samples to improve the reliability of the data. In these cases, freeze-dried muscle tissue was combined from two samples (matched for group and time point) during the extraction procedure. This method increased the mass of muscle sample available for extraction and was utilized to remove some of the experimental error associated with weighing and extracting the muscles.

Three specific assays were used to identify the relative concentration of the metabolites of interest (ATP-PCr, Cr, La^-). Concentrations of ADP and inorganic phosphate (P_i) were calculated from known K_{eq} values and delta-PCr, respectively. Raw metabolite concentrations were normalized for mean total creatine content. For detailed procedures of muscle extraction, metabolite assays, and calculation for ADP and inorganic phosphate (P_i) please refer to appendix 2 and 3.

4.9.2 Myosin RLC Phosphorylation

Mouse EDL muscles were frozen prior to, during, and following 5-minutes of repetitive stimulation. Myosin RLC phosphate content was quantified using 2 dimensional-isoelectric focusing. Muscle samples were ~4-6mg (dry weight).

4.10.0 Data Analysis & Statistics

The central intervention investigated was the effect of skMLCK KO on contractile performance at rest and during fatigue. Measurement of muscle metabolites and myosin RLC phosphorylation provided additional data to compare WT and KO muscle performance at rest and during fatigue. To determine the effect of skMLCK knockout (WT vs. KO) and treatment (i.e., time, length), a significant difference between means was determined using a two-way ANOVA. For the analysis of contractile data, a repeated measures ANOVA was used. Metabolic analysis was completed with a standard two-way ANOVA, as each muscle sample was assayed only once for a given metabolite.

Given a significant interaction between group and treatment, Post-hoc analysis was completed using Tukey's HSD test. All data are presented as the sampled mean +/- SEM. For comparison of mean mouse age and absolute force production, a two-tailed Student's t-test was performed.

V. RESULTS

5.1.0 Myosin RLC Phosphorylation

Myosin RLC phosphate content was quantified as the proportion of RLC molecules in the phosphorylated state versus total myosin (P-skRLC/Total skRLC). Muscles from KO mice exhibited low myosin RLC phosphorylation at rest, and were not influenced by repetitive stimulation for the duration of the fatigue protocol (see Table 1). WT myosin RLC phosphorylation was significantly higher at all time points when compared to KO muscles ($p<0.001$). Myosin RLC phosphate content increased significantly during the first minute of the fatigue protocol, rapidly reaching maximal phosphorylation (0.63 ± 0.03). The remaining 4 minutes of repetitive stimulation did not significantly influence myosin RLC phosphorylation, although the myosin RLC was phosphorylated to a lesser degree at 5-minutes (0.57 ± 0.02 P-skRLC/Total-skRLC).

Group	Rest	1min	5min
WT	0.39 ± 0.05 *	0.63 ± 0.03 *†	0.57 ± 0.02 *†
KO	0.08 ± 0.02	0.07 ± 0.01	0.07 ± 0.02

Table 1. Summary of myosin RLC phosphate content in WT and KO muscles prior to, during and following 5-minutes of fatiguing contractions (n=5-8). Myosin RLC phosphorylation is quantified as the ratio of phosphorylated myosin to total myosin content (P-skRLC/Total-skRLC). (*) Significant difference between groups (within time point, $p<0.001$). (†) Significant difference from Rest value (within group analysis, $p<0.001$).

5.2.0 Mouse Characteristics

No significant difference was found between WT and KO groups for mean mouse age, peak tetanic force (P_o), or peak twitch force (P_t) in the contractile experiments. The mean age of WT mice used in the biochemical analysis experiments was significantly lower than mean KO mouse age (92.5 ± 1.1 vs. 152.0 ± 5.5 days). In addition, the mice used in the contractile experiments were significantly older than those used for the muscle freezing experiments ($p<0.01$). It is unclear whether this average difference in age (~160 days) would influence contractile performance or muscle phenotypic expression. For the present discussion, it is assumed that age did not influence the structure or function of the EDL muscles enough to significantly alter myosin RLC phosphorylation or metabolic accumulation.

Absolute (mN) and Relative (mN/mm) Baseline Force Values				
Group	Tetanic Force (P_o)		Twitch Force (P_t)	
	Absolute	Normalized	Absolute	Normalized
WT	269.2 ± 40.5	122.9 ± 16.7	56.1 ± 12.7	22.4 ± 4.1
KO	302.3 ± 29.5	122.5 ± 11.8	40.6 ± 4.9	17.8 ± 2.2

Mean Mouse Age (days)		
Group	Contractile Experiments	Biochemical Analysis Experiments
WT	277.9 ± 36.5	92.5 ± 1.1 < *
KO	302.3 ± 29.5	152.9 ± 5.5

Table 2. Mean mouse age and baseline force values for individual muscles used in the contractile experiments (n=12) and mean age for muscles frozen for biochemical analysis (n=20-24). Data are presented as mean ± SEM. (*) Significant difference between mean age of WT vs. KO mice in biochemical analysis experiments (Student's t-test, $p<0.05$). Force is normalized to muscle diameter (mm), which was measured at L_o prior to each contractile experiment using a stereo zoom microscope. This is not a true evaluation of muscle specific force, as cross-sectional area was not measured.

5.3.0 Posttetanic Potentiation (PTP) & Muscle Length

Analysis of posttetanic potentiation (PTP) established a main effect for muscle length (0.9 L_o vs. 1.0 L_o) and group (WT vs. KO), and a significant positive interaction between group and treatment ($p<0.001$). KO muscles did not exhibit any force potentiation, as mean PTP was 2.5 ± 0.02% and 1.2 ± 0.02% for 1.0 L_o and 0.9 L_o, respectively. WT muscles potentiated significantly more at both 0.9 L_o than 1.0 L_o ($p<0.001$). Twitch force in WT muscles was potentiated 37.2 ± 0.04% at 0.9 L_o and 12.5 ± 0.01% at 1.0 L_o.

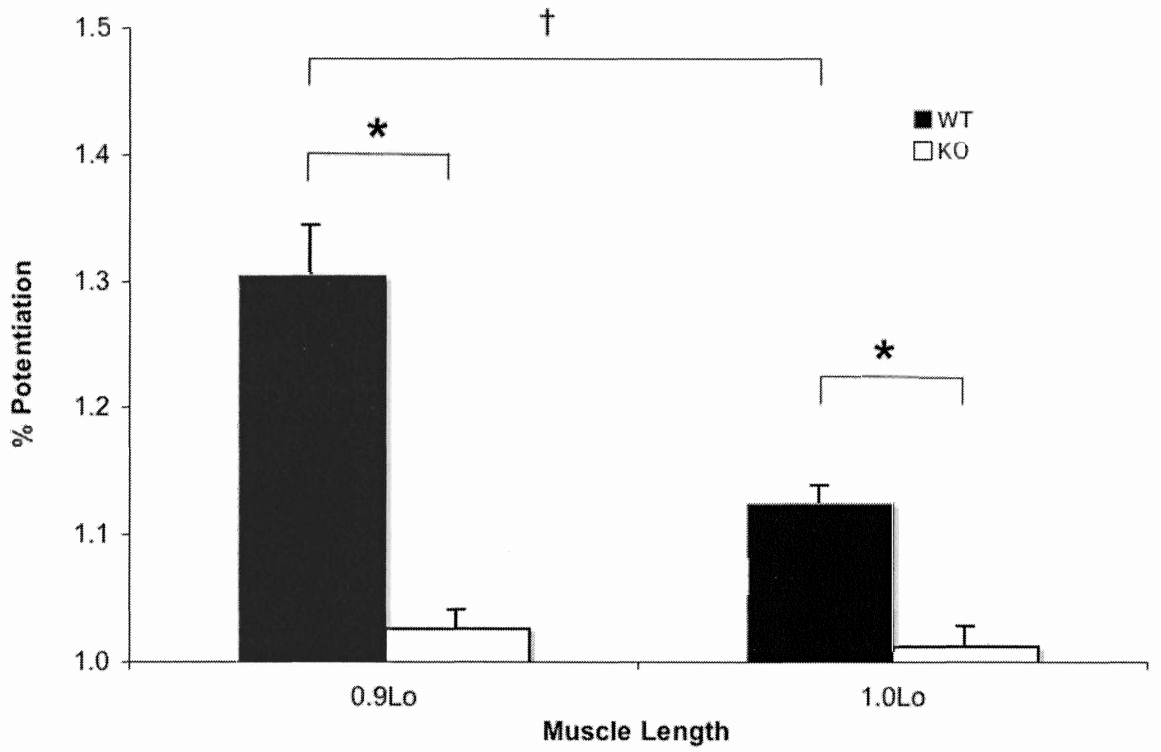

Figure 13. The effect of length on Posttetanic Potentiation (PTP) at rest (n=15). (*) Significant difference between groups within a given muscle length ($p<0.001$). (†) Significant effect of length on PTP in WT muscles (within group analysis, $p<0.001$).

5.4.0 Twitch (P_t) & Tetanic (P_o) Force Production During Fatigue

5.4.1 Low Frequency Force Modulation

Low frequency force production was measured every 5-seconds throughout the 5-minute fatigue protocol (Figure 14). Statistical comparison between WT and KO twitch force was completed only for the first minute of the fatigue protocol. The relative difference in P_t between WT and KO muscles during the remainder of the fatigue protocol (1-5minutes) was clearly minimal and was therefore excluded from statistical analysis so as not to obscure the acute group and time interaction (0-35 seconds).

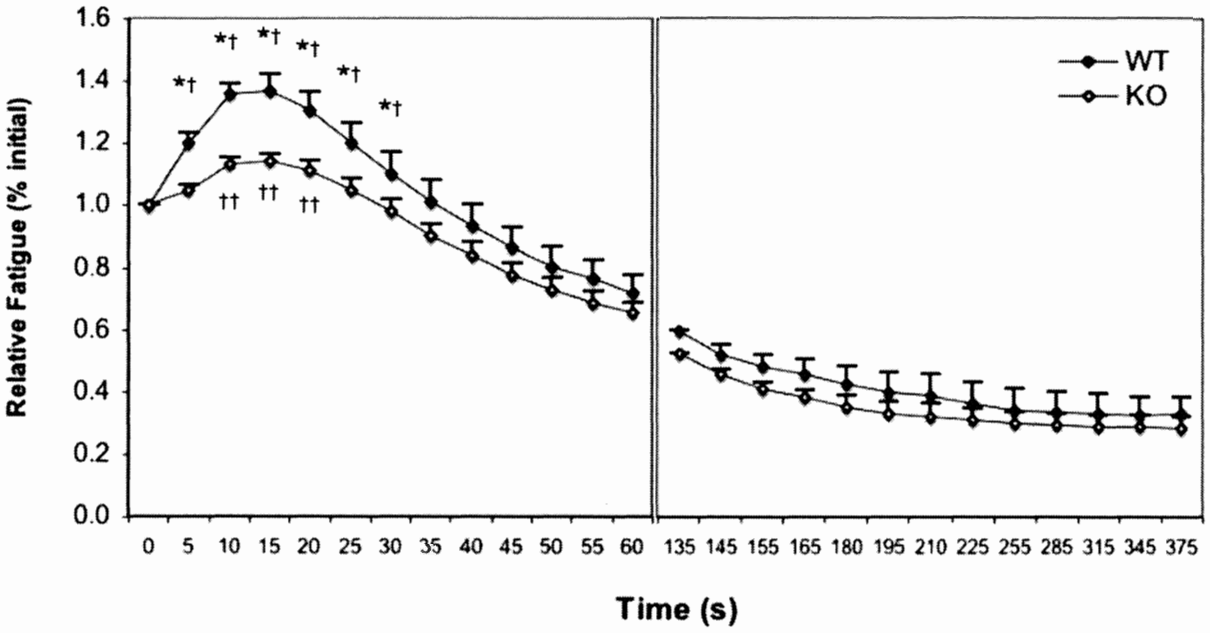

Figure 14. Relative twitch force (P_t) during fatigue (n=12). The fatigue protocol was suspended from 60s until 135s for measurement of unloaded shortening velocity (n=12). (*) Significant difference in relative twitch force between groups. (†) WT twitch force potentiated above baseline twitch force. (††) KO twitch force potentiated above baseline twitch force.

The analysis of twitch forces during fatigue yielded a significant main effect for group and time ($p=0.02$ and $p<0.001$) and a significant interaction between group and time ($p<0.001$). The five minutes of repetitive stimulation reduced twitch force to ~75% in both WT and KO muscles. WT muscles exhibited significantly greater twitch force than KO muscles during the first 35-seconds of the fatigue protocol. Interestingly, both WT and KO muscles exhibited significant force potentiation above the reference twitch (although to a different extent). Within group analysis revealed that WT twitch force was significantly potentiated above the reference twitch value for the first 30-seconds of the fatigue protocol, peaking at 15-seconds (37.2 ± 0.05%). Alternatively, KO twitch force was significantly potentiated above the reference twitch value for a brief time (10-20 seconds of the fatigue protocol). KO twitch force potentiation also peaked at 15-seconds at 14.3 ± 0.02%. There was no significant difference in twitch force between groups for the 1-5 minute component of the fatigue protocol.

5.4.2 High Frequency Fatigue

Five minutes of repetitive, high frequency stimulation depressed maximal tetanic force production in WT and KO muscles equally. There was no significant difference in relative tetanic force (% initial) between WT and KO muscles during any individual time point, despite very low within-group variability (SEM). Statistical analysis produced a main effect for time ($p<0.001$), as mean tetanic force production declined ~90% in both WT and KO muscles. The largest proportion of this force degradation occurred during the first minute of stimulation as tetanic forces declined to ~40% of initial.

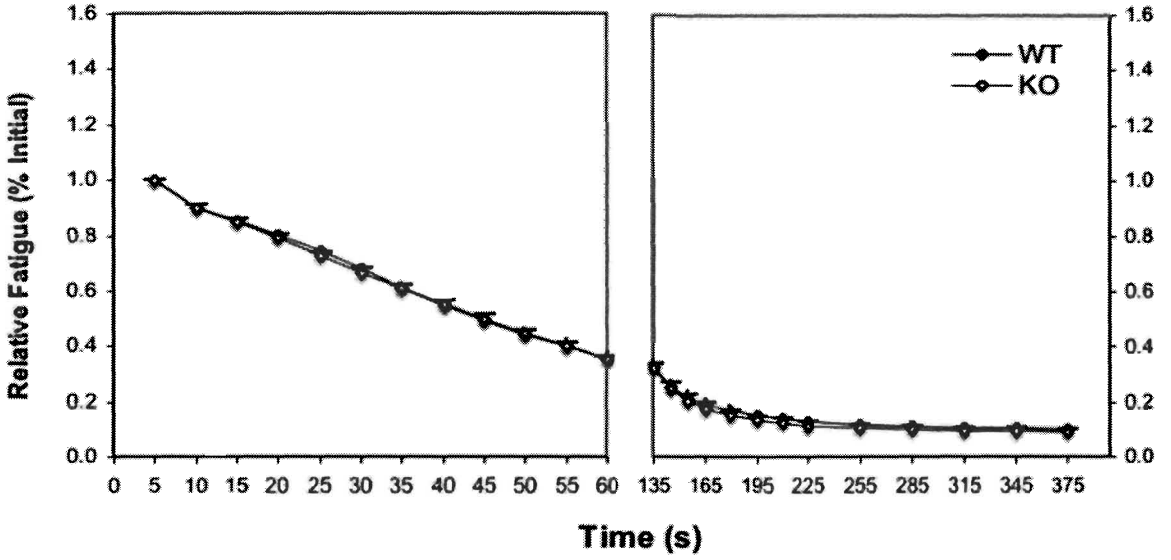

Figure 15. Tetanic force (P_o) degradation during 5-minutes of repetitive stimulation. The fatigue protocol was paused from 60s until 135s for measurement of unloaded shortening velocity (V_o) (n=12). Both WT and KO muscles were slightly more fatigued after the measurement of V_o at 1-minute (≤7%), although this effect was not different between groups.

5.5.0 Maximal Unloaded Shortening Velocity (V_o)

The intrinsic capacity to shorten the contractile apparatus (slack test) was assessed prior to (Rest), during (1min), and following (5min) the 5-minute fatigue protocol (Figure 16 & 17). WT muscles exhibited a slightly higher absolute V_o value at all time points, although the difference between means was not statistically significant ($p=0.304$). There was a significant main effect for time as V_o decreased significantly during the fatigue protocol ($p<0.001$). Repetitive stimulation depressed shortening velocity ~20% within the first minute and a further 15% during the remaining period of fatiguing contractions (1-5 minutes). WT shortening velocity decreased from 14.96 ± 0.78 fibre lengths/s (Rest) to 11.56 ± 0.59 at 1-minute, further degrading to 9.60 ± 0.57 at the cessation of the fatigue protocol. Analysis of KO muscles demonstrated that resting V_o (13.95 ± 1.07) was reduced to 10.53 ± 0.62 at 1-minute before diminishing to 8.39 ± 0.36 at 5-minutes.

The relative degradation of shortening velocity during fatigue was compared between groups, although no significant group effects were found when WT and KO means were compared (Figure 18). As with the absolute V_o values, the relative degradation of shortening velocity demonstrated a significant main effect for time ($p<0.001$). Both absolute and relative comparisons demonstrated that the majority of the degradation of V_o occurred during the first minute of repetitive stimulation. This was evident from the absence of a significant difference between 1min and 5min time points for absolute and relative pooled means.

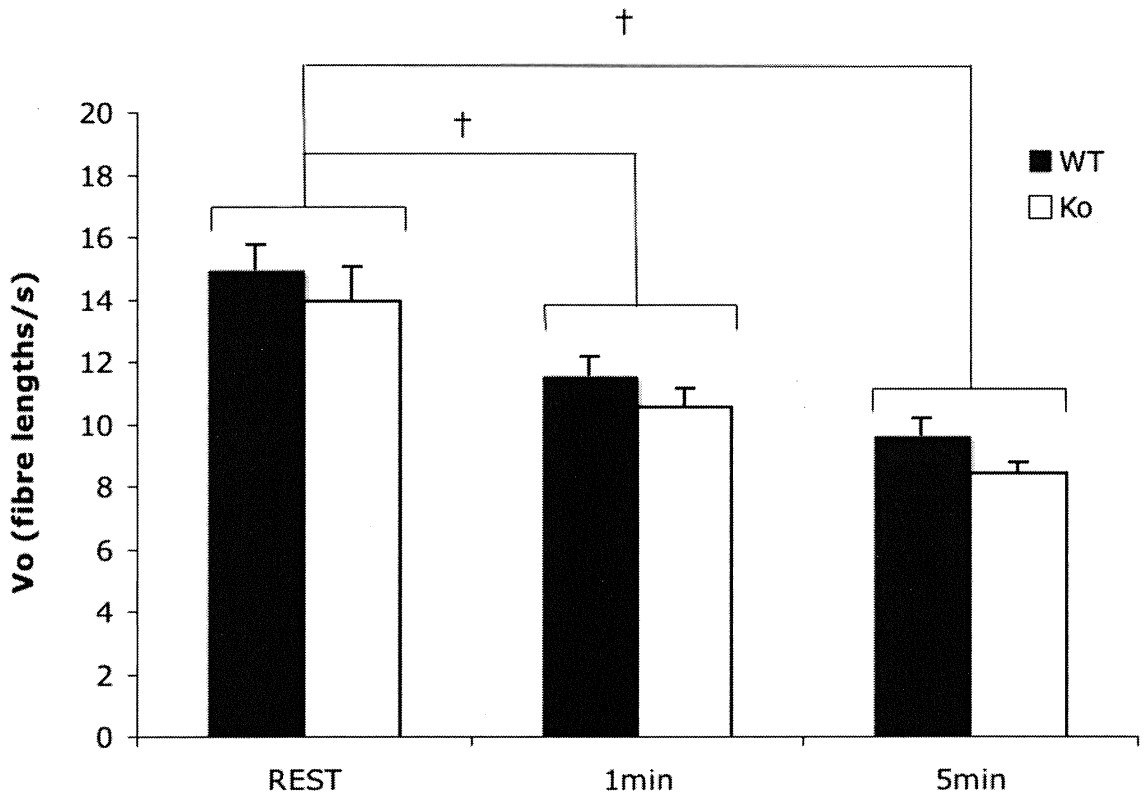

Figure 16. Maximal Unloaded Shortening Velocity (V_o) during fatigue (n=9-10). (†) Significant difference in absolute V_o compared to Rest.

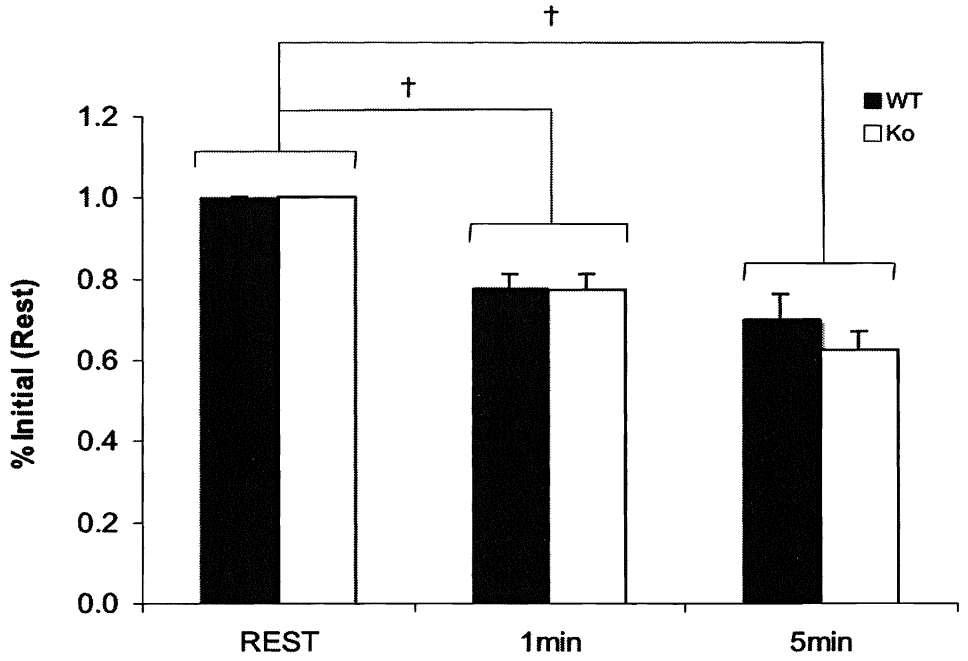

Figure 17. Relative degradation of Unloaded Shortening Velocity (V_o) during fatigue (n=9-10). (†) Significant difference in relative V_o degradation compared to Rest.

5.6.0 Rate of Force Development (+dP/dt)

Rate of force development was assessed during the first contraction of each slack test (Rest, 1min, 5min). The +dP/d*t* value was objectively calculated as the instantaneous rate of force development when the muscle had developed 20% of peak tetanic force (see methods section 4.7.2 for details). Three measures of +dP/d*t* were analyzed in the present project. First, peak +dP/d*t* during the initial rise of force during a tetanic contraction was quantified (Figure 18). Second, the +dP/d*t* during force redevelopment was calculated following a 20% Lo length step (at the midpoint of the same contraction). These values were also used for the calculation of shortening-induced deactivation (see Figure 21 & 22). Finally, peak +dP/d*t* values were used to calculate the relative degradation of force development during fatigue (Figure 20). Analysis of peak +dP/d*t* revealed a main effect for time ($p<0.001$) and group ($p<0.001$), and a significant genotype vs. time interaction ($p<0.001$). Peak +dP/d*t* at Rest was almost twice as high in WT muscles when compared

to KO muscles (5490 ± 573 vs. 2920 ± 208 mN/s). Although absolute +dP/d*t* decreased significantly with time, the difference between groups remained proportionally the same at 1-minute (4349 ± 461 vs. 2311 ± 270) and 5min (2255 ± 256 vs. 1171 ± 120). Rate of force development (+dP/d*t*) after shortening was statistically equal in WT and KO muscles, although a significant main effect for time was produced ($p<0.001$). The relative degradation of +dP/d*t* during fatigue was similar in both WT and KO (no significant main effect for group). WT and KO muscles demonstrated a ~20% decline in +dP/d*t* at 1-minute and a further 40% decline during the remainder of the fatigue protocol (1-5 minutes). These differences produced a significant main effect for time ($p<0.001$), as all pairwise comparisons were significant (Rest vs. 1min, 1min. vs. 5min, Rest vs. 5min).

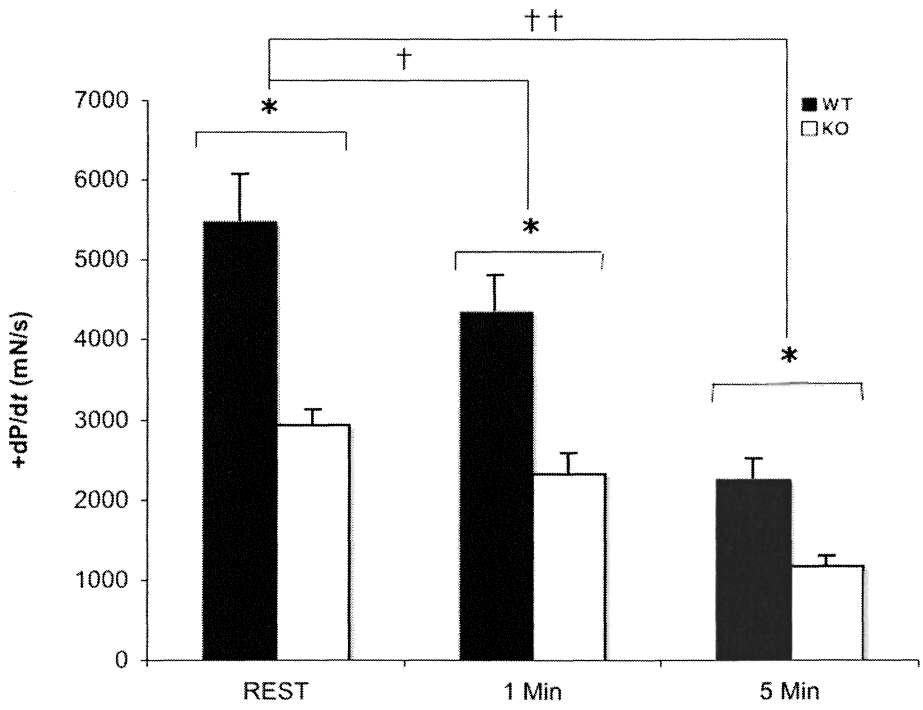

Figure 18. Peak rate of force development (+dP/d*t*) during the initial rise in force during the 20% L_o length step of each slack test (n=9-10).(*) significant difference between groups at each time point ($p<0.001$). (†) Significant difference from Rest +dP/d*t* (within group analysis, $p<0.001$). (††). Significant difference from 1min +dP/d*t* (within group analysis, $p<0.001$). These values were normalized by finding the instantaneous +dP/d*t* value measured at 20% of peak force production (see section 4.7.2).

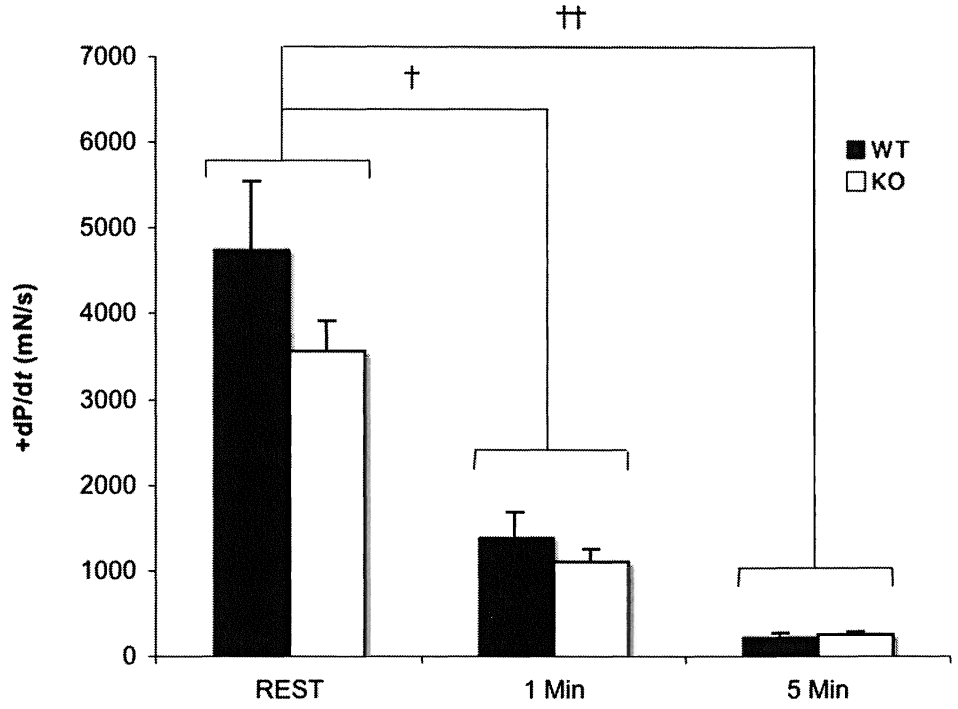

Figure 19. Rate of force development (+dP/d*t*) following a 20% L_o length step (n=9-10). (†) Significant difference from Rest +dP/d*t* ($p<0.001$). (††) Significant difference from 1min +dP/d*t* ($p<0.001$).

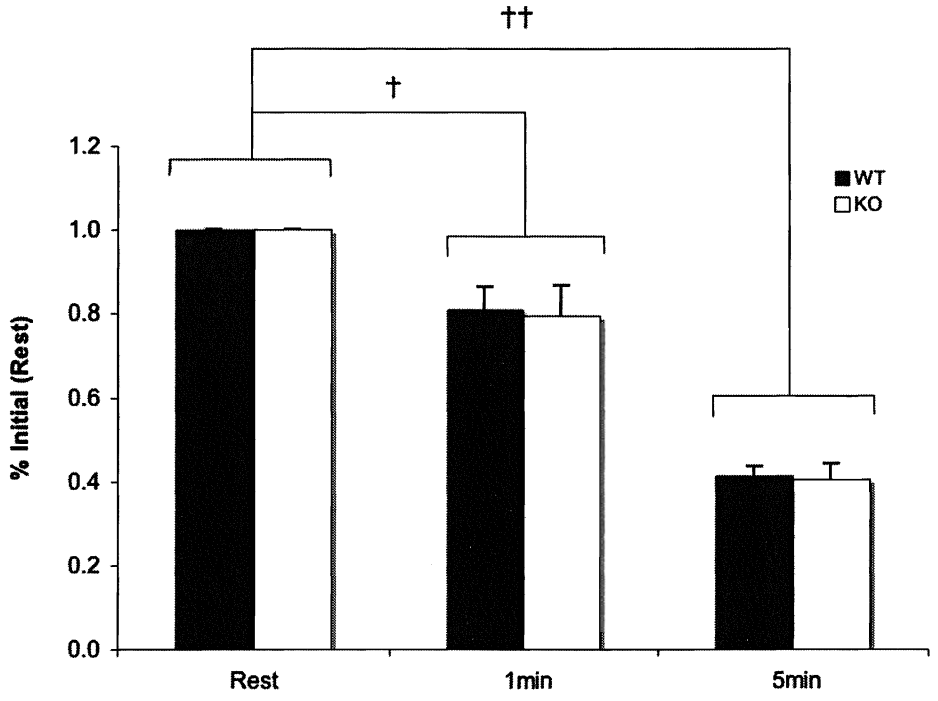

Figure 20. Relative degradation of +dP/d*t* during fatigue (n=9-10). (†) Significant difference from Rest ($p<0.001$). (††) Significant difference from 1min ($p<0.001$).

5.7.0 Shortening-Induced Deactivation (SID)

Shortening-induced deactivation (SID) measured the effect of a 20% L_o length step on subsequent rate of force development. Rapid shortening during a maximal tetanic contraction *in vivo* is thought to deactivate the thin filament to a substantial degree such that +dP/d*t* is attenuated as force is redeveloped. For each muscle, a ratio was created from the +dP/dt values measured before and after the 20% L_o length step. These values were pooled within group and time point for statistical comparison of means (Figure 21).

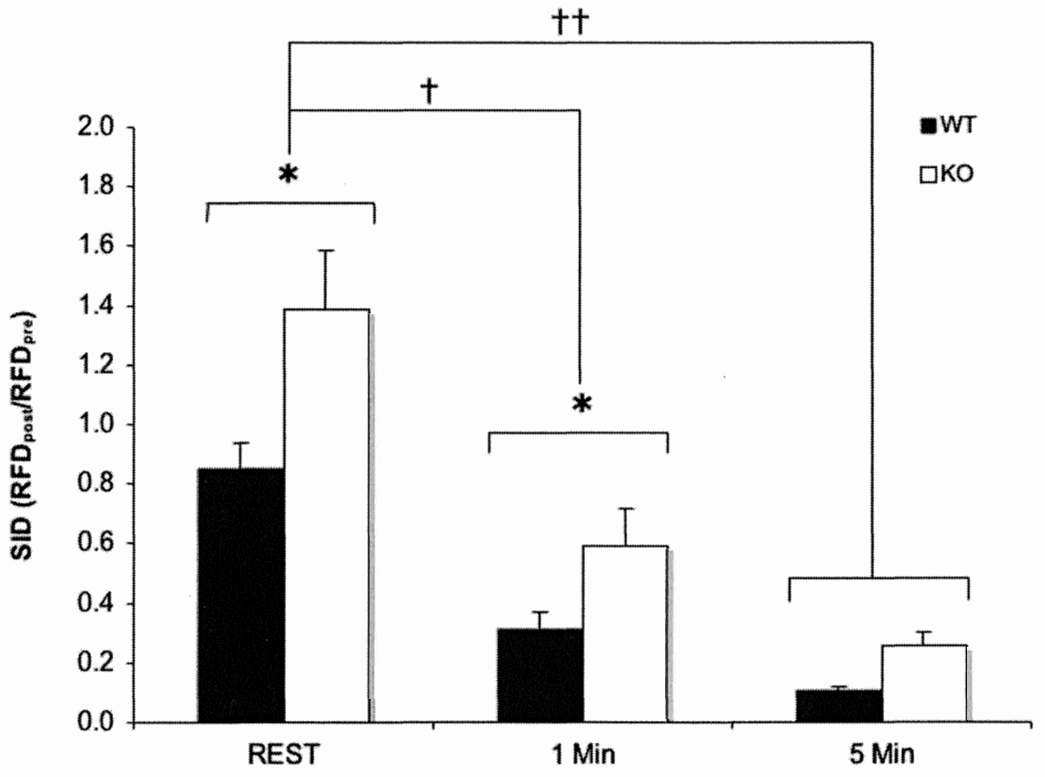

Figure 21. Shortening-induced Deactivation during fatigue (n=9-10). (*) Significant difference between groups at each time point ($p<0.05$), (†) Significant difference from Rest +dP/d*t* (within group analysis, $p<0.001$). (††) Significant difference from 1min +dP/d*t* (within group analysis, $p<0.05$).

Statistical analysis established a significant main effect for group ($p<0.001$) and time ($p<0.001$), and a significant genotype vs. time interaction ($p=0.024$). SID was significantly greater in WT muscles at Rest and 1-minute (Figure 21), however, this difference was not observed in the 5-minute values. SID was 1.39 ± 0.02 for KO muscles at rest, demonstrating that higher +dP/d*t* was observed after rather than prior to active shortening. The net effect of repetitive stimulation on SID was depressive, as +dP/dt following the length step (Figure 19) diminished more rapidly than peak +dP/dt (Figure 18). The degradation of SID was statistically similar in both WT and KO muscles.

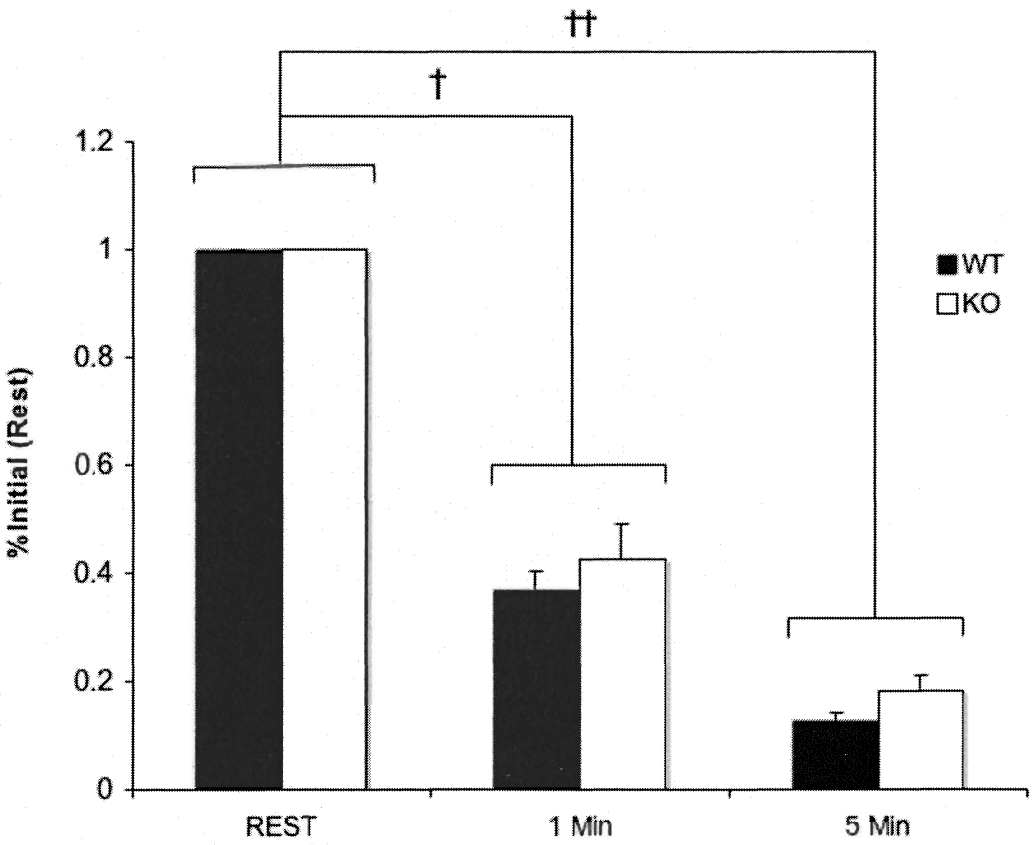

Figure 22. Degradation of SID during fatigue (n=9-10). (†) Significant difference between Rest and 1min ($p<0.001$). (††) Significant difference between 1min and 5min ($p<0.001$).

5.8.0 Biochemical Analysis

5.8.1 Muscle Metabolites

Muscle metabolite concentrations were found to be statistically similar in WT and KO muscles (Figure 24), as there was no significant group interaction found in the analysis of ATP, ADP, P_i, PCr, Cr, or La^-. In each case, however, there was a significant main effect for time ($p<0.05$) as repetitive stimulation altered the concentration of each metabolite from resting values within the first minute of stimulation.

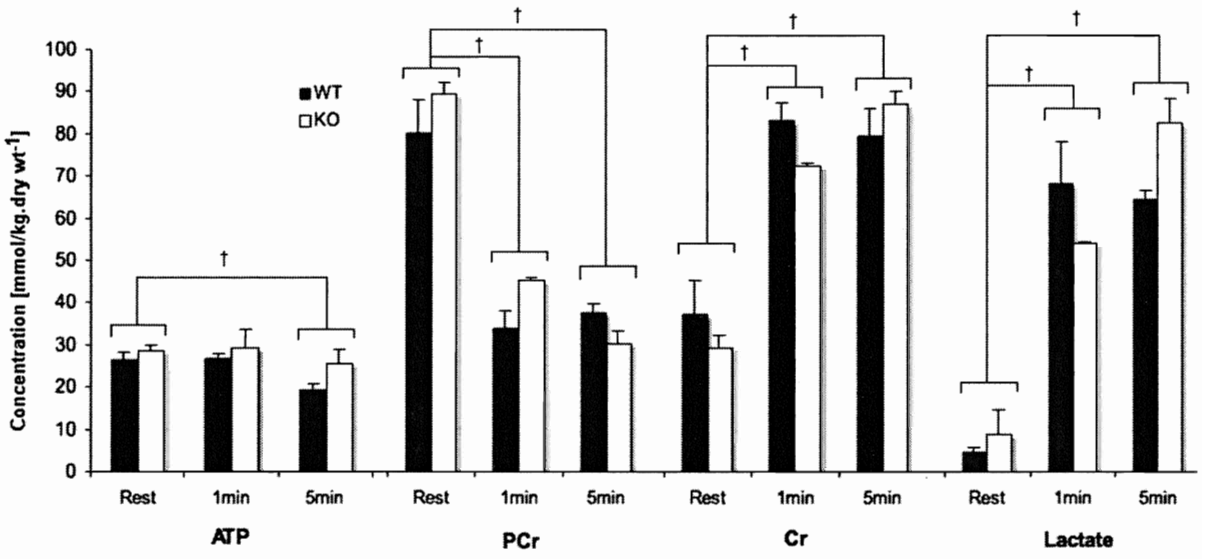

Figure 23. Muscle metabolites during fatigue (n=2-5). (†) Significantly different metabolite concentration compared to Rest ($p<0.05$).

A trend emerged in the metabolite data from the 1-minute time point to 5-minutes. WT muscles exhibited a small but consistent metabolic improvement in the remainder of the fatigue protocol, such that [PCr] increased while Cr, La^-, ADP and P_i concentrations decreased. This trend was in stark contrast to that of KO muscles, which displayed a decrease in [PCr] and increased [Cr], [La^-], and [P_i]. The concentration of ATP was depressed to a larger extent in WT muscles at 5-minutes, although this difference was not significant (19.3±1.3 vs. 25.5±3.5 mmol/kg.dry wt^{-1}). Similarly, the concentration of ADP was lower at 5-minutes in WT muscles, although the absence of a significant group effect and significant interaction did not allow this individual statistical comparison.

Group	Inorganic Phosphate (mmol/kg.dry wt^{-1})			ADP (µmol/kg.dry wt^{-1})		
	Rest	1min	5min	Rest	1min	5min
WT	2.30	48.4 †	44.8 †	67.2 ± 21	207.2 ± 7 †	158.1 ± 32 †
KO	2.30	46.2 †	60.1 †	57.4 ± 9	211.6 ± 28 †	203.3 ± 11 †

Table 3. Concentrations of inorganic phosphate (P_i) and ADP_{free} during fatigue in WT and KO muscles (n=2-5). (†) Significant difference from Rest value ($p<0.05$). For detailed explanations of the calculations involved, please refer to the appendixes.

5.9.0 Summary of Findings & Statistics

The important parameters of contractile performance studied in this project did not respond similarly to repetitive stimulation. It is clear that individual contractile parameters have different sensitivities to fatigue. Moreover, the percentage of fatigue that occurred during the first minute of stimulation was variable from measure to measure-suggesting that intrinsic contractile properties are differentially influenced by various environmental factors. Tables 4 and 5 summarize the most important findings observed in this study, including statistical analysis where applicable. Independent of muscle genotype, the ability to produce maximal force (P_o) was the most susceptible to repetitive stimulation, fatiguing ~90% during the 5-minute protocol (71% during the first minute). Unloaded shortening velocity (V_o) degraded the least during fatigue (declining only 36%). Tetanic force and shortening velocity were especially susceptible to fatigue within the first minute.

Measure	Group	Fatigue (1min)	Fatigue (5min)	% of Total Fatigue	
		%	%	0-1min	1-5min
Twitch Force (P_t)	WT	28	67	42%	58%
	KO	34	71	48%	52%
Peak Tetanic Force (P_o)	WT	64	90	71%	29%
	KO	64	91	70%	30%
Unloaded Shortening Velocity (V_o)	WT	23	33	70%	30%
	KO	25	40	63%	38%
Rate of Force Development (+dP/dt)	WT	19	58	33%	67%
	KO	20	59	34%	66%

Table 4. Summary of the relative fatigue associated with each contractile measure, including the proportion of fatigue that occurred during the acute (0-1min) and subacute (1-5min) segments of the experiments.

Variable	Group	0.9 Lo	1.0 Lo		Main Effect - Length	Main Effect - Group	Interaction	Power
PTP: % Potentiation	WT	30.4 ± 0.04 > *	12.5 ±0.01 > *		p<0.001	p<0.001	p<0.001	1.000
	KO	2.5 ± 0.02	1.2 ± 0.02					
Variable	**Group**	**Rest**	**1Min**	**5Min**	**Main Effect - Time**	**Main Effect - Group**	**Interaction**	**Power**
V_o: Fibre lengths/s	WT	14.96 ± 0.78	11.56 ± 0.59	9.60 ± 0.57	p<0.001			
	KO	13.95 ± 1.07	10.53 ± 0.62	8.39 ± 0.36				
V_o Degradation During Fatigue (%)	WT	1.00 ± 0.00	0.78 ± 0.03	0.66 ± 0.06	p<0.001			
	KO	1.00 ± 0.00	0.78 ± 0.04	0.62 ± 0.04				
Rate of Force Development (+dP/dt): mN/s	WT	5490 ± 573 > *	4349 ± 461 > *	2255 ± 256 > *	p<0.001	p<0.001	p=0.001	0.918
	KO	2920 ± 208	2311 ± 270	1171 ± 120				
(+dP/dt) Degradation During Fatigue (%)	WT	1.00 ± 0	0.810 ± 0.05	0.41 ± 0.02	p<0.001			
	KO	1.00 ± 0	0.79 ± 0.07	0.40 ± 0.04				
(+dP/dt) After a Length Step: mN/s	WT	4762 ± 766	1394 ± 289	236 ± 30	p<0.001			
	KO	3561 ± 350	1101 ± 138	248 ± 41				
SID: $[+dP/dt_{Post}]$ / $[+dP/dt_{Pre}]$	WT	0.85 ± 0.09 > *	0.31 ± 0.06 > *	0.11 ± 0.01	p<0.001	p=0.011	p=0.024	0.561
	KO	1.39 ± 0.2	0.68 ± 0.1	0.25 ± 0.05				
SID Degradation During Fatigue (%)	WT	1.00 ± 0.00	0.36 ± 0.04	0.13 ± 0.01	p<0.001			
	KO	1.00 ± 0.00	0.42 ± 0.06	0.18 ± 0.03				
Variable	**Group**	**Peak PTP (%)**	**Within Group (PTP)**	**PTP Between Group**	**Main Effect - Time**	**Main Effect - Group**	**Interaction**	**Power**
Twitch Force (Pt) During Fatigue: mN	WT	37.2 ± 0.05 > *	5-30 seconds	5-35 seconds *	p<0.001	p=0.02	p<0.001	0.995
	KO	14.3 ± 0.02	10-20 seconds					
Tetanic Force During Fatigue (P_o): mN	WT	N/A	N/A	N/A	p<0.001			
	KO	N/A	N/A					

Table 5. Summary of contractile data and associated statistical analysis.

VI. DISCUSSION

6.1.0 Coincident Myosin RLC Phosphorylation & Fatigue

The present results illustrate that the elimination of myosin RLC phosphorylation by skMLCK KO does not significantly influence maximal force production (P_o), shortening velocity (V_o), or the accumulation of metabolic byproducts during fatigue. In addition, there is no evidence that the presence of elevated myosin RLC phosphate content significantly intensifies any of the measured markers of fatigue. The following discussion explores these concepts to justify the central finding that myosin RLC phosphorylation maintains the contractile performance of WT muscles during fatigue with no associated metabolic cost. Investigation of the single muscle twitch and the kinetics of force development has substantiated the previous findings that myosin RLC phosphorylation is an important modulator of crossbridge attachment during contraction and is the primary mechanism of force potentiation in skeletal muscle. The observation that muscle twitch force is transiently maintained in WT muscles in the presence of considerable fatigue agrees with the present hypothesis that myosin RLC phosphorylation initially preserves the mechanical function of skeletal muscle during repetitive high frequency stimulation. The similar reduction of $+dP/dt$ in KO muscles throughout the fatigue protocol provides evidence that the mechanical benefit of myosin RLC phosphorylation persists independent of muscular fatigue. Finally, metabolic analysis highlighted that while the accumulation of specific metabolites was not statistically different between WT and KO muscles, it seems likely that the elevated metabolic cost of myosin RLC phosphorylation early in fatigue may be offset by more energy efficient crossbridge cycling in the phosphorylated state.

6.2.0 Contractile Mechanics

6.2.1 Force Modulation: Potentiation & Fatigue

Posttetanic Potentiation (PTP) following a brief conditioning stimulus was eliminated in skMLCK knockout muscles. Myosin RLC phosphate content was not measured before and after the conditioning stimulus. However, the current conditioning stimulus (four 150Hz, 400ms stimuli) was similar to that used previously (150Hz, 2s) to elicit a significant elevation of myosin RLC phosphate content in WT muscles (Zhi et al. 2005). The observation of significant PTP in WT muscles and the absence of PTP in KO muscles confirms the hypothesis that myosin RLC phosphorylation is the mechanistic basis of twitch force potentiation in rested skeletal muscle following brief, high intensity activation. The additional observation that PTP is length-dependent in WT muscles suggests that the beneficial spatial alteration of myosin crossbridges in the phosphorylated state is more important at short muscle lengths where interfilament spacing is significantly greater (Yang et al. 1998). Muscle length is therefore a critical consideration in future studies aiming to observe force potentiation and the influence of myosin RLC phosphorylation on contractile performance in all experimental models (*in vitro*, *in situ*, *in vivo*).

The finding that skMLCK KO does not eliminate twitch force potentiation during repetitive, intermittent stimulation implies that an additional mechanism is present which produces the same effect as myosin RLC phosphorylation. The most likely explanation is that myoplasmic [Ca^{2+}], in the absence of stimulation, was not stable throughout the fatigue protocol. Specifically, if the concentration of Ca^{2+} within the muscle remained transiently elevated following each tetanic contraction, the resulting twitch force would

be potentiated (as seen during the early stages of fatigue). This possibility has been discussed by Allen et al. (2008b), who suggest that rapidly increasing P_i during fatigue may inhibit SR Ca^{2+} pumping. As Ca^{2+} is actively pumped into the SR against its concentration gradient, any factor that could reduce the affinity for ATP hydrolysis would theoretically reduce the rate and efficiency of Ca^{2+} reuptake. This mechanism could explain why skMLCK KO muscles selectively exhibit force potentiation during repetitive intermittent stimulation and not following a brief, isolated conditioning stimulus. Although the current study did not measure calcium during the fatigue protocol, the perturbation to calcium handling that may have occurred in the skMLCK KO muscles is likely to have occurred in the WT muscles as well, as both displayed similar $[P_i]$. Future studies should incorporate the measurement of intracellular calcium during fatigue to corroborate this theory.

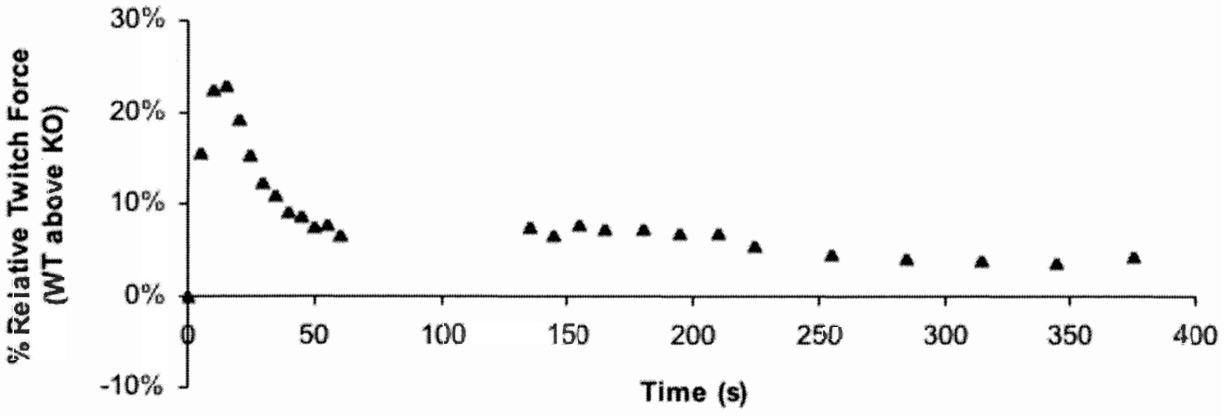

Figure 24. The difference in twitch force between WT and KO muscles during fatigue. Each point in figure 25 was calculated from the difference in relative twitch force between WT and KO muscles at a given time point. Myosin RLC phosphorylation itself potentiated twitch force ~23% within the initial 15-seconds of stimulation and continued to protect twitch force for the remainder of the fatigue protocol (although this difference was not statistically significant after 35-seconds).

Assuming that the SR Ca^{2+} pump was also inhibited in WT muscles, the relative role of myosin RLC phosphorylation in potentiation of twitch force during fatigue was calculated as the difference between peak potentiation in WT muscles (37.2 ± 0.05%) and peak potentiation in KO muscles (14.3 ± 0.02%). Therefore, myosin RLC phosphorylation itself potentiated twitch force by approximately 23%, accounting for approximately 62% of total twitch force potentiation. Figure 24 tracks the difference in relative twitch force (% initial) between WT and KO muscles to highlight the beneficial effect of myosin RLC phosphorylation above and beyond the mechanism that potentiated KO twitch force (i.e. possible Ca^{2+} effects).

6.2.2 Maximal Force Production: Peak Tetanic Force (P_o)

The absence of skMLCK and the resulting absence of elevated myosin RLC phosphate content was not expected to influence peak tetanic force production because the Ca^{2+}-sensitizing effect of myosin RLC phosphorylation is of limited importance at saturating [Ca^{2+}] (Persechini et al. 1985). Accordingly, both WT and KO muscles exhibited similar high frequency fatigue profiles. Peak tetanic force was depressed ~90% in both groups over the 5-minute period of repetitive high frequency stimulation. The mechanisms of force depression during fatigue were assumed to be similar in WT and KO muscles, as decreased Ca^{2+} release during contraction and decreased sensitivity to Ca^{2+} (due to end-product inhibition) limit the quantity and quality of force-producing actin-myosin interactions. Calcium measurements were not obtained during the experiments to quantify the influence of altered Ca^{2+}-handling on force production. However, metabolite data demonstrate that the most effective inhibitor of force

production, inorganic phosphate, was significantly elevated in both WT and KO muscles. In conclusion, the current experiments establish that skMLCK KO has no significant effect on the maximal force produced in response to 1-second high frequency tetanic contractions *in vitro*.

6.2.3 Crossbridge Cycling Rate: Velocity of Shortening (V_o)

Crossbridge cycling rate governs the velocity at which skeletal muscle can shorten in response to zero external load (Edman, 1975). As hypothesized, WT and KO muscles produced statistically similar values of unloaded shortening velocity at rest, during and after fatigue. In addition, the relative degradation of V_o during fatigue was statistically similar in both WT and KO groups.

Perhaps the most important predictor of shortening velocity is the predominant myosin isoform present. Fast myosin isoforms (IIA<IIX<IIB) catalyze the hydrolysis of ATP at a greater rate than type I fibres and therefore exhibit higher rates of crossbridge cycling and ATP turnover. Muscle fibre type was not controlled for in the present study; however, there is some evidence to suggest that both WT and KO muscles expressed similar myosin phenotypes. Both groups produced similar maximal force levels at rest. There was no visual evidence to suggest that muscle diameter was significantly different between WT and KO muscles during any of the experiments (as assessed visually with the stereo zoom microscope). It can be assumed, therefore, that if KO muscles had expressed significantly more or less type II fibres than WT muscles, that average differences in muscle specific force would have influenced this measure. Furthermore, mean mouse age was not different in the contractile experiments, reducing the possibility that age-induced fibre type shifts could influence the comparison. Additional evidence

can be found in the fatigue profiles of WT and KO muscles. Both groups fatigued almost identically throughout five minutes of repetitive stimulation. It seems likely that a significant difference in fibre type would have manifested itself in altered rates of fatigue due to the different metabolic capacity associated with a change in myosin isoform expression.

The rate-limiting step of the crossbridge cycle during muscle contraction is the release of ADP, which facilitates the binding of a new ATP molecule to the myosin head and catalyzes crossbridge detachment from the thin filament (Chase & Kushmerick, 1995; Cooke & Pate, 1985). The results of metabolic analysis did not produce any statistical difference in [ADP] between WT and KO muscles. This outcome is in agreement with the contractile data described above, as no difference in V_o was observed between WT and KO muscles.

In conclusion, the ablation of skMLCK does not seem to significantly influence the maximal unloaded shortening velocity in isolated mouse skeletal muscle. This finding supports previous reports that unloaded shortening velocity is insensitive to myosin RLC phosphorylation, and refutes more recent evidence that myosin RLC phosphorylation contributes to the reduction of unloaded shortening velocity during conditions that mimic fatigue (Karatzaferi et al., 2008). The discrepancy in these conclusions may lie in subtle differences inherent to the individual models of study. The current experiments were completed on whole muscles *in vitro* at 25°C, while those reporting the opposite findings were completed at 30°C on isolated skinned muscle fibres with chemically induced myosin RLC phosphorylation (Karatzaferi et al., 2008; Franks-Skiba et al., 2007). It is possible that the effect of myosin RLC phosphorylation on shortening velocity may be

different at temperatures that approach physiological temperatures; however, the current results demonstrate that this modulatory mechanism does not influence maximal shortening velocity in whole muscles *in vitro* at 25°C (as measured using the slack test).

6.2.4 Rate of Force Development (+dP/dt) & Shortening-induced Deactivation (SID)

The present finding that skMLCK knockout significantly impairs rate of force development is in agreement with the theory that myosin crossbridges in the phosphorylated state bind more rapidly and effectively with actin during muscle activation. When measured during the initial rise in force of a fully fused tetanic contraction, KO muscles exhibited only half the mean +dP/d*t* when compared to WT muscles at all stages of fatigue. This finding has significant implications for the contractile performance of skeletal muscles *in vivo*. The fact that +dP/d*t* is augmented during high frequency stimulation provides evidence that peak force production for contractions of shorter duration may be considerably improved in the presence of myosin RLC phosphorylation.

The traces shown in Figure 25 suggest that ablation of skMLCK may attenuate the peak force produced during fused tetanic contractions lasting less than ~300ms. This effect may be highly significant for patterns of brief, repetitive muscle activation found during various movements and locomotion, as peak force produced during a brief contraction may be sensitive to high rates of force development.

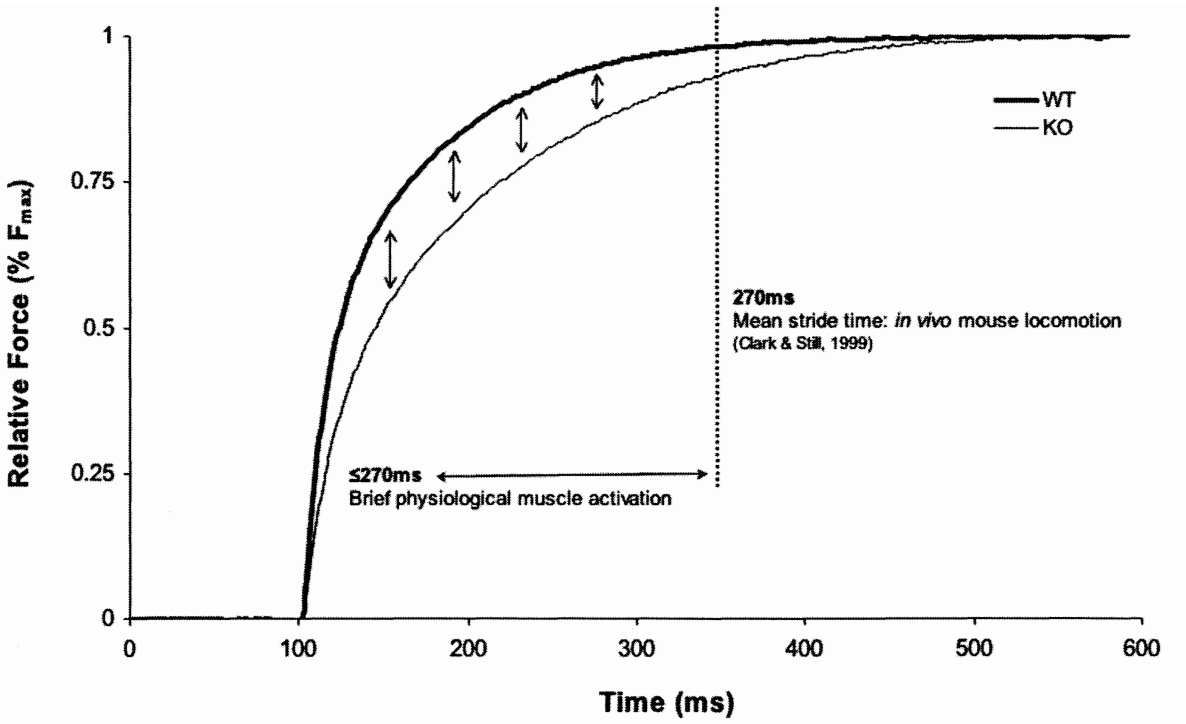

Figure 25. Force-time traces of WT and KO muscles during a fully fused tetanic contraction at 25°C. The ablation of skMLCK attenuated +dP/d*t* in KO muscles, an effect which could influence the peak force produced prior to reaching peak tetanic force during physiological muscle contractions *in vivo* (the initial ~300ms of stimulation).

In specific gait analysis of mouse walk/trot locomotion, Clarke and Still (1999) established that mean stride frequency was ~3.7Hz, demonstrating that fore and hind limb muscles are being activated approximately every 270ms. Given that each stride includes both agonist and antagonist muscle activity, each muscle would be activated for a brief period of time during these types of locomotion (likely much shorter than 270ms). These findings provides clear evidence that mouse muscles are not simulated for sufficient duration *in vivo* to reach maximal force. Furthermore, potentiation of high frequency force production for short duration contractions by augmented +dP/d*t* could be possible and quite meaningful for *in vivo* contractile performance. Specifically, myosin RLC phosphorylation could provide fatigue resistant benefits if peak force production during brief contractions could be maintained throughout fatigue by augmented +dP/d*t*.

Despite the almost two-fold difference in absolute +dP/d*t* values between WT and KO muscles at each time point, the depressive effect of fatigue on this contractile parameter was equal between groups as both exhibited a similar relative depression in +dP/d*t* at 1-minute and 5-minute (Figure 21). This observation demonstrates that the ablation of skMLCK does not significantly influence the fatigue mechanisms responsible for the decline in +dP/d*t* during fatigue. In addition, the relative difference in absolute +dP/d*t* between WT and KO muscles did not differ noticeably during fatigue in spite of a significant increase in myosin RLC phosphate content found in WT muscles between Rest and 1-minute. This result suggests that the beneficial effect of myosin RLC phosphorylation on +dP/d*t* may have been present at rest or very early during fatigue; and furthermore, that there may be no extra benefit to myosin RLC phosphorylation above some submaximal level of myosin RLC phosphate content.

Shortening-induced deactivation (SID) was assessed indirectly by comparison of the +dP/dt before and after the 20% L_o length step of each slack test. The rationale for this analysis was to investigate whether myosin RLC phosphorylation influences the rapid deactivation of the thin filament during active shortening. SID was treated as a mechanism distinct from muscle relaxation and from those factors that influence crossbridge detachment during crossbridge cycling. As explained previously, maximal crossbridge cycling is rate-limited by the rate of crossbridge detachment, which is in turn restricted by factors that influence the affinity for ATP hydrolysis and the release of ADP. SID is therefore a unique mechanism whereby rapid shortening of muscle length imposed during an isometric contraction causes reduces the activation level of the thin filament. In the present analysis, SID was quantified as the ratio of +dP/d*t* before and

after a 20% L_o length step. The ability of the muscle to redevelop force after rapid shortening therefore represented an indirect measure of the activation level of the thin filament where an observed depression in +dP/d*t* was assumed to be a product of SID.

The novel finding that SID was attenuated in skMLCK KO muscles reveals that myosin RLC phosphorylation may act as an important modulator of thin filament activation during active shortening. Specifically, it appears that muscles deactivate to a greater extent during active shortening in the presence of elevated myosin RLC phosphate content. Initially, this observation seemed to provide evidence that myosin RLC phosphate exacerbates fatigue by making WT muscles more susceptible to SID. It is possible that greater SID would transiently impede subsequent contractile performance, inducing a greater energy cost for activation in WT muscles to compensate for this mechanism. However, the absolute +dP/dt measured following the rapid length step in WT muscles was the same or greater than in KO muscles. This observation demonstrates that although WT muscles exhibited relatively more SID than KO muscles, this did not occur at a substantial cost to contractile performance. The question that emerges from this analysis is, does more SID benefit the contractile performance of WT muscles during fatigue? The observation that myosin RLC phosphorylation enhances rapid deactivation during active shortening without diminishing absolute rate of force development below skMLCK KO muscles suggests that this mechanism could be important for rapid cycles of muscle activation. For example, a muscle with elevated myosin RLC phosphate content could improve the repetitive rapid attachment and detachment of myosin crossbridges. However, the present results only represent a theoretical model for analysis, as the mechanism(s) that actually limit maximal stride frequency of muscles *in vivo* have

not been well established. Despite this, myosin RLC phosphorylation could represent an important mechanism that facilitates both the rapid activation and deactivation of the contractile apparatus during rapid cycles of muscle contraction. It is unclear, however, how the presence of elevated myosin RLC phosphorylation would exacerbate SID and what affect this would have on the physiological function of skeletal muscles *in vivo*.

6.3.0 Myosin RLC Phosphorylation

As hypothesized, myosin RLC phosphate content was depressed in skMLCK knockout mice and did not increase in response to repetitive high frequency stimulation. The low level of phosphorylation measured in KO muscles (0.07 P-skRLC/Total-skRLC) cannot be accounted for in the present study, as total skMLCK was not measured. An additional kinase could have be present to phosphorylate the RLC, however, this enzyme would not likely be contraction activated, as myosin RLC phosphate content did not increase in KO muscles during fatigue. WT muscles exhibited increased myosin RLC phosphate content during the first minute of stimulation and remained similarly elevated throughout the five minutes of stimulation ($p<0.001$). Although not significant, the small decrease in RLC phosphate content from 1-minute to 5-minutes suggests that myoplasmic [Ca^{2+}] may have been progressively decreasing as muscular fatigue progressed, decreasing the activity of skMLCK.

The myosin RLC phosphate content of WT muscles at rest (0.39 P-skRLC/Total-skRLC) was higher than previously reported values of ~0.15 and ~0.1 (Zhi et al, 2005; Vandenboom et al. 1993). A probable explanation for this result is that the handling of the mouse EDL muscle immediately prior to rapid freezing may mechanically induce a small release of Ca^{2+} in the muscle, thus activating skMLCK. This possibility highlights

the importance of adopting a freezing method that minimizes the physical manipulation of a muscle before it is frozen. A second possibility for the elevated resting myosin RLC phosphate content is that preceding contractile activity had elevated myosin RLC phosphorylation. However, muscles frozen for myosin RLC phosphorylation analysis were always subjected to a 20-minute period of quiescence before freezing and twitch pacing was employed during these 20-minute periods to ensure the full decline in twitch force potentiation to baseline values, so it appears to be unlikely that myosin RLC phosphorylation could persist in the absence of potentiation.

The present results confirm the efficacy of skMLCK gene ablation for the purpose of studying the mechanism of myosin RLC phosphorylation. Given the substantial difference in myosin RLC phosphorylation between WT and KO muscles at all time points, it is likely that the observed differences in contractile function were largely associated with this primary intervention.

6.4.0 Relative Change in Metabolic Accumulation Throughout Fatigue

The present results provide evidence that the metabolic requirement of skeletal muscles with elevated myosin RLC phosphate content may not be constant during fatigue; and moreover, that a higher metabolic cost may be evident in skMLCK knockout muscles during more prolonged periods of fatigue. However, statistical investigation demonstrated that mean metabolite concentrations did not differ between WT and KO muscles. This finding may be a product of the study design itself, however, and might well have obscured an important trend.

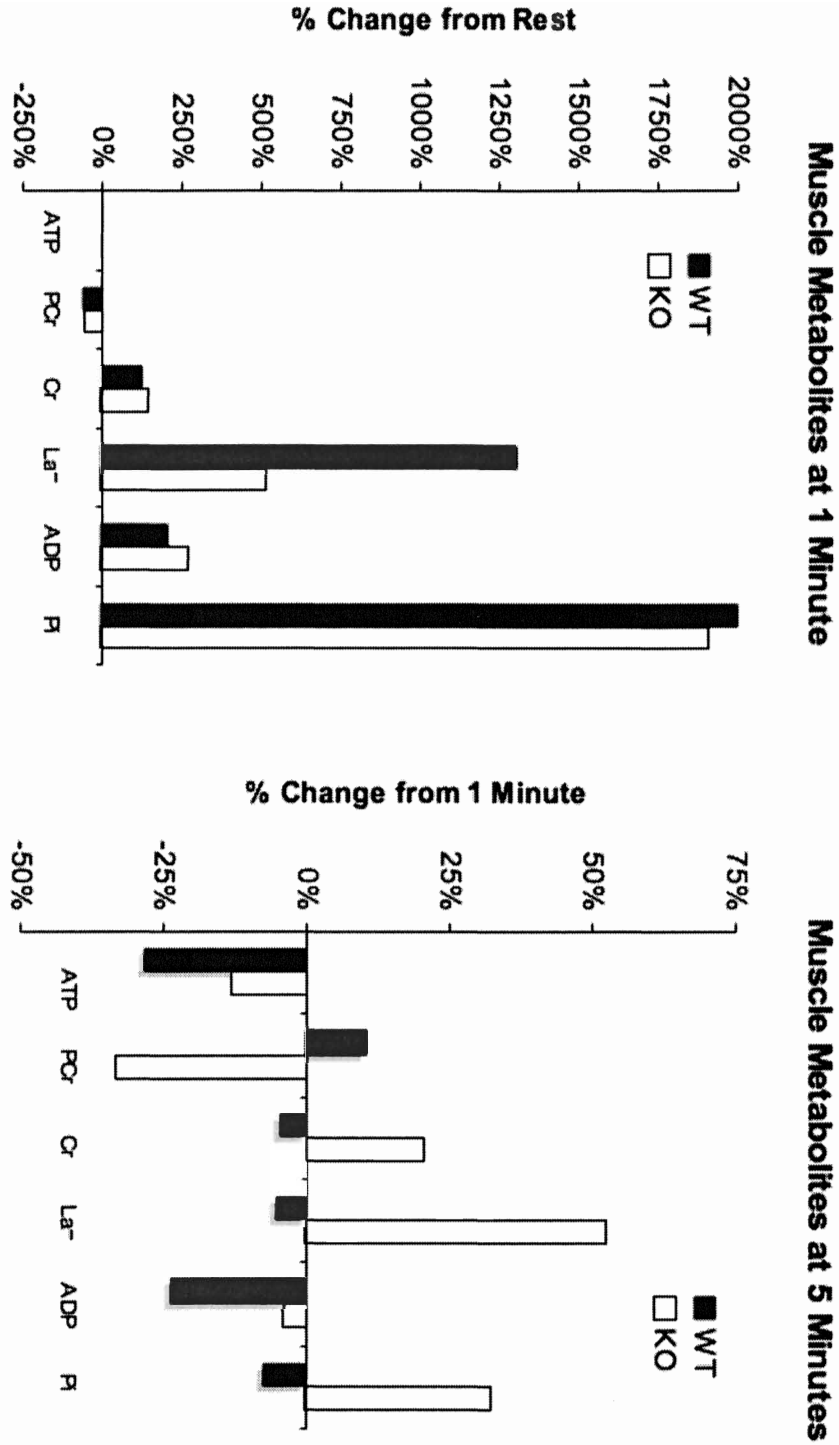

Figure 26. The relative change in concentration of each metabolite from rest to 1-minute (Left) and from 1-minute to 5-minutes (Right). The initial effect of fatigue was similar in both WT and KO muscles, however, this pattern was not recapitulated in the remaining 4-minutes of stimulation. In most cases, WT and KO muscles exhibited opposite changes in metabolite concentrations. KO muscles displayed changes that suggested further progression of fatigue, whereas WT muscles actually demonstrated relative improvements in most measures (increased PCr, decreased Cr, La^-, P_i). These results were not evaluated statistically as each was simply calculated as the dividend between mean metabolite concentrations at each time point and expressed as a percentage.

The data presented in Figure 26 demonstrate that WT and KO muscles did not perform similarly in terms of the metabolic cost of contraction during the second, more prolonged portion of the fatigue protocol. In both groups, the majority of the absolute change in metabolite concentrations occurred during the first minute of fatigue. Discounting the variable muscle lactate values, the metabolic response of WT and KO muscles during the first minute of stimulation was reasonably similar. During this period of time, peak force output (P_o) and shortening velocity (V_o) were similar in WT and KO muscles. Twitch force potentiation and rate of force development were significantly greater in WT muscles throughout this interval, an observation in agreement with the concurrent increase in myosin RLC phosphate content. In comparison, the remaining 4-minutes of the fatigue protocol demonstrated similar trends in terms of contractile performance (P_o, V_o, $+dP/dt$, SID) despite a marked variation in the metabolic cost of contraction in WT and KO muscles.

A reasonable supposition would be that WT muscles may incur a larger metabolic cost during the initial stages of fatigue due to the increased ATP cost of myosin RLC phosphorylation; and once myosin RLC phosphate content is elevated, that the metabolic cost of contraction may decrease to some degree. This hypothesis cannot be elucidated with the current data but is in agreement with the findings of Abbate et al. (2001) that the metabolic cost of contraction was greater than the increase in mechanical work output in potentiated rat fast skeletal muscle during 10 intermittent contractions at 60Hz. The protocol utilized in the aforementioned study was considerably shorter than the current experiments, lasting approximately 1-minute. Had Abbate et al. (2001) extended their protocol to 5-minutes, their findings may have more closely resembled the present

results. In addition, Crow and Kushmerick (1982b) demonstrated that elevated myosin light chain phosphorylation was associated with a decrease in the total splitting of high-energy phosphates during an isometric contraction, and suggested that this observation is likely the product of reduced myosin ATPase activity. The current experiments did not produce a statistically significant difference in metabolite concentrations, therefore the hypothesis that a decrease in the energy cost for contraction mitigated by elevated myosin RLC phosphorylation cannot be satisfactorily answered.

The absence of statistically significant results in the present metabolic data was likely the product of small sample sizes (n=2-5) and relatively high within group variability. These sources of inconsistency were attributed to human error within the extraction procedure and during each metabolic assay itself. An inherent difficulty with the current metabolic analysis is the task of quantifying very low concentrations of metabolites in such small muscle samples ($\leq$ 1mg dry wt). In future studies, muscle samples of ~1.5mg dry wt are likely necessary to produce accurate and consistent data.

VII. CONCLUSIONS & SIGNIFICANCE

7.1.0 Primary Findings

- Myosin RLC phosphorylation was virtually nonexistent in skMLCK knockout mouse EDL muscles and did not increase significantly with repetitive stimulation.
- Myosin RLC phosphate content rapidly increased in WT muscles with repetitive stimulation to ~0.63 P-skRLC/Total-skRLC at 1-minute, and remained similarly elevated throughout the fatigue protocol to 5-minutes.
- Muscle twitch force was protected in WT muscles for the first 35-seconds of the fatigue protocol, whereas P_o was depressed up to 40%.
- skMLCK KO muscles did not exhibit PTP following a conditioning stimulus, although a small degree of twitch force potentiation (~13%) was observed during the first 20-seconds of fatigue.
- The presence (or absence) of myosin RLC phosphorylation did not influence maximal force production (P_o) or maximal unloaded shortening velocity (V_o).
- Rate of force development (+dP/d*t*) was almost two-fold greater in WT compared to KO muscles at all stages of fatigue. The relative degradation of +dP/d*t* was similar in WT and KO muscles.
- Shortening-induced deactivation (SID) was exacerbated in WT muscles at all stages of fatigue.
- WT and skMLCK KO muscles exhibited statistically similar concentrations of muscle metabolites prior to, during, and following the 5-minute fatigue protocol.
- A noteworthy trend in energy utilization occurred, however, as WT muscles demonstrated a noticeably larger energy cost during the first minute of stimulation (greater PCr depletion, pronounced Cr and La^- accumulation).
- WT muscles may be more efficient metabolically when myosin RLC phosphorylation is high, as seen during the remaining 4-minutes of stimulation (increased PCr, decreased Cr and La^-).

7.2.0 Significance of Findings

The purpose of the present study was to explore whether myosin RLC phosphorylation resists fatigue by maintaining the performance response of the contractile apparatus during repeated activation. The inhibition of myosin RLC phosphorylation in skMLCK KO muscles provided an important experimental control to study both contractile and metabolic measures in the absence of the modulatory mechanism of interest. The interpretation of the present study is that the absence of myosin RLC phosphorylation does not meaningfully modify the progressive loss of maximal force and shortening velocity that characterizes muscle fatigue. However, the potentiation of low frequency force production in WT muscles is a clear indication that myosin RLC phosphorylation may preserve contractile function at low or moderate intensities during repetitive stimulation. The stimulation protocol used in the present study is likely more severe than almost all types of activity in humans (peak force was depressed ~60% in the first minute). Therefore, the role of low frequency force potentiation and myosin RLC phosphorylation in resisting fatigue during less rigorous patterns of activation may be more important and longer lasting than reported here.

The current results provide substantial evidence that myosin RLC phosphorylation may delay fatigue *in vivo*, where different patterns of stimulation intensity and duration during physiological movements could make the most of the various contractile benefits associated with myosin RLC phosphorylation. Of these benefits, an augmented rate of force development appears to be the most likely to maintain contractile function at all stages of muscle fatigue. The finding that both rate of force development and deactivation are attenuated in skMLCK KO muscles also suggests

that myosin RLC phosphorylation may also play a modulatory role in the rapid application and removal of force-producing actin-myosin interactions during repetitive cycles of muscle activation.

The observation that myosin RLC phosphorylation may impose an additional ATP demand while concurrently improving Ca^{2+} sensitivity and mechanical function demonstrates that this mechanism could play an important role in muscle metabolism. It is possible that myosin RLC phosphorylation offers a contractile benefit to muscles early in fatigue by maintaining low frequency forces, but imposes a greater ATP demand until myosin RLC phosphate content is elevated maximally. At this point, the mechanical benefits are likely still present (increased +dP/d*t*) but the energy cost of contraction may actually decrease during the subsequent period of repetitive stimulation. It is presently unclear if elevated myosin RLC phosphorylation significantly decreases the metabolic economy of working muscles, and furthermore, whether this may occur due to an alteration in the affinity for ATP hydrolysis to spare ATP turnover.

The *in vitro* preparation does not contain natural feedback systems that may be important to physiological function *in vivo*. Of these, the most important is the theory that as myosin RLC phosphorylation increases the contractile performance of a muscle (Ca^{2+} sensitivity), the activation requirement (i.e. motor unit firing rates) may diminish accordingly to ensure a steady mechanical output (see Appendix 5 for schematic). This mechanism would have the potential to decrease metabolic demand and ATP turnover by reducing the Ca^{2+} handling requirements in the muscle (Ca^{2+} release and active reuptake), and more importantly, may help spare the strength of activation required for a given contractile output in the muscle.

7.3.0 Future Research & Considerations

Investigation of the following research questions would directly extend the scope of the present findings, and contribute to the continued production of new knowledge in the fields of muscle and exercise physiology.

- *To what extent does myosin RLC phosphorylation contribute to low-frequency force potentiation during repetitive contractions, and is there a calcium-handling component to this phenomenon?*

- *Although myosin RLC phosphorylation may not influence maximal unloaded shortening velocity, is shortening velocity at various submaximal forces significantly influenced?*

- *Does myosin RLC phosphorylation improve high-frequency force production during brief contractions (≤300ms) by enhancing the initial rate of force development? Does this contractile benefit prevent fatigue or just delay its effect?*

- *Does myosin RLC phosphorylation enhance SID across different contraction types or during concentric/eccentric work cycles? Are either of these mechanisms present during active lengthening, is there lengthening-induced deactivation?*

- *What is the metabolic cost of contraction in the phosphorylated state and is there a transitional period of increased metabolic demand when myosin RLC phosphate content increases rapidly?*

- *What is the relationship between force output and central nervous muscle activation? Can the body sense an improvement in Ca^{2+} sensitivity and does this feed forward to alter or pace motor unit firing rates in fast twitch skeletal muscle?*

7.4.0 Assumptions

- The procedures involved in the storage, homogenization and analysis of muscle tissue will accurately reflect the true metabolic conditions sampled at the time of freezing.
- Electrical field stimulation of EDL muscles *in vitro* similarly reflects how muscles are activated *in vivo*.
- The Tyrode solution provides an exercising muscle with similar ions concentrations found *in vivo*.
- The decrement in rate of force development after active shortening is a function of shortening-induced deactivation.
- That statistical conclusions extracted from the present experiments truly represent the population being sampled.

7.5.0 Limitations

- The observations and conclusions of the current study are principally limited to exploring the function of fast twitch mammalian skeletal muscle in carefully controlled *in vitro* conditions. Mouse EDL muscle is relatively homogeneous in nature, and extrapolating the physiological role of myosin RLC phosphorylation to larger, heterogeneous muscles may be problematic.
- *In vivo* muscle activity is not well approximated by isometric contractions, as physiological contractile performance is highly dependent on muscle length and changes thereof.
- The present *in vitro* experiments were conducted at sub-physiological temperatures (25°C). The findings presented previously may not accurately reflect the true effect of myosin RLC phosphorylation on muscle function at 37° C.
- The quantification of unloaded shortening velocity (V_o) represents only the maximal capacity of the fastest fibres to redevelop force. The physiological range of maximal shortening at zero load (V_{max}) *in vivo* is typically an underestimation of V_o (Claflin & Faulkner, 1985). The differences between V_o and V_{max} therefore represents the shortening capacity of the slower fibres found in whole muscles with heterogeneous fibre types.

REFERENCES

Abbate, F., Van Der Velden, J., Stienen, G. J., & De Haan, A. (2001). Post-tetanic potentiation increases energy cost to a higher extent than work in rat fast skeletal muscle. *Journal of Muscle Research and Cell Motility, 22*(8), 703-710.

Allen, D. G. (2004). Skeletal muscle function: Role of ionic changes in fatigue, damage and disease. *Clinical and Experimental Pharmacology & Physiology, 31*(8), 485-493.

Allen, D. G., Lamb, G. D., & Westerblad, H. (2008a). Impaired calcium release during fatigue. *Journal of Applied Physiology (Bethesda, Md.: 1985), 104*(1), 296-305.

Allen, D. G., Lamb, G. D., & Westerblad, H. (2008b). Skeletal muscle fatigue: Cellular mechanisms. *Physiological Reviews, 88*(1), 287-332.

Allen, D. G., Lannergren, J., & Westerblad, H. (1995). Muscle cell function during prolonged activity: Cellular mechanisms of fatigue. *Experimental Physiology, 80*(4), 497-527.

Allen, D. G., & Westerblad, H. (2001). Role of phosphate and calcium stores in muscle fatigue. *The Journal of Physiology, 536*(Pt 3), 657-665.

Altringham, J. D., & Johnston, I. A. (1985). Effects of phosphate on the contractile properties of fast and slow muscle fibres from an antarctic fish. *The Journal of Physiology, 368*, 491-500.

Aydin, J., Korhonen, T., Tavi, P., Allen, D. G., Westerblad, H., & Bruton, J. D. (2007). Activation of ca(2+)-dependent protein kinase II during repeated contractions in single muscle fibres from mouse is dependent on the frequency of sarcoplasmic reticulum ca(2+) release. *Acta Physiologica (Oxford, England), 191*(2), 131-137.

Baldwin, K. M., Klinkerfuss, G. H., Terjung, R. L., Mole, P. A., & Holloszy, J. O. (1972). Respiratory capacity of white, red, and intermediate muscle: Adaptative response to exercise. *The American Journal of Physiology, 222*(2), 373-378.

Balnave, C. D., & Allen, D. G. (1996). The effect of muscle length on intracellular calcium and force in single fibres from mouse skeletal muscle. *The Journal of Physiology, 492 (Pt 3)*(Pt 3), 705-713.

Barclay, C.J. (2005). Modelling diffusive O2 supply to isolated preparations of mammalian skeletal and cardiac muscle. *Journal of Muscle Research and Cell Motility. (26),* 225-235.

Baudry, S., & Duchateau, J. (2007). Postactivation potentiation in a human muscle: Effect on the load-velocity relation of tetanic and voluntary shortening

contractions. *Journal of Applied Physiology (Bethesda, Md.: 1985), 103*(4), 1318-1325.

Bottinelli, R. (2001). Functional heterogeneity of mammalian single muscle fibres: Do myosin isoforms tell the whole story? *Pflugers Archiv : European Journal of Physiology, 443*(1), 6-17.

Bowditch, H. P. (1871). Uber die eigenthumlichkeiten der reizbarkeit welche die muskelfasern des herzens zeigen. *Ber Sächs Ges Wiss, 23*, 652-689.

Brenner, B. (1988). Effect of Ca2+ on cross-bridge turnover kinetics in skinned single rabbit psoas fibres: implications for regulation of muscle contraction. Proc. *Natl. Acad. Sci. USA* 85, 3265-3269

Brown, L. T., & Tuttle, W. W. (1926). The phenomenon of treppe in intact human skeletal muscle. *Am Physiol Soc., 77*, 483-490.

Bruton, J. D., Lannergren, J., & Westerblad, H. (1998). Mechanisms underlying the slow recovery of force after fatigue: Importance of intracellular calcium. *Acta Physiologica Scandinavica, 162*(3), 285-293.

Chase, P. B., & Kushmerick, M. J. (1995). Effect of physiological ADP concentrations on contraction of single skinned fibres from rabbit fast and slow muscles. *The American Journal of Physiology, 268*(2 Pt 1), C480-9.

Claflin, D. R., & Faulkner, J. A. (1985). Shortening velocity extrapolated to zero load and unloaded shortening velocity of whole rat skeletal muscle. *The Journal of Physiology, 359*, 357-363.

Clarke, K. A., & Still, J. (1999). Gait Analysis in the Mouse. *Physiology and Behavior. 66(5).* 723-729.

Close, R., & Hoh, J. F. (1968). The after-effects of repetitive stimulation on the isometric twitch contraction of rat fast skeletal muscle. *The Journal of Physiology, 197*(2), 461-477.

Cooke, R. (1997). Actomyosin interaction in striated muscle. *Physiological Reviews, 77*(3), 671-697.

Cooke, R. (2007). Modulation of the actomyosin interaction during fatigue of skeletal muscle. *Muscle & Nerve, 36*(6), 756-777.

Cooke, R., & Pate, E. (1985). The effects of ADP and phosphate on the contraction of muscle fibres. *Biophysical Journal, 48*(5), 789-798.

Crow, M. T., & Kushmerick, M.J. (1982a). Chemical Energetics of Slow- and Fast-Twitch Muscles of the Mouse. *Journal of General Physiology.* (79). 147-166.

Crow, M. T., & Kushmerick, M. J. (1982b). Myosin Light Chain Phosphorylation Is Associated with a Decrease in the Energy Cost for Contraction in Fast Twitch Mouse Muscle. *The Journal of Biological Chemistry, 257(5).* 2121-2124.

Debold, E. P., Dave, H., & Fitts, R. H. (2004). Fibre type and temperature dependence of inorganic phosphate: Implications for fatigue. *American Journal of Physiology.Cell Physiology, 287*(3), C673-81.

Dudley, G. A., Tullson, P. C., & Terjung, R.L. (1987). Influence of Mitochondrial Content on the Sensitivity of Respiratory Control. *The Journal of Biological Chemistry. 269*(19), 9101-9114.

Edman, K. A. (1975). Mechanical deactivation induced by active shortening in isolated muscle fibres of the frog. *The Journal of Physiology, 246*(1), 255-275.

Edman, K. A. (1979). The velocity of unloaded shortening and its relation to sarcomere length and isometric force in vertebrate muscle fibres. *The Journal of Physiology, 291*, 143-159.

Edman, K. A. (1996). Fatigue vs. Shortening-induced deactivation in striated muscle. *Acta Physiologica Scandinavica, 156 (3)*, 183-192.

Fabiato, A., & Fabiato, F. (1978). Effects of pH on the myofilaments and the sarcoplasmic reticulum of skinned cells from cardiace and skeletal muscles. *The Journal of Physiology, 276*, 233-255.

Fitts, R. H. (2008). The cross-bridge cycle and skeletal muscle fatigue. *Journal of Applied Physiology (Bethesda, Md.: 1985), 104*(2), 551-558.

Fowles, J. R., & Green, H. J. (2003). Coexistence of potentiation and low-frequency fatigue during voluntary exercise in human skeletal muscle. *Canadian Journal of Physiology and Pharmacology, 81*(12), 1092-1100.

Franks-Skiba, K., Lardelli, R., Goh, G., & Cooke, R. (2007). Myosin light chain phosphorylation inhibits muscle fibre shortening velocity in the presence of vanadate. *American Journal of Physiology.Regulatory, Integrative and Comparative Physiology, 292*(4), R1603-12.

Godt, R. E., & Nosek, T. M. (1989). Changes of intracellular milieu with fatigue or hypoxia depress contraction of skinned rabbit skeletal and cardiac muscle. *The Journal of Physiology, 412*, 155-180.

Gordon, A. M., Homsher, E., & Regnier, M. (2000). Regulation of contraction in striated muscle. *Physiological Reviews, 80*(2), 853-924.

Gordon, A. M., Regnier, M., & Homsher, E. (2001). Skeletal and cardiac muscle contractile activation: Tropomyosin "rocks and rolls". *News in Physiological Sciences : An International Journal of Physiology Produced Jointly by the International Union of Physiological Sciences and the American Physiological Society, 16*, 49-55.

Grange, R. W., Cory, C. R., Vandenboom, R., & Houston, M. E. (1995). Myosin phosphorylation augments force-displacement and force-velocity relationships of mouse fast muscle. *The American Journal of Physiology, 269*(3 Pt 1), C713-24.

Grange, R. W., Vandenboom, R., & Houston, M. E. (1993). Physiological significance of myosin phosphorylation in skeletal muscle. *Canadian Journal of Applied Physiology = Revue Canadienne De Physiologie Appliquee, 18*(3), 229-242.

Grange, R. W., Vandenboom, R., Xeni, J., & Houston, M. E. (1998). Potentiation of *in vitro* concentric work in mouse fast muscle. *Journal of Applied Physiology (Bethesda, Md.: 1985), 84*(1), 236-243.

Gulick, A. M., & Rayment, I. (1997). Structural studies on myosin II: Communication between distant protein domains. *BioEssays : News and Reviews in Molecular, Cellular and Developmental Biology, 19*(7), 561-569.

Hanson, J., & Huxley, H. E. (1953). Structural basis of the cross-striations in muscle. *Nature, 172*(4377), 530-532.

Hodgson, M., Docherty, D., & Robbins, D. (2005). Post-activation potentiation: Underlying physiology and implications for motor performance. *Sports Medicine (Auckland, N.Z.), 35*(7), 585-595.

Houston, M.E. (2006). Biochemistry Primer for Exercise Science. Windsor, ON: Human Kinetics.

Huxley, H., & Hanson, J. (1954). Changes in the cross-striations of muscle during contraction and stretch and their structural interpretation. *Nature, 173*(4412), 973-976.

Huxley, H. E. (1953). Electron microscope studies of the organisation of the filaments in striated muscle. *Biochimica Et Biophysica Acta, 12*(3), 387-394.

Huxley, H. E. (1957). The double array of filaments in cross-striated muscle. *The Journal of Biophysical and Biochemical Cytology, 3*(5), 631-648.

Huxley, H. E. (1969). The mechanism of muscular contraction. *Science (New York, N.Y.), 164*(886), 1356-1365.

Jiang, Y., & Julian, F. J. (1999). Effects of ramp shortening during linear phase of relaxation on [Ca2+]i in intact skeletal muscle fibres. *The American Journal of Physiology, 276*(1 Pt 1), C152-60.

Kabbara, A. A., & Allen, D. G. (1999). The role of calcium stores in fatigue of isolated single muscle fibres from the cane toad. *The Journal of Physiology, 519 Pt 1*, 169-176.

Karatzaferi, C., Franks-Skiba, K., & Cooke, R. (2008). Inhibition of shortening velocity of skinned skeletal muscle fibres in conditions that mimic fatigue. *American Journal of Physiology.Regulatory, Integrative and Comparative Physiology, 294*(3), R948-55.

Klug, G. A., Botterman, B. R., & Stull, J. T. (1982). The effect of low frequency stimulation on myosin light chain phosphorylation in skeletal muscle. *The Journal of Biological Chemistry, 257*(9), 4688-4690.

Krarup, C. (1981). Temperature dependence of enhancement and diminution of tension evoked by staircase and by tetanus in rat muscle. *The Journal of Physiology, 311*, 373-387.

Kushmerick, M. J., Moerland, T. S., & Wiseman, R. W. (1993). Two classes of mammalian skeletal muscle fibres distinguished by metabolite content. *Advances in Experimental Medicine and Biology, 332*, 749-60; discussion 760-1.

Kushmerick, M. J., Moerland, T. S., & Wiseman, R. W. (1992). Mammalian skeletal muscle fibres distinguished by contents of phosphocreatine, ATP, and pi. *Proceedings of the National Academy of Sciences of the United States of America, 89*(16), 7521-7525.

Lee, F. S. (1906). The cause of treppe. *Am Physiol Soc., 18*, 267-282.

Manning, D. R., & Stull, J. T. (1979). Myosin light chain phosphorylation and phosphorylase A activity in rat extensor digitorum longus muscle. *Biochemical and Biophysical Research Communications, 90*(1), 164-170.

Manning, D. R., & Stull, J. T. (1982). Myosin light chain phosphorylation-dephosphorylation in mammalian skeletal muscle. *The American Journal of Physiology, 242*(3), C234-41.

McKillop, D. F., & Geeves, M. A. (1993). Regulation of the interaction between actin and myosin subfragment 1: Evidence for three states of the thin filament. *Biophysical Journal, 65*(2), 693-701.

Metzger, J. M. (1996). Effects of phosphate and ADP on shortening velocity during maximal and submaximal calcium activation of the thin filament in skeletal muscle fibres. *Biophysical Journal, 70*(1), 409-417.

Morgan, M., Perry, S. V., & Ottaway, J. (1976). Myosin light-chain phosphatase. *The Biochemical Journal, 157*(3), 687-697.

Persechini, A., Stull, J. T., & Cooke, R. (1985). The effect of myosin phosphorylation on the contractile properties of skinned rabbit skeletal muscle fibres. *The Journal of Biological Chemistry, 260*(13), 7951-7954.

Pette, D., & Staron, R. S. (2000). Myosin isoforms, muscle fibre types, and transitions. *Microscopy Research and Technique, 50*(6), 500-509.

Posterino, G. S., & Dunn, S. L. (2008). Comparison of the effects of inorganic phosphate on caffeine-induced Ca2+ release in fast- and slow-twitch mammalian skeletal muscle. *American Journal of Physiology.Cell Physiology, 294*(1), C97-105.

Rassier, D. E., & Macintosh, B. R. (2000). Coexistence of potentiation and fatigue in skeletal muscle. *Brazilian Journal of Medical and Biological Research = Revista Brasileira De Pesquisas Medicas e Biologicas / Sociedade Brasileira De Biofisica ...[Et Al.], 33*(5), 499-508.

Rassier, D. E., & MacIntosh, B. R. (2000). Length dependence of staircase potentiation: Interactions with caffeine and dantrolene sodium. *Canadian Journal of Physiology and Pharmacology, 78*(4), 350-357.

Rassier, D. E., & MacIntosh, B. R. (2002). Sarcomere length-dependence of activity-dependent twitch potentiation in mouse skeletal muscle. *BMC Physiology, 2*, 19.

Rassier, D. E., Tubman, L. A., & MacIntosh, B. R. (1997). Length-dependent potentiation and myosin light chain phosphorylation in rat gastrocnemius muscle. *The American Journal of Physiology, 273*(1 Pt 1), C198-204.

Rassier, D. E., Tubman, L. A., & MacIntosh, B. R. (1998). Caffeine and length dependence of staircase potentiation in skeletal muscle. *Canadian Journal of Physiology and Pharmacology, 76*(10-11), 975-982.

Rayment, I., Holden, H. M., Whittaker, M., Yohn, C. B., Lorenz, M., Holmes, K. C., et al. (1993). Structure of the actin-myosin complex and its implications for muscle contraction. *Science (New York, N.Y.), 261*(5117), 58-65.

Rijkelijkhuizen, J. M., de Ruiter, C. J., Huijing, P. A., & de Haan, A. (2005). Low-frequency fatigue, post-tetanic potentiation and their interaction at different muscle lengths following eccentric exercise. *The Journal of Experimental Biology, 208*(Pt 1), 55-63.

Ritz-Gold, C. J., Cooke, R., Blumenthal, D. K., & Stull, J. T. (1980). Light chain phosphorylation alters the conformation of skeletal muscle myosin. *Biochemical and Biophysical Research Communications, 93*(1), 209-214.

Ryder, J. W., Lau, K. S., Kamm, K. E., & Stull, J. T. (2007). Enhanced skeletal muscle contraction with myosin light chain phosphorylation by a calmodulin-sensing kinase. *The Journal of Biological Chemistry, 282*(28), 20447-20454.

Sahlin. K., Harris, R. C., Nylind, B., & Hultman, E. (1976). Lactate Content and pH in Muscle Samples Obtained after Dynamic Exercise. *European Journal of Physiology.* 367, 143-149.

Sale, D. G. (2002). Postactivation potentiation: Role in human performance. *Exercise and Sport Sciences Reviews, 30*(3), 138-143.

Spriet, L.L. (1989). ATP utilization and provision in fast-twitch skeletal muscle during tetanic contractions. *American Journal of Physiology,* 257, E595-605.

Stein, R. B., Gordon, T., & Shriver, J. (1982). Temperature dependence of mammalian muscle contractions and ATPase activities. *Biophysical Journal, 40*(2), 97-107.

Szczesna, D., Zhao, J., Jones, M., Zhi, G., Stull, J., & Potter, J. D. (2002). Phosphorylation of the regulatory light chains of myosin affects Ca2+ sensitivity of skeletal muscle contraction. *Journal of Applied Physiology (Bethesda, Md.: 1985), 92*(4), 1661-1670.

Vandenboom, R., Grange, R. W., & Houston, M. E. (1993). Threshold for force potentiation associated with skeletal myosin phosphorylation. *The American Journal of Physiology, 265*(6 Pt 1), C1456-62.

Vandenboom, R., Grange, R. W., & Houston, M. E. (1995). Myosin phosphorylation enhances rate of force development in fast-twitch skeletal muscle. *The American Journal of Physiology, 268*(3 Pt 1), C596-603.

Vandenboom, R., & Houston, M. E. (1996). Phosphorylation of myosin and twitch potentiation in fatigued skeletal muscle. *Canadian Journal of Physiology and Pharmacology, 74*(12), 1315-1321.

Vandenboom, R., Xeni, J., Bestic, N. M., & Houston, M. E. (1997). Increased force development rates of fatigued mouse skeletal muscle are graded to myosin light chain phosphate content. *The American Journal of Physiology, 272*(6 Pt 2), R1980-4.

Vandenboom, R., Claflin, D. R., & Julian, F. J. (1998). Effects of rapid shortening on rate of force regeneration and myoplasmic [Ca2+] in intact frog skeletal muscle fibres. *The Journal of Physiology, 511 (Pt 1)*(Pt 1), 171-180.

Vandenboom, R., Hannon, J. D., & Sieck, G. C. (2002). Isotonic force modulates force redevelopment rate of intact frog muscle fibres: Evidence for cross-bridge induced thin filament activation. *The Journal of Physiology, 543*(Pt 2), 555-566.

Vandenboom, R. (2004). The myofibrillar complex and fatigue: A review. *Canadian Journal of Applied Physiology = Revue Canadienne De Physiologie Appliquee, 29*(3), 330-356.

Westerblad, H., & Allen, D. G. (1991). Changes of myoplasmic calcium concentration during fatigue in single mouse muscle fibres. *The Journal of General Physiology, 98*(3), 615-635.

Westerblad, H., Allen, D. G., Bruton, J. D., Andrade, F. H., & Lannergren, J. (1998). Mechanisms underlying the reduction of isometric force in skeletal muscle fatigue. *Acta Physiologica Scandinavica, 162*(3), 253-260.

Westerblad, H., Allen, D. G., & Lannergren, J. (2002). Muscle fatigue: Lactic acid or inorganic phosphate the major cause? *News in Physiological Sciences : An International Journal of Physiology Produced Jointly by the International Union of Physiological Sciences and the American Physiological Society, 17*, 17-21.

Yang, Z., Stull, J. T., Levine, R. J., & Sweeney, H. L. (1998). Changes in interfilament spacing mimic the effects of myosin regulatory light chain phosphorylation in rabbit psoas fibres. *Journal of Structural Biology, 122*(1-2), 139-148.

Zhi, G., Ryder, J. W., Huang, J., Ding, P., Chen, Y., Zhao, Y., et al. (2005). Myosin light chain kinase and myosin phosphorylation effect frequency-dependent potentiation of skeletal muscle contraction. *Proceedings of the National Academy of Sciences of the United States of America, 102*(48), 17519-17524.

APPENDIX 1: Force & Length Tracings

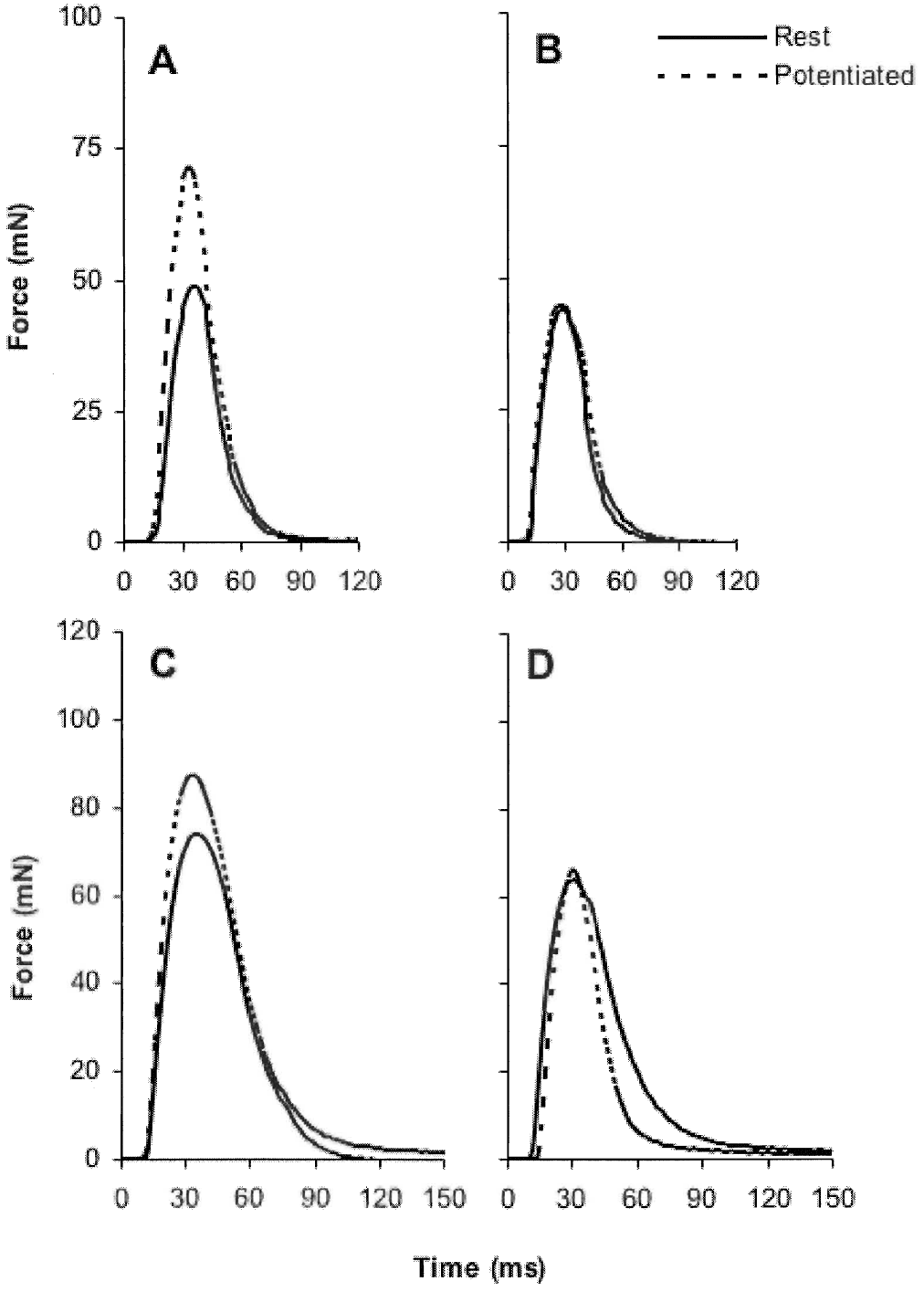

Figure 27. Potentiation of muscle twitch force following the standard conditioning stimulus. Traces **A** & **B** are from WT and KO muscles at $0.9L_o$. Traces **C** & **D** were collected from WT and KO muscles at $1.0L_o$.

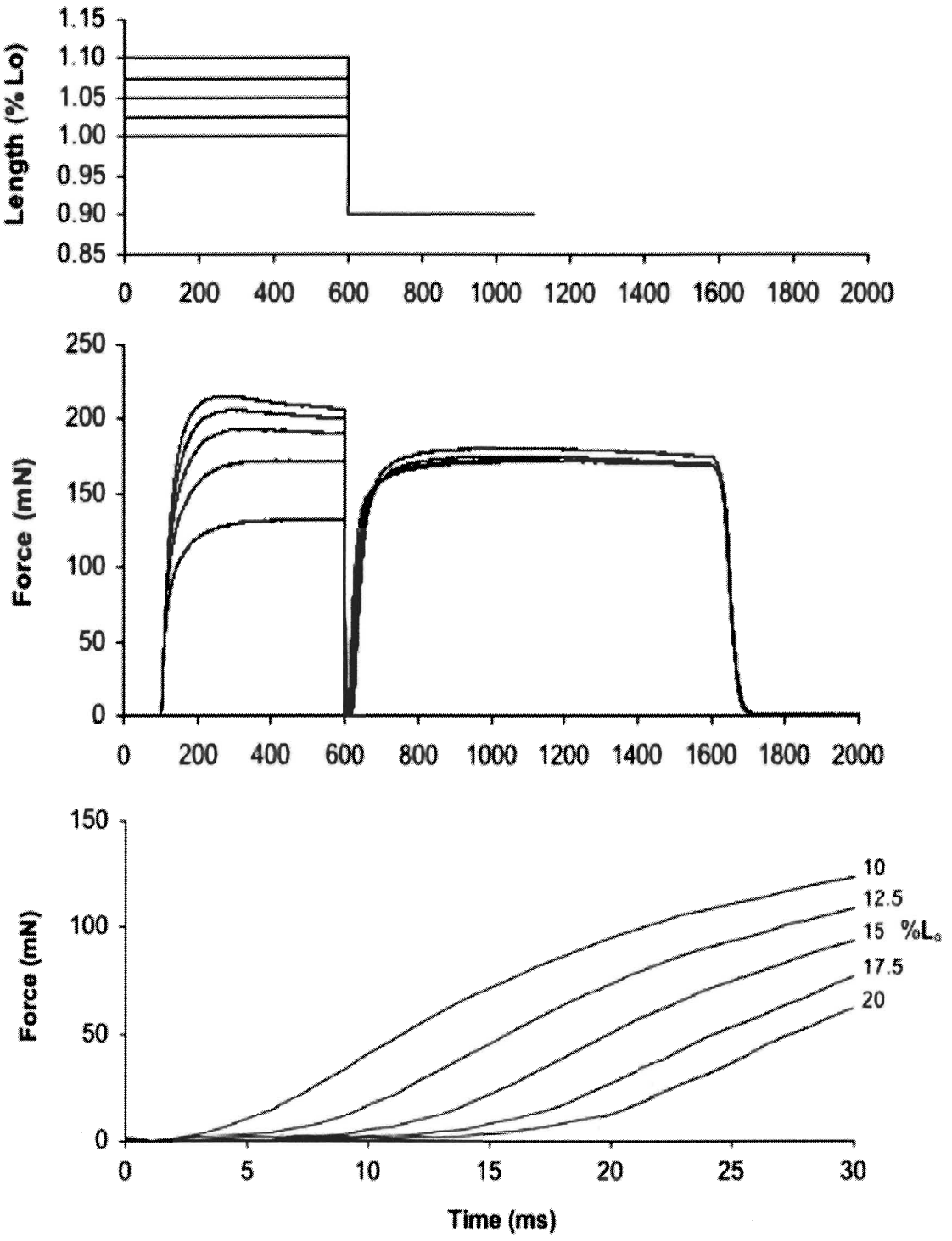

Figure 28. Force and length tracings sampled from a Slack Test. (Top) Length steps are induced during a fully fused tetanic contraction. (Middle) Tetanic force production prior to and following the rapid length step. (Bottom) Force redevelopment tracings after a length step. Slack time increases linearly with increasing step size from 10% L_o to 20% L_o. This relationship was used to calculate unloaded shortening velocity (V_o).

APPENDIX 2: Methods for Metabolic Assays & Fluorometry

Metabolite Extraction

Often the preparation of the tissue is the most critical. In the case of metabolite assays, the most hazardous period is usually the period between the moment the O_2 supply is cut off and the moment the enzyme activity is finally stopped. Rapid freezing is essential. Therefore, most metabolite analysis is performed on extracts prepared from frozen tissue. Most metabolites are assayed in protein-free extracts prepared with perchloric acid ($HClO_4$). $HClO_4$ is preferred because most of it can be easily removed by precipitation as a potassium salt. All of the following analyses are performed on freeze-dried tissue. Not only does it circumvent the problem of changing water contents in tissue, but also because the tissue is much easier to work with. Enzymes are rendered inactive in a water-free environment, and will remain so until water is re-added. Therefore, the weighing of the samples can be performed at room temperature and the tissue can be dissected free of connective tissues and blood.

Procedure

1. Freeze dry tissue (overnight to ensure all water is removed)
2. Store with dry rite in freezer until powdering
3. Tease out connective tissue and powder
4. Place in pre-weighed microcentrifuge tube and weigh (0.6 – 1.0 mg)
5. Place tubes in an ice bucket (make sure tubes remain cold)
6. Add 240 µL of pre-cooled 0.5 M PCA
7. Extract for 10 minutes, vortexing several times (ensure all tissue is in contact with PCA)
8. Centrifuge for 10 minutes at 15 000 G (spinning helps remove some of the enzymes that can influence concentration)
9. Remove 216 µL and place in freezer (-20°C) for 10 min
10. To the frozen supernatant add 54 µL of 2.2 M $KHCO_3$ and vortex until liquid (addition of $KHCO_3$ to a frozen supernatant prevents foaming over)
11. Centrifuge 10 min 4°C at 15 000G. Remove supernate to assay metabolites.

* Note: Dilution factors were varied for individual muscle size. PCA, Supernatent, $KHCO_3$ were altered accordingly. For samples <0.6mg [100/85/21.25], 0.6-1.5mg (200/180/45), >1.5mg (240/126/54).

Muscle Adenosine Triphosphate (ATP) and Phosphocreatine (PCr) Assay

CREATINE KINASE

P-CREATINE + ADP----------→ CREATINE + ATP

HEXOKINASE

ATP + GLUCOSE----------→ ADP + GLUCOSE-6-P

G-6-P-DH

GLUCOSE-6-P + NADP----------→ GLUCANOLACTONE + NADPH

Reagent	STOCK CONC.	FINAL CONC.	VOLUME 25ML	VOLUME 50ML	VOLUME 100ML
1. Tris Buffer (on shelf) **(pH 8.1)** *stored in fridge*	0.1 M	50 mM	1.25 ml	2.5 ml	5.00 ml
2. $MgCl_2$ (on shelf) fresh (.2033g/ml)	1.00 M	1.0 mM	25.00 µL	50.00 µL	100.00 µL
3. D.T.T. (found in -20) *aliquots -80*	0.5 M	0.5 mM	25.00 µL	50.00 µL	100.00 µL
4. Glucose (on shelf) *aliquots (-80)*	100.0 mM	100.0 µM	25.00 µL	50.00 µL	100.00 µL
5. NADP (found in -20) *aliquots (-80)*	50.0 mM	50.0 µM	25.00 µL	50.00 µL	100.00 µL
6. G-6-P-DH (found in fridge) Sigma (G-5760)	2660 U/ml	0.02 U/ml	1.00 µL	2.00 µL	4.00 µL
8. ADP (found in -20) Sigma (A-2754)	Solid				
9. Creatine Kinase (found in -20) Sigma (C-3755)	324 U/mg				

Note: Mix reagents 1-5 together. Bring to volume with distilled water and adjust to pH 8.1. Then add reagent 6. Mix by inversion with enzymes.

Procedure for Assay (Note: Run everything in triplicate)

Part 1.

1. Fill three wells with a blank (10.00 µL dH_2O per well)
2. a. Vortex each concentration mixture before pipetting
   b. Fill the next five wells with 10.00µL of varying concentrations of ATP standard (0.05 mM, 0.1 mM, 0.2 mM, 0.3 mM, 0.4 mM)
3. a. Vortex each concentration mixture before pipetting
   b. Fill the next five wells with 10.00 µL of varying concentrations of the PCr standard. (0.1 mM, 0.2 mM, 0.4 mM, 0.8 mM, 1.2 mM)
4. a. Vortex each sample before pipetting
   b. Add 10.00 µL of sample to the appropriately wells
5. Add 185 µL of reagent to each well
6. Incubate for 25 minutes.
7. Read the plate at sensitivity of 80 (excitation setting 340, emission setting 460) (base line reading)

Part 2.

Preparation: Mix 2.5 µL of Hexokinase with 1ml of tris buffer. Mix by inversion.

1. Add 6 µL of dilute Hexokinase to all of the wells
2. Place in the dark for 80 minutes
3. Read the plate at sensitivity of 80 (excitation setting 340, emission setting 460) (R2-R1= reflects ATP in extract)

Part 3.

Preparation: Mix ~1.5 mg of phosphocreatine kinase and 5 mg of ADP into 5 ml of tris buffer. Mix by inversion.

1. Add 6 µL of dilute CPK/ADP mixture to all of the wells
2. Place in the dark for 120 minutes
3. Read the plate at sensitivity of 80 (excitation setting 340, emission setting 460) (R3-R2= reflects PCr in extract)

ATP (Sigma A-7699) Standard Curve
-Make fresh 5.51 mg into 5 mL dH_2O

Conc (mM)	Stock (µL)	dH_2O (µL)
0.05	25	975
0.1	50	950
0.2	100	900
0.3	150	850
0.4	200	800

Phosphocreatine (Sigma P-7936) Standard Curve
-Stored in 7.6 mM aliquots in the -80°C
-To make 7.6 mM stock: mix 96.94mg PCr into 50mL dH_2O

Conc (mM)	Stock (µL)	dH_2O (µL)
0. 076	10	990
0.152	20	980
0.304	40	960
0.608	80	920
0.912	120	880

$C_4H_8N_3O_5PNa \bullet 4.4$ mol $H_2O \bullet mol^{-1}$ substance

Therefore its effective weight is 334.3 $g \bullet mol^{-1}$

Muscle Creatine (Cr) Assay

CREATINE KINASE

CREATINE + ATP----------→ P-CREATINE + ADP

PYRUVATE KINASE

ADP + P-PYRUVATE----------→ ATP + PYRUVATE

LDH

PYRUVATE + NADH----------→ LACTATE + NAD

Reagent	STOCK CONC	FINAL CONC	VOLUME 25ml	VOLUME 50 ml	VOLUME 100ml
1. Imidazole (on shelf) **(pH 8.1)** *stored in aliquots (-80)*	1.00 M	50 mM	1.25 ml	2.5 ml	5.00 ml
2. $MgCl_2$ (on shelf) make fresh (.2033g/ml)	1.00 M	5.0 mM	125.00 µL	250.00 µL	500.00 µL
3. KCl (on shelf) make fresh (.148g/2ml)	1.00 M	30.00 mM	0.75 ml	1.5 ml	3.00 ml
4. PEP (found in -20) *stored in aliquots (-80)*	10.0 mM	25.0 µM	60.00 µL	120.00 µL	240.00 µL
5. ATP (found in -20) make fresh	SOLID	2OO µM	3 mg	6 mg	12 mg
6. NADH (found in -20) Sigma (N-8129) *make fresh 10.5 mg/ml*	15 mM	45 µM	75.00 µL	150.00 µL	300.00 µL
7. LDH (found in fridge) Sigma (L-5132)	5264 U/ml	0.24 U/ml	1.10 µL	2.3 µL	4.6 µL
8. Pyruvate Kinase (found in fridge) Sigma (P-1506)	1252 U/ml	0.75 U/ml	15.00 µL	30.00 µL	60.00 µL
9. Creatine Kinase (found in -20) Sigma (C-3755)	324 U/mg	3.6 U/ml			

Note: Mix reagents 1-6 together. Bring to volume with distilled water and adjust to pH 7.5. Then add reagents 7 & 8. Mix by inversion when enzymes added.

Before beginning to pipette the samples you must test the fluorescence of the buffer (might have to change gain)

Procedure for Assay

Prepare Standards

Part 1.

1. Fill three wells with a blank (10.00 µL dH_2O per well)
2. a. Vortex each concentration mixture before pipetting
   b. Fill the next five wells with 10.00µL of varying concentrations of Cr standard (0.1mM, 0.2 mM, 0.4 mM, 0.8 mM, 1.2 mM)
3. a. Vortex each sample before pipetting
   b. Add 10.00 µL of sample to the appropriately wells
4. Add 185 µL of buffer to each well
5. Incubate for 30 minutes
6. Read the plate at a sensitivity of 100 (excitation setting 340, emission setting 460) (base line reading)

Part 2.

Preparation: Mix 1.0 mg of Creatine Kinase with 2.6 ml of buffer. Mix by inversion.

1. Add 6 µL of dilute Creatine Kinase to all of the wells
2. Place in the dark for 55 minutes
3. Read the plate (excitation setting 340, emission setting 460)

Note: Everything analyzed in triplicate

Creatine (Sigma C0780-50g) Standard Curve

-Stored in 10 mM aliquots in the -80°C

-To make 10 mM stock: 131.1 mg into 100 ml dH_2O

Conc (mM)	Stock (uL)	dH_2O ($umol \cdot L^{-1}$)
0.1	10	990
0.2	20	980
0.4	40	960
0.8	80	920
1.2	120	880

Muscle Lactate Assay

$$\text{Lactate} + NAD^+ \xrightarrow{\text{LDH}} \text{Pyruvate} + NADH + H^+$$

$$\text{PYRUVATE} + \text{Hydrazine} \longrightarrow \text{Pyruvate Hydrazone}$$

Reagent	STOCK CONC	FINAL CONC	VOLUME 25ml	VOLUME 50 ml	VOLUME 100ml
1. Hydrazine *stored in fridge* *make fresh bi-weekly*	1.00M	100.0 mM	2.5 ml	5.00 ml	10.00 ml
2. Glycine *stored in fridge* *make fresh bi-weekly*	1.00 M	100.0 mM	2.5 ml	5.00 ml	10.00 µL
3. NAD^+ (found in -20) *stored in aliquots (-80)*	100.0 mM	0.5 mM	125 µL	250 µL	500.00 µL
4. LDH (found in fridge) Sigma (L-5132)	5264 U/ml	8 U/ml	See	Procedure	

Note: Mix reagents 1-3 together. Bring to volume with distilled H_2O and adjust to pH 10.

Preparation of Dilute Enzyme (dependant on LDH)

Sigma L-5132

-Add 60 µL of LDH to 1.0 ml of reagent. Mix by inversion. (For 50 ml do 120 µL of reagent).

Sigma L-2500

-17.25 µL if using L-2500, LDH

Procedure for Assay

Prepare Standards

Part 1.

1. Fill three wells with a blank (10.00 µL dH_2O per well)
2. a. Vortex each concentration mixture before pipetting
   b. Fill the next five wells with 10.00µL of varying concentrations of lactate standard (0.025 mM, 0.05 mM, 0.1 mM, 0.2 mM, 0.8 mM)
3. a. Vortex each sample before pipetting
   b. Add 10.00 µL of sample to the appropriately wells
4. Add 185 µL of buffer to each well
5. Incubate for 15 minutes
6. Read the plate at a sensitivity of 100 (excitation setting 340, emission setting 460) (base line reading)

Part 2.

1. Add 10 µL of dilute LDH to all of the wells
2. Place in the dark for 120 minutes
3. Read the plate at a sensitivity of 100 (excitation setting 340, emission setting 460)

Note: Run everything in triplicate

Lactate Standard Curve

-Pre-made lactate standard (4.44 mM)

Conc (mM)	Stock (uL)	dH_2O (umol•L^{-1})
0.1	23	977
0.2	45	955
0.4	90	910
0.8	180	820
1.2	270	730

Conc (mM)	Stock (uL)	dH_2O (umol•L^{-1})
0.025	5.6	994
0.05	11.25	988
0.1	22.5	978
0.2	45	955
0.8	180	820
1.2	*270*	*730*

*Preferred Curve – 1.2mM not always necessary

APPENDIX 3: Calculation of ADP_{free} & Inorganic Phosphate Concentrations

Calculation of $[P_i]$ & Estimating Resting $[P_i]$

$$[Pi] = delta\ PCr\ (Rest - Exercise) + resting\ Pi$$

Resting inorganic phosphate concentrations were estimated according to the specific fibre-type composition of mouse EDL muscles reported previously (Crow & Kushmerick, 1982a; Kushmerick et al. 1992; Kushmerick et al. 1993).

Mouse EDL contains ~
.63 type IIB
.36 type IIX
.01 type I

Resting P_i measured in each fibre type ~
Type IIA, IIB: 0.8 mM/kg.dry wt^{-1}
Type I, IIX: 6.0 mM/kg.dry wt^{-1}

Resting $[P_i]$ was therefore calculated according to the following relationship:

$$[P_i] = (.63*0.8)+(.36*6.0)+(.01*6.0)$$
$$= 2.27\ mM/kg.dry\ wt^{-1}$$

Calculating muscle pH & Estimating [Pyruvate]

Muscle pH was calculated from the relationship of La^+ & Pyruvate (Sahlin. et al. 1976).

$$pH = -0.00413\ x\ (La^-\ + Pyr) + 7.06$$

Muscle [Pyruvate] was not directly measured but estimated according to the results of Sahlin et al. (1976), where [Pyruvate] equals between 0.5-4% of muscle lactate. This range was ~0.4 – 0.7mM. Muscle pyruvate content was therefore calculated as 2.25% of muscle lactate concentration.

$$pH = -\ log\ [H^+]$$

$$[H^+] = 10^{\wedge(-pH)}\ M$$

Calculating ADP_{free}

ADP_{free} was calculated using the known equilibrium constant K_{eq} for the creatine kinase reaction, as previously described by Dudley et al. (1987).

$$K_{eq} = 1.66\ x\ 10^6\ \mu M = [ATP]\ [Cr]\ /\ [H+]\ [PCr]\ [ADP]$$

$$[ADP] = [ATP]*[Cr]\ /\ 1.66\ x\ 10^6\ x\ [PCr]\ x\ [H+]$$

To calculate ADP in μmol/kg.dry wt^{-1}, concentrations of metabolites must be entered as mmol/kg.dry wt^{-1}. H^+ must be entered in mmol.

APPENDIX 4: Metabolic Changes During Skeletal Muscle Fatigue

Table 6. The following table of values represents the approximate change in concentration of specific muscle metabolites and pH in skeletal muscle during fatigue. Where available, values were selected from studies of intact, mammalian skeletal muscle. All other sources were compiled from studies of human, murine, and/or amphibian skeletal muscle preparations. The actual metabolite concentration measured in working skeletal muscle is largely determined by the species from which the sample was obtained and the manner in which the sample was analyzed; although the intensity and duration of muscle activation are important considerations for the evaluation of 'normal' metabolite values within a given fatigue protocol. Values are presented as mol/kg wet weight.

Metabolite	Rest	Fatigued
ATP	5-6mM [1,4]	2-4mM [1.4]
ADP_{free}	20μM [1]	250μM [1]
AMP_{free}	~ 0μM [2]	2μM [2]
IMP	~ 0mM [3]	5mM [3]
P_i	2mM [1]	25mM [1]
PCr	20mM [4]	≤5mM [3]
Cr	15mM [4]	30mM [4]
Lactate	1-2mM [3,4]	30-40mM [3,4]
pH (-log[H^+])	7.0 [1]	6.2 [1]

[1] as reviewed by Vandenboom (2004)
[2] as reviewed by Houston (2006)
[3] as reviewed by Allen, Lamb & Westerblad (2008)
[4] Spriet (1989)

APPENDIX 5: Myosin RLC Phosphorylation & Muscle Activation *In Vivo*

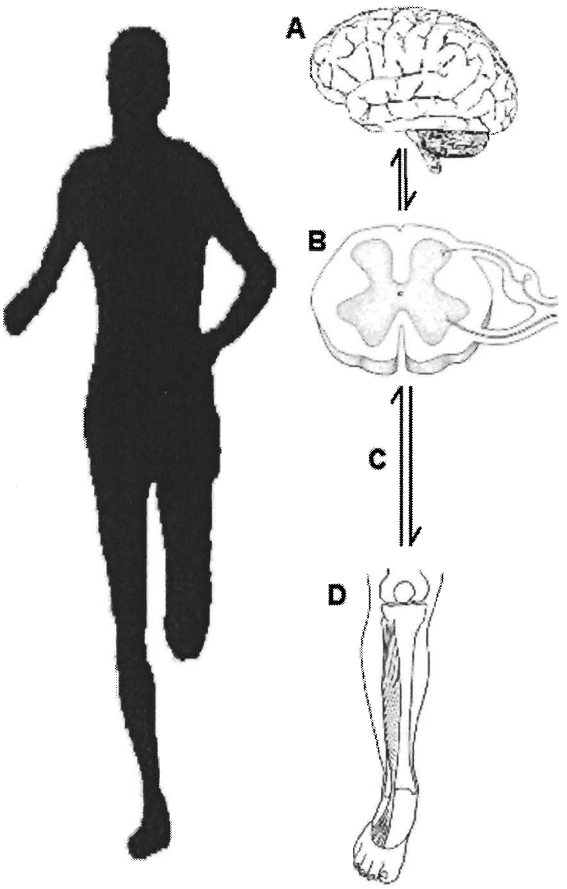

Figure 29. Afferent feedback (mechanical & metabolic) from working muscles may be used as important physiological information that regulates pacing strategies and peripheral motor unit firing frequencies *in vivo*. In this model, the body is subconsciously aware of muscle performance and the intensity of activation required to maintain a given steady-state activity. This information is processed by higher cortical structures (sensory & motor cortex, basal ganglia, cerebellum), and is applied to the coordination of complex movements and activities. It is assumed that the body will intrinsically alter complex physiological processes to operate in the most economical way possible during voluntary exercise. Applying the mechanism of myosin RLC phosphorylation to this model suggests that a given increase in contractile performance (increased Ca^{2+} sensitivity) for the same activation requirement (motor unit firing rate) may allow the body to decrease motor unit firing rates while maintaining some steady pace or muscle performance. A) The brain. The control of human movement requires complex processing that takes afferent (sensory) information into account when producing efferent signals to effector organs (i.e. working muscles). B) The spinal cord is the conduit that transfers all afferent and efferent information throughout the body. C) The peripheral nervous system is the local system of nerves that transfers sensory information from to the spinal cord, and additionally, carries the descending signals that activate muscles at the neuromuscular junction. D) The effector organ (i.e. muscle) is activated by the peripheral motor neuron and contains structures that measure and produce feedback information that is sent back to the brain (i.e. Golgi tendon organs, muscle spindles).